

# An axiomatic characterization of the Brownian map

Jason Miller and Scott Sheffield

## Abstract

The Brownian map is a random sphere-homeomorphic metric measure space obtained by “gluing together” the continuum trees described by the  $x$  and  $y$  coordinates of the Brownian snake. We present an alternative “breadth-first” construction of the Brownian map, which produces a surface from a certain decorated branching process. It is closely related to the peeling process, the hull process, and the Brownian cactus.

Using these ideas, we prove that the Brownian map is the only random sphere-homeomorphic metric measure space with certain properties: namely, scale invariance and the conditional independence of the inside and outside of certain “slices” bounded by geodesics. We also formulate a characterization in terms of the so-called Lévy net produced by a metric exploration from one measure-typical point to another. This characterization is part of a program for proving the equivalence of the Brownian map and Liouville quantum gravity with parameter  $\gamma = \sqrt{8/3}$ .

# Contents

|          |   |           |
|----------|---|-----------|
| <b>1</b> | <b>Introduction</b>   | <b>3</b>  |
| 1.1      | Overview . . . . .  | 3         |
| 1.2      | Relation with other work . . . . .                                    | 5         |
| 1.3      | Theorem statement . . . . .   | 5         |
| 1.4      | Outline . . . . .   | 8         |
| 1.5      | Discrete intuition . . . . .  | 10        |
| <b>2</b> | <b>Preliminaries</b>  | <b>18</b> |
| 2.1      | Metric measure spaces . . . . .                                       | 18        |
| 2.2      | Observations about metric spheres . . . . .                           | 19        |
| 2.3      | A consequence of slice independence/scale invariance . . . . .        | 25        |
| 2.4      | A $\sigma$ -algebra on the space of metric measure spaces . . . . .   | 27        |
| <b>3</b> | <b>Tree gluing and the Lévy net</b>                                   | <b>36</b> |
| 3.1      | Gluing together pair of continuum random trees . . . . .              | 36        |
| 3.2      | Gluing together pair of stable looptrees . . . . .                    | 37        |
| 3.3      | Gluing stable looptree to itself to obtain the Lévy net . . . . .     | 37        |
| 3.4      | A second approach to the Lévy net quotient . . . . .                  | 43        |
| 3.5      | Characterizing continuous state branching processes . . . . .         | 44        |
| 3.6      | A breadth-first approach to the Lévy net quotient . . . . .           | 48        |
| 3.7      | Topological equivalence of Lévy net constructions . . . . .           | 56        |
| 3.8      | Recovering embedding from geodesic tree quotient . . . . .            | 62        |
| <b>4</b> | <b>Tree gluing and the Brownian map</b>                               | <b>65</b> |
| 4.1      | Gluing trees given by Brownian-snake-head trajectory . . . . .        | 65        |
| 4.2      | Brownian maps and Lévy nets . . . . .                                 | 70        |
| 4.3      | Axioms that characterize the Brownian map . . . . .                   | 73        |
| 4.4      | Adding a third marked point along the geodesic . . . . .              | 86        |
| 4.5      | The martingale property holds if and only if $\alpha = 3/2$ . . . . . | 89        |
|          | <b>References</b>   | <b>94</b> |

**Acknowledgments.** We have benefited from conversations about this work with many people, a partial list of whom includes Omer Angel, Itai Benjamini, Nicolas Curien, Hugo Duminil-Copin, Amir Dembo, Bertrand Duplantier, Ewain Gwynne, Jean-François Le Gall, Gregory Miermont, Rémi Rhodes, Steffen Rohde, Oded Schramm, Stanislav Smirnov, Xin Sun, Vincent Vargas, Samuel Watson, Wendelin Werner, David Wilson, and Hao Wu.

We would also like to thank the Isaac Newton Institute (INI) for Mathematical Sciences, Cambridge, for its support and hospitality during the program on Random Geometry where part of this work was completed. Both authors were partially supported by a grant from the Simons Foundation while at the INI. J.M.’s work was also partially supported by DMS-1204894 and S.S.’s work was also partially supported by DMS-1209044, a fellowship from the Simons Foundation, and EPSRC grants EP/L018896/1 and EP/I03372X/1.

# 1 Introduction

## 1.1 Overview

In recent years, numerous works have studied a random measure-endowed metric space called the *Brownian map*, which can be understood as the  $n \rightarrow \infty$  scaling limit of the uniformly random quadrangulation (or triangulation) of the sphere with  $n$  quadrilaterals (or triangles). We will not attempt a detailed historical account here. Miermont’s recent St. Flour lecture notes are a good place to start for a general overview and a list of additional references [Mie14].<sup>1</sup>

This paper will assemble a number of ideas from the literature and use them to derive some additional fundamental facts about the Brownian map: specifically, we explain how the Brownian map can be constructed from a certain branching “breadth-first” exploration. This in turn will allow us to characterize the Brownian map as the only random metric measure space with certain properties.

---

<sup>1</sup>To give an extremely incomplete sampling of other papers relevant to this work, let us mention the early planar map enumerations of Tutte and Mullin [Tut62, Mul67, Tut68], a few early works on tree bijections by Schaeffer and others [CV81, JS98, Sch99, BMS00, CS02], early works on path-decorated surfaces by Duplantier and others [DK88, DS89, Dup98], the pioneering works by Watabiki and by Angel and Schramm on triangulations and the so-called peeling process [Wat95, Ang03, AS03], Krikun’s work on reversed branching processes [Kri05], the early Brownian map definitions of Marckert and Mokkadem [MM06a] and Le Gall and Paulin [LGP08] (see also the work [Mie08] of Miermont), various relevant works by Duquesne and Le Gall on Lévy trees and related topics [DLG02, DLG05, DLG06, DLG09], the Brownian cactus of Curien, Le Gall, and Miermont [CLGM13], the stable looptrees of Curien and Kortchemski [CK13], and several recent breakthroughs by Le Gall and Miermont [LG10, LG13, Mie13, LG14].

Roughly speaking, in addition to some sort of scale invariance, the main property we require is the conditional independence of the inside and the outside of certain sets (namely, filled metric balls and “slices” formed by pairs of geodesics from the center to the boundary of a filled metric ball) given an associated boundary length parameter. Section 1.5 explains that certain discrete models satisfy discrete analogs of this conditional independence; so it is natural to expect their limits to satisfy a continuum version. Our characterization result is in some sense analogous to the characterization of the Schramm-Loewner evolutions (SLEs) as the only random paths satisfying conformal invariance and the so-called domain Markov property [Sch00], or the characterization of conformal loop ensembles (CLEs) as the only random collections of loops with a certain Markov property [SW12].

The reader is probably familiar with the fact that in many random planar map models, when the total number of faces is of order  $n$ , the length of a macroscopic geodesic path has order  $n^{1/4}$ , while the length of the outer boundary of a macroscopic metric ball has order  $n^{1/2}$ . Similarly, if one rescales an instance of the Brownian map so that distance is multiplied by a factor of  $C$ , the area measure is multiplied by  $C^4$ , and the length of the outer boundary of a metric ball (when suitably defined) is multiplied by  $C^2$  (see Section 4). One might wonder whether there are other continuum random surface models with other scalings exponents in place of the 4 and the 2 mentioned above, perhaps arising from other different types of discrete models. However, in this paper the exponents 4 and 2 are shown to be determined by the axioms we impose; thus a consequence of this paper is that any continuum random surface model with different exponents must fail to satisfy at least one of these axioms.

One reason for our interest in this characterization is that it plays a role in a larger program for proving the equivalence of the Brownian map and the Liouville quantum gravity (LQG) sphere with parameter  $\gamma = \sqrt{8/3}$ . Both  $\sqrt{8/3}$ -LQG and the Brownian map describe random measure-endowed surfaces, but the former comes naturally equipped with a conformal structure, while the latter comes naturally equipped with the structure of a geodesic metric space. The program in progress provides a bridge between these objects, effectively endowing each one with the *other’s* structure, and showing that once this is done, the laws of the objects agree with each other.

Other parts of this program appear in [She10, MS12a, MS12b, MS12c, MS13a, MS13b, DMS14], and additional work in preparation by the current authors [MS15a, MS15b, MS15c, MS15d] (see also Curien’s work on the discrete side of this question [Cur13]). After using a quantum Loewner evolution (QLE) exploration to impose a metric structure on the LQG sphere, the papers [MS15b, MS15c] will prove that the law of this metric has the properties that characterize the law of the Brownian map, and hence is equivalent to the law of the Brownian map.

## 1.2 Relation with other work

We have learned in recent months of several independent works in preparation by other authors that will complement and partially overlap the work done here in interesting ways. Bertoin, Curien, and Kortchemski are working independently on a project [BCK15] to construct a breadth-first exploration of the Brownian map, which may also contain an independent proof that the Brownian map is uniquely determined by the information encoding this exploration. They draw from the theory of fragmentation processes to describe the evolution of the whole countable collection of unexplored component boundaries. They also explore the relationship to discrete breadth-first searches in some detail. Abraham and Le Gall [ALG15] are studying an infinite measure on Brownian snake excursions in the positive half-line (with the individual Brownian snake paths stopped when they return to 0). These excursions correspond to disks cut out by a metric exploration of the Brownian map, and play a role in this work as well. Finally, Bettinelli and Miermont [BM15] are constructing and studying properties of *Brownian disks* with an interior marked point and a given boundary length  $L$  (corresponding to the measure we call  $\mu_{\text{DISK}}^{1,L}$ ) including a decomposition of these disks into geodesic slices, which is related to the decomposition employed here for metric balls of a given boundary length (chosen from the measure we call  $\mu_{\text{MET}}^L$ ). They show that as a point moves around the boundary of Brownian disk, its distance to the marked point evolves as a type of Brownian bridge. In particular, this implies that the object they call the Brownian disk has finite diameter almost surely.

## 1.3 Theorem statement

In this subsection, we give a quick statement of our main theorem. However, we stress that several of the objects involved in this statement (leftmost geodesics, the Brownian map, the various  $\sigma$ -algebras, etc.) will not be formally defined until later in the paper. Let  $\mathcal{M}_{\text{SPH}}$  be the space of geodesic metric spheres that come equipped with a *good* measure (i.e., a finite measure that has no atoms and assigns positive mass to each open set). In other words,  $\mathcal{M}_{\text{SPH}}$  is the space of (measure-preserving isometry classes of) triples  $(S, d, \nu)$ , where  $d: S \times S \rightarrow [0, \infty)$  is a distance function on a set  $S$  such that  $(S, d)$  is topologically a sphere, and  $\nu$  is a good measure on the Borel  $\sigma$ -algebra of  $S$ .

Denote by  $\mu_{\text{SPH}}^{A=1}$  the standard unit area (sphere homeomorphic) Brownian map, which is a random variable that lives on the space  $\mathcal{M}_{\text{SPH}}$ . We will also discuss a closely related *doubly marked Brownian map* measure  $\mu_{\text{SPH}}^2$  on the space  $\mathcal{M}_{\text{SPH}}^2$  of elements of  $\mathcal{M}_{\text{SPH}}$  that come equipped with two distinguished marked points  $x$  and  $y$ . This  $\mu_{\text{SPH}}^2$  is an *infinite* measure on the space of *finite* volume surfaces. The quickest way to describe it is to say that sampling from  $\mu_{\text{SPH}}^2$  amounts to first choosing a real number  $A$  from the infinite measure  $A^{-3/2}dA$ , then independently choosing a measure-endowed surface from  $\mu_{\text{SPH}}^{A=1}$ , then choosing two marked points  $x$  and  $y$  independently from the measure on the surface, and then “rescaling” the resulting doubly marked surface so that its area is  $A$

(scaling area by  $A$  and distances by  $A^{1/4}$ ). The measure  $\mu_{\text{SPH}}^2$  turns out to describe the natural “grand canonical ensemble” on doubly marked surfaces. We formulate our main theorems in terms of  $\mu_{\text{SPH}}^2$  (although they can indirectly be interpreted as theorems about  $\mu_{\text{SPH}}^{A=1}$  as well).

Given an element  $(S, d, \nu, x, y) \in \mathcal{M}_{\text{SPH}}^2$ , and some  $r \geq 0$ , we let  $B^\bullet(x, r)$  denote the *filled* metric ball of radius  $r$  centered at  $x$ , as viewed from  $y$ . That is,  $B^\bullet(x, r)$  is the complement of the  $y$ -containing component of the complement of  $\overline{B(x, r)}$ , where  $B(x, r)$  is the open metric ball with radius  $r$  and center  $x$ . One can also understand  $S \setminus B^\bullet(x, r)$  as the set of points  $z$  such that there exists a path from  $z$  to  $y$  along which the function  $d(x, \cdot)$  stays strictly larger than  $r$ . Note that if  $0 < r < d(x, y)$  then  $B^\bullet(x, r)$  is a closed set whose complement contains  $y$  and is topologically a disk. In fact, one can show (see Proposition 2.1) that the boundary  $\partial B^\bullet(x, r)$  is topologically a circle, so that  $B^\bullet(x, r)$  is topologically a closed disk. We will sometimes interpret  $B^\bullet(x, r)$  as being itself a metric measure space with one marked point (the point  $x$ ) endowed with the internal metric it inherits from  $(S, d)$  (i.e., the distance between two points is the  $d$  length of the shortest path between them that stays in the interior of  $B^\bullet(x, r)$ ) and a measure obtained by restricting  $\nu$  to  $B^\bullet(x, r)$ . Whenever we make reference to metric balls or slices (as in the statement of Theorem 1.1 below) we understand them as marked metric measure spaces (endowed with the internal metric induced by  $d$ , and the restriction of  $\nu$ ) in this way.

We will later see that in the doubly marked Brownian map, if we fix  $r > 0$ , then on the event that  $d(x, y) > r$ , the circle  $\partial B^\bullet(x, r)$  almost surely comes endowed with a certain “boundary length measure” (which scales like the square root of the area measure). This is not too surprising given that the Brownian map is a scaling limit of random triangulations, and the discrete analog of a filled metric ball clearly comes with a notion of boundary length. We review this idea, along with more of the discrete intuition behind Theorem 1.1, in Section 1.5.

We will also see in Section 2 that there is a certain  $\sigma$ -algebra on the space of doubly marked metric measure spaces (which induces a  $\sigma$ -algebra  $\mathcal{F}^2$  on  $\mathcal{M}_{\text{SPH}}^2$ ) that is in some sense the “weakest reasonable”  $\sigma$ -algebra to use. We formulate Theorem 1.1 in terms of that  $\sigma$ -algebra (since in this case a weaker  $\sigma$ -algebra corresponds to a stronger theorem). We will also need to have some discussion in Section 2 to explain why the assumptions in the theorem statement are meaningful (e.g., why objects like  $B^\bullet(x, r)$  are measurable random variables), and to explain the term “leftmost” (which makes sense once one of the two orientations of the sphere has been fixed). However, let us clarify one point upfront: whenever we discuss geodesics in this paper, we will refer to paths between two endpoints that have minimal length among *all* paths between those endpoints (i.e., they do not just have this property in a some local sense).

**Theorem 1.1.** *The (infinite) doubly marked Brownian map measure  $\mu_{\text{SPH}}^2$  is the only measure on  $(\mathcal{M}_{\text{SPH}}^2, \mathcal{F}^2)$  with the following properties. (Here a sample from the measure is denoted by  $(S, d, \nu, x, y)$ .)*

1. The law is invariant under the Markov operation that corresponds to forgetting  $x$  (or  $y$ ) and then resampling it from the measure  $\nu$ . In other words, given  $(S, d, \nu)$ , the points  $x$  and  $y$  are conditionally i.i.d. samples from  $\nu$ .
2. Fix  $r > 0$  and let  $\mathcal{E}_r$  be the event that  $d(x, y) > r$ . Then  $\mu_{\text{SPH}}^2(\mathcal{E}_r) \in (0, \infty)$ , so that the restriction of  $\mu_{\text{SPH}}^2$  to  $\mathcal{E}_r$  can be normalized to be a probability measure. On the event  $\mathcal{E}_r$ , the following are true for  $s = r$  and also for  $s = d(x, y) - r$ .
  - (a) There is a random variable that we denote by  $L_s$  (which we interpret as a “boundary length” of  $\partial B^\bullet(x, s)$ ) such that given  $L_s$ , the random metric measure spaces  $B^\bullet(x, s)$  and  $S \setminus B^\bullet(x, s)$  are conditionally independent of each other. The conditional law of each of these random spaces depends only on the quantity  $L_s$ , and does so in a scale invariant way; i.e., the law given  $L_s = C$  is the same as the law given  $L_s = 1$  except that areas and distances are respectively scaled by  $C^a$  and  $C^b$  (for some fixed  $a$  and  $b$ ).
  - (b) In the case that  $s = d(x, y) - r$ , the boundary  $\partial B^\bullet(x, s)$  (necessarily homeomorphic to a circle) comes endowed with a good measure whose total mass is  $L_s$ , and which we interpret as a boundary length measure on  $\partial B^\bullet(x, s)$ . If  $z_1$  is chosen uniformly from this measure, and  $z_2, z_3, \dots, z_n$  are positioned so that  $z_1, \dots, z_n$  are evenly spaced around  $\partial B^\bullet(x, s)$  (according to the boundary measure) and  $\partial B^\bullet(x, s)$  is oriented according to the flip of an independent fair coin, then the  $n$  “slices” produced by cutting  $B^\bullet(x, s)$  along the leftmost geodesics from  $z_i$  to  $x$  are conditionally i.i.d. (as suggested by Figure 1.2 and Figure 1.3) and the law of each slice depends only on  $L_s/n$ , and does so in a scale invariant way (with the same exponents  $a$  and  $b$  as above).

We remark that the statement that we have a good measure can be reformulated as the statement that we have (for each  $n$ ) a way of choosing the cyclically ordered set of points  $z_1, \dots, z_n$  such that a.s. the orderings are consistent, a.s. there is no  $n$  for which two of the  $z_i$  are equal (the measure is non-atomic) and a.s. the points become dense on  $\partial B^\bullet(x, s)$  as  $n \rightarrow \infty$  (the measure assigns positive mass to open sets). We also note that the condition that  $L_r$  is equal to the total mass of a good measure implies that  $L_r > 0$ .

Among other things, the conditions of Theorem 1.1 will ultimately imply that  $L_r$  can be viewed as a process indexed by  $r \in [0, d(x, y)]$ , and that both  $L_r$  and its time reversal can be understood as excursions derived from Markov processes. We will see *a posteriori* that the time reversal of  $L_r$  is given by a certain time change of a 3/2-stable Lévy excursion with only positive jumps. One can also see *a posteriori* (when one samples from a measure which satisfies the axioms in the theorem — i.e., from the Brownian map measure  $\mu_{\text{SPH}}^2$ ) that the definition of the “slices” above is not changed if one replaces “leftmost” with “rightmost” because, in fact, from almost all points on  $\partial B^\bullet(x, s)$  the geodesic to  $x$  is unique. We remark that the last condition in Theorem 1.1

can be understood as a sort of “infinite divisibility” assumption for the law of a certain filled metric ball, given its boundary length.

Before we prove Theorem 1.1, we will actually first formulate and prove another closely related result: Theorem 4.6. To explain roughly what Theorem 4.6 says, note that for any element of  $\mathcal{M}_{\text{SPH}}^2$ , one can consider the union of the boundaries  $\partial B^\bullet(x, r)$  taken over all  $r \in [0, d(x, y)]$ . This union is called the *metric net* from  $x$  to  $y$  and it comes equipped with certain structure (e.g., there is a distinguished leftmost geodesic from any point on the net back to  $x$ ). Roughly speaking, Theorem 4.6 states that  $\mu_{\text{SPH}}^2$  is the only measure on  $(\mathcal{M}_{\text{SPH}}^2, \mathcal{F}^2)$  with certain basic symmetries and the property that the infinite measure it induces on the space of metric nets corresponds to a special object called the  $\alpha$ -(stable) *Lévy net* that we will define in Section 3.

## 1.4 Outline

In Section 2 we discuss some measure theoretic and geometric preliminaries. We begin by defining a *metric measure space* (a.k.a. *mm-space*) to be a triple  $(S, d, \nu)$  where  $(S, d)$  is a complete separable metric space,  $\nu$  is a measure defined on its Borel  $\sigma$ -algebra, and  $\nu(S) \in (0, \infty)$ .<sup>2</sup> Let  $\mathcal{M}$  denote the space of all metric measure spaces. Let  $\mathcal{M}^k$  denote the set of metric measure spaces that come with an ordered set of  $k$  marked points.

As mentioned above, before we can formally make a statement like “The doubly marked Brownian map is the only measure on  $\mathcal{M}^2$  with certain properties” we have to specify what we mean by a “measure on  $\mathcal{M}^2$ ,” i.e., what  $\sigma$ -algebra a measure is required to be defined on. The weaker the  $\sigma$ -algebra, the stronger the theorem, so we would ideally like to consider the weakest “reasonable”  $\sigma$ -algebra on  $\mathcal{M}$  and its marked variants. We argue in Section 2 that the weakest reasonable  $\sigma$ -algebra on  $\mathcal{M}$  is the  $\sigma$ -algebra  $\mathcal{F}$  generated by the so-called Gromov-weak topology. We recall that this topology can be generated by various natural metrics that make  $\mathcal{M}$  a complete separable metric space, including the so-called Gromov-Prohorov metric and the Gromov- $\square_1$  metric [GPW09, Löh13].

We then argue that this  $\sigma$ -algebra is at least strong enough so that the statement of our characterization theorem makes sense: for example, since our characterization involves surfaces cut into pieces by ball boundaries and geodesics, we need to explain why certain simple functions of these pieces can be understood as measurable functions

---

<sup>2</sup>Elsewhere in the literature, e.g., in [GPW09], the definition of a metric measure space also requires that the measure be a *probability* measure, i.e., that  $\nu(S) = 1$ . It is convenient for us to relax this assumption so that the definition includes area-measure-endowed surfaces whose total area is different from one. Practically speaking, the distinction does not matter much because one can always recover a probability measure by dividing the area measure by the total area. It simply means that we have one extra real parameter — total mass — to consider. Any topology or  $\sigma$ -algebra on the space of metric *probability*-measure spaces can be extended to the larger space we consider by taking its product with the standard Euclidean topology (and Borel- $\sigma$ -algebra) on  $\mathbf{R}$ .

of the original surface. All of this requires a bit of a detour into metric geometry and measure theory, a detour that occupies the whole of Section 2. The reader who is not interested in the details may skip or skim most of this section.

In Section 3, we recall the tree gluing results from [DMS14]. In [DMS14] we proposed using the term *peanosphere*<sup>3</sup> to describe a space, topologically homeomorphic to the sphere, that comes endowed with a good measure and a distinguished space-filling loop (parameterized so that a unit of area measure is filled in a unit of time) that represents an interface between a continuum “tree” and “dual tree” pair. Several of the constructions in [DMS14] describe natural measures on the space of peanospheres, and we note that the Brownian map also fits into this framework.

Some of the constructions in [DMS14] also involve the  $\alpha$ -stable *looptrees* introduced by Curien and Kortchemski in [CK13], which are in turn closely related to the Lévy stable random trees explored by Duquesne and Le Gall [DLG02, DLG05, DLG06, DLG09]. For  $\alpha \in (1, 2)$  we show how to glue an  $\alpha$ -stable looptree “to itself” in order to produce an object that we call the  $\alpha$ -stable *Lévy net*, or simply the  $\alpha$ -*Lévy net* for short. The Lévy net can be understood as something like a Peano *carpet*. It is a space homeomorphic to a closed subset of the sphere (obtained by removing countably many disjoint open disks from the sphere) that comes with a natural measure and a path that fills the entire space; this path represents an interface between a geodesic tree (whose branches also have well defined length parameterizations) and its dual (where in this case the dual object is the  $\alpha$ -stable looptree itself).

We then show how to explore the Lévy net in a breadth-first way, providing an equivalent construction of the Lévy net that makes sense for all  $\alpha \in (1, 2)$ . Our results about the Lévy net apply for general  $\alpha$  and can be derived independently of their relationship to the Brownian map. Indeed, the Brownian map is not explicitly mentioned at all in Section 3.

In Section 4 we make the connection to the Brownian map. To explain roughly what is done there, let us first recall recent works by Curien and Le Gall [CL14a, CL14b] about the so-called *Brownian plane*, which is an infinite volume Brownian map that comes with a distinguished origin. They consider the *hull process*  $L_r$ , where  $L_r$  denotes an appropriately defined “length” of the outer boundary of the metric ball of radius  $r$  centered at the origin, and show that  $L_r$  can be understood in a certain sense as the time-reversal of a continuous state branching process (which is in turn a time change of a  $3/2$ -stable Lévy process). See also the earlier work by Krikun on reversed branching processes associated to an infinite planar map [Kri05].

Section 4 will make use of *finite-volume* versions of the relationship between the Brownian map and  $3/2$ -stable Lévy processes. In these settings, one has two marked points  $x$  and

---

<sup>3</sup>The term emerged in a discussion with Kenyon. On the question of whether to capitalize (*à la* Laplacian, Lagrangian, Hamiltonian, Jacobian, Bucky Ball) or not (*à la* boson, fermion, newton, hertz, pascal, ohm, einsteinium, algorithm, buckminsterfullerene) the authors express no strong opinion.

$y$  on a finite-diameter surface, and the process  $L_r$  indicates an appropriately defined “length” of  $\partial B^\bullet(x, r)$ . The restriction of the Brownian map to the union of these boundary components is itself a random metric space (using the shortest path distance within the set itself) and we will show that it agrees in law with the  $3/2$ -Lévy net.

Given a single instance of the Brownian map, and a single fixed point  $x$ , one may let the point  $y$  vary over some countable dense set of points chosen i.i.d. from the associated area measure; then for each  $y$  one obtains a different instance of the Lévy net. We will observe that, given this collection of coupled Lévy net instances, it is possible to reconstruct the entire Brownian map. Indeed, this perspective leads us to the “breadth-first” construction of the Brownian map. (As we recall in Section 4, the conventional construction of the Brownian map from the Brownian snake involves a “depth-first” exploration of the geodesic tree associated to the Brownian map.)

The characterization will then essentially follow from the fact that  $\alpha$ -stable Lévy processes (and the corresponding continuous state branching processes) are themselves characterized by certain symmetries (such as the Markov property and scale invariance; see Proposition 3.10) and these correspond to geometric properties of the random metric space. An additional calculation will be required to prove that  $\alpha = 3/2$  is the only value consistent with the axioms that we impose, and to show that this determines the other scaling exponents of the Brownian map.

## 1.5 Discrete intuition

This paper does not address discrete models directly. All of our theorems here are formulated and stated in the continuum. However, it will be useful for intuition and motivation if we recall and sketch a few basic facts about discrete models. We will not include any detailed proofs in this subsection.

### 1.5.1 Infinite measures on singly and doubly marked surfaces

The literature on planar map enumeration begins with Mullin and Tutte in the 1960’s [Tut62, Mul67, Tut68]. The study of geodesics and the metric structure of random planar maps has roots in an influential bijection discovered by Schaeffer [Sch97], and earlier by Cori and Vauquelin [CV81].

The Cori-Vauquelin-Schaeffer construction is a way to encode a planar map by a pair of trees: the map  $M$  is a quadrangulation, and a “tree and dual tree” pair on  $M$  are produced from  $M$  in a deterministic way. One of the trees is a breadth-first search tree of  $M$  consisting of geodesics; the other is a type of dual tree.<sup>4</sup> In this setting, as one

---

<sup>4</sup>It is slightly different from the usual dual tree definition. As in the usual case, paths in the dual tree never “cross” paths in the tree; however, the dual tree is defined on the same vertices as the tree itself; it has some edges that cross quadrilaterals diagonally and others that overlap the tree edges.

traces the boundary between the geodesic tree and the dual tree, one may keep track of the distance from the root in the dual tree, and the distance in the geodesic tree itself; Chassaing and Schaeffer showed that the scaling limit of this random two-parameter process is the continuum random path in  $\mathbf{R}^2$  traced by the head of a Brownian snake [CS02], whose definition we recall in Section 4. The Brownian map<sup>5</sup> is a random metric space produced directly from this continuum random path; see Section 4.

Let us remark that tracing the boundary of a tree counterclockwise can be intuitively understood as performing a “depth-first search” of the tree, where one chooses which branches to explore in a left-to-right order. In a sense, the Brownian snake is associated to a *depth-first search of the tree of geodesics* associated to the Brownian map. We mention this in order to contrast it with the *breadth-first search* of the same geodesic tree that we will introduce later.

The scaling limit results mentioned above have been established for a number of types of random planar maps, but for concreteness, let us now focus our attention on triangulations. According to [AS03, Theorem 2.1] (applied with  $m = 0$ , see also [Ang03]), the number of triangulations (with no loops allowed, but multiple edges allowed) of a sphere with  $n$  triangles and a distinguished oriented edge is given by

$$\frac{2^{n+1}(3n!)}{n!(2n+2)!} \approx C(27/2)^n n^{-5/2} \quad (1.1)$$

where  $C > 0$  is a constant. Let  $\mu_{\text{TRI}}^1$  be the probability measure on triangulations such that the probability of each specific  $n$ -triangle triangulation (with a distinguished oriented edge — whose location one may treat as a “marked point”) is proportional to  $(27/2)^{-n}$ . Then (1.2) implies that the  $\mu_{\text{TRI}}^1$  probability of obtaining a triangulation with  $n$  triangles decays asymptotically like a constant times  $n^{-5/2}$ . One can define a new (non-probability) measure on random metric spaces  $\mu_{\text{TRI},k}^1$ , where the area of each triangle is  $1/k$  (instead of constant) but the measure is multiplied by a constant to ensure that the  $\mu_{\text{TRI},k}^1$  measure of the set of triangulations with area in the interval  $(1, 2)$  is given by  $\int_1^2 x^{-5/2} dx$ , and distances are scaled by  $k^{-1/4}$ . As  $k \rightarrow \infty$  the vague limit (as defined w.r.t. the Gromov-Hausdorff topology on metric spaces) is an infinite measure on the set of measure-endowed metric spaces. Note that we can represent any instance of one of these scaled triangulations as  $(M, A)$  where  $A$  is the total area of the triangulation and  $M$  is the measure-endowed metric space obtained by rescaling the area of each triangle by a constant so that the total becomes 1 (and rescaling all distances by the fourth root of that constant).

As  $k \rightarrow \infty$  the measures  $\mu_{\text{TRI},k}^1$  converge vaguely to the measure  $dM \otimes A^{-5/2} dA$ , where  $dM$  is the standard *unit volume* Brownian map measure (see [LG13] for the case of

---

<sup>5</sup>The Brownian map was introduced in works by Marckert and Mokkadem and by Le Gall and Paulin [MM06b, LGP08]. For a few years, the term “Brownian map” was used to refer to any one of the subsequential Gromov-Hausdorff scaling limits of certain random planar maps. Works by Le Gall and by Miermont established the uniqueness of this limit, and proved its equivalence to the metric space constructed directly from the Brownian snake [LG13, Mie13, LG14].

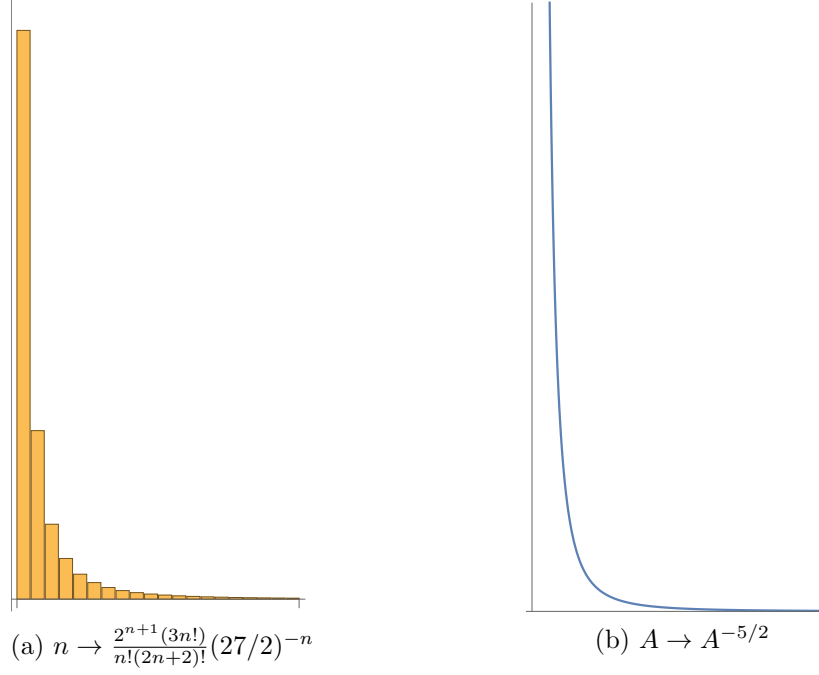


Figure 1.1: Up to constant factor, the right graph is the  $C \rightarrow \infty$  limit of the left graph rescaled (squeezed by factor of  $C$  horizontally, stretched by factor of  $C^{5/2}$  vertically). This explains why the “total surface area” marginal of the measure  $\mu_{\text{TRI},k}^1$  converges vaguely to the infinite measure  $A^{-5/2}dA$  as  $k \rightarrow \infty$ . One can deduce from this that the area marginal of  $\mu_{\text{TRI},k}^2$  converges vaguely to  $A^{-3/2}dA$ . (Note the relationship between  $\mu_{\text{TRI},k}^2$  and the “slice law” suggested by Figure 1.3.)

triangulations and  $2p$ -angulations for  $p \geq 2$  and [Mie13] for the case of quadrangulations); a sample from  $dM$  comes equipped with a single marked point. See Figure 1.1. The measure  $dM \otimes A^{-5/2}dA$  can be understood as type of grand canonical or Boltzmann measure on the space of (singly marked) Brownian map instances.

Now suppose we consider the set of *doubly marked* triangulations such that in addition to the root vertex (the first point on the distinguished oriented edge), there is an additional distinguished or “marked” vertex somewhere on the triangulation. Since, given an  $n$ -triangle triangulation, there are (by Euler’s formula)  $n/2$  other vertices one could “mark,” we find that the number of these doubly marked triangulations is (up to constant factor) given by  $n$  times the expression in (1.2), i.e.

$$\frac{n2^{n+1}(3n!)}{2n!(2n+2)!} \approx C(27/2)^n n^{-3/2}. \quad (1.2)$$

Let  $\mu_{\text{TRI},k}^2$  denote this probability measure on doubly marked surfaces (the doubly marked analog of  $\mu_{\text{TRI},k}^1$ ). Then the scaling limit of  $\mu_{\text{TRI},k}^2$  is an infinite measure of the

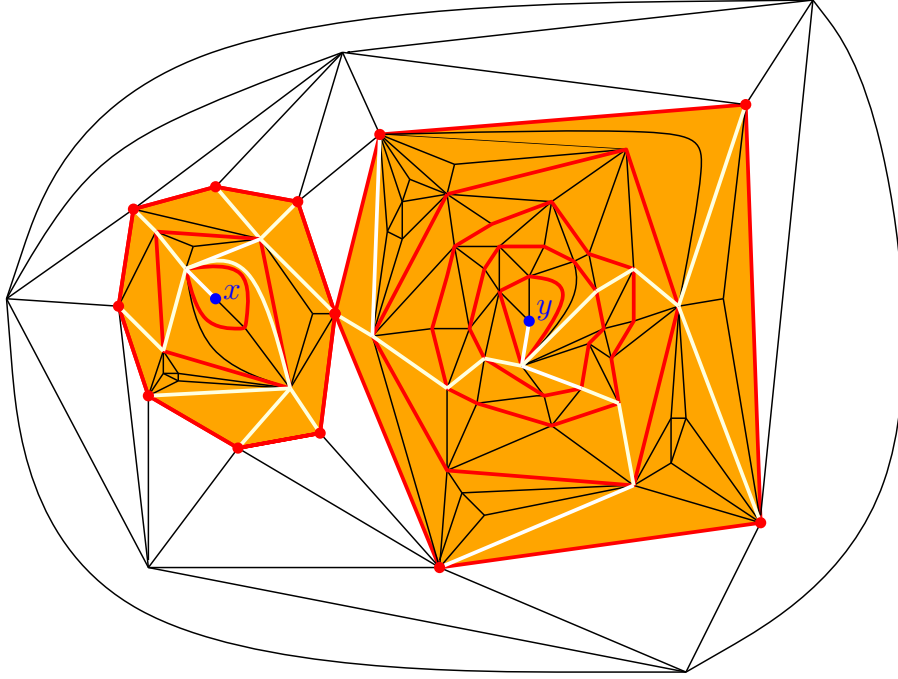


Figure 1.2: Shown is a triangulation of the sphere (the outer three edges form one triangle) with two marked points: the blue dots labeled  $x$  and  $y$ . The red cycles are outer boundaries of metric balls centered at  $x$  (of radii 1, 2, 3) and at  $y$  (of radii 1, 2, 3, 4, 5). From each point on the outer boundary of  $B^\bullet(x, 3)$  (resp.  $B^\bullet(y, 5)$ ) a geodesic toward  $x$  (resp.  $y$ ) is drawn in white. The geodesic drawn is the “leftmost possible” one; i.e., to get from a point on the circle of radius  $k$  to the circle of radius  $k - 1$ , one always takes the leftmost edge (as viewed from the center point). “Cutting” along white edges divides each of  $B^\bullet(x, 3)$  and  $B^\bullet(y, 5)$  into a collection of triangulated surfaces (one for each boundary edge) with left and right boundaries given by geodesic paths of the same length. Within  $B^\bullet(x, 3)$  (resp.  $B^\bullet(y, 5)$ ), there happens to be a single longest slice of length 3 (resp. 5) reaching all the way from the boundary to  $x$  (resp.  $y$ ). Parts of the left and right boundaries of these longest slices are identified with each other when the slice is embedded in the sphere. This is related to the fact that all of the geodesics shown in white have “merged” by their final step. Between  $B^\bullet(x, 3)$  and  $B^\bullet(y, 5)$ , there are  $8 + 5 = 13$  slices in total, one for each boundary edge. The white triangles outside of  $B^\bullet(x, 3) \cup B^\bullet(y, 5)$  form a triangulated disk of boundary length 13.

form  $dM \otimes A^{-3/2}dA$ , where  $M$  now represents a unit area *doubly marked* surface with distinguished points  $x$  and  $y$ . Note that if one ignores the point  $y$ , then the law  $dM$  in this context is exactly the same as in the one marked point context.

Generalizing the above analysis to  $k$  marked points, we will write  $\mu_{\text{SPH}}^k$  to denote the natural limiting infinite measure on  $k$ -marked spheres, which can be understood (up to a constant factor) as the  $k$ -marked point version of the Brownian map. To sample from

$\mu_{\text{SPH}}^k$ , one may

1. Choose  $A$  from the infinite measure  $A^{-7/2+k}dA$ .
2. Choose  $M$  as an instance of the standard unit area Brownian map.
3. Sample  $k$  points independently from the measure with which  $M$  is endowed.
4. Rescale the resulting  $k$ -marked sphere so that it has area  $A$ .

Of the measures  $\mu_{\text{SPH}}^k$ , we mainly deal with  $\mu_{\text{SPH}}^1$  and  $\mu_{\text{SPH}}^2$  in this paper. As mentioned earlier, we also sometimes use the notation  $\mu_{\text{SPH}}^{A=1}$  to describe the standard unit-area Brownian map measure, i.e., the measure described as  $dM$  above.

### 1.5.2 Properties of the doubly marked Brownian map

In this section, we consider what properties of the measure  $\mu_{\text{SPH}}^2$  on doubly marked measure-endowed metric spaces (as described above) can be readily deduced from considerations of the discrete models and the fact that  $\mu_{\text{SPH}}^2$  is a scaling limit of such models. These will include the properties contained in the statement of Theorem 1.1. Although we will not provide fully detailed arguments here, we note that together with Theorem 1.1, this subsection can be understood as a justification of the fact that  $\mu_{\text{SPH}}^2$  is the only measure one can reasonably expect to see as a scaling limit of discrete measures such as  $\mu_{\text{TRI}}^2$  (or more precisely as the vague limit of the rescaled measures  $\mu_{\text{TRI},k}^2$ ). In principle it might be possible to use the arguments of this subsection along with Theorem 1.1 (and a fair amount of additional detail) to give an alternate proof of the fact that the measures  $\mu_{\text{TRI}}^2$  have  $\mu_{\text{SPH}}^2$  as scaling limit. But we will not do that here.

Let us stress again that all of the properties discussed in this subsection can be proved rigorously for the doubly marked Brownian map measure  $\mu_{\text{SPH}}^2$ . But for now we are simply using discrete intuition to argue (somewhat heuristically) that these are properties that any scaling limit of the measures  $\mu_{\text{TRI}}^2$  should have.

Although  $\mu_{\text{SPH}}^2$  is an infinite measure, we have that  $\mu_{\text{SPH}}^2[A > c]$  is finite whenever  $c > 0$ . Based on what we know about the discrete models, what other properties would we expect  $\mu_{\text{SPH}}^2$  to have? One such property is obvious; namely, the law  $\mu_{\text{SPH}}^2$  should be invariant under the operation of resampling one (or both) of the two marked points from the (unit) measure on  $M$ . This is a property that  $\mu_{\text{TRI}}^2$  clearly has. If we fix  $x$  (with its directed edge) and resample  $y$  uniformly, or vice-versa, the overall measure is preserved. Another way to say this is the following: to sample from  $dM$ , one may first sample  $M$  as an unmarked unit-measure-endowed metric space (this space has no non-trivial automorphisms, almost surely) and then choose  $x$  and  $y$  uniformly from the measure on  $M$ .

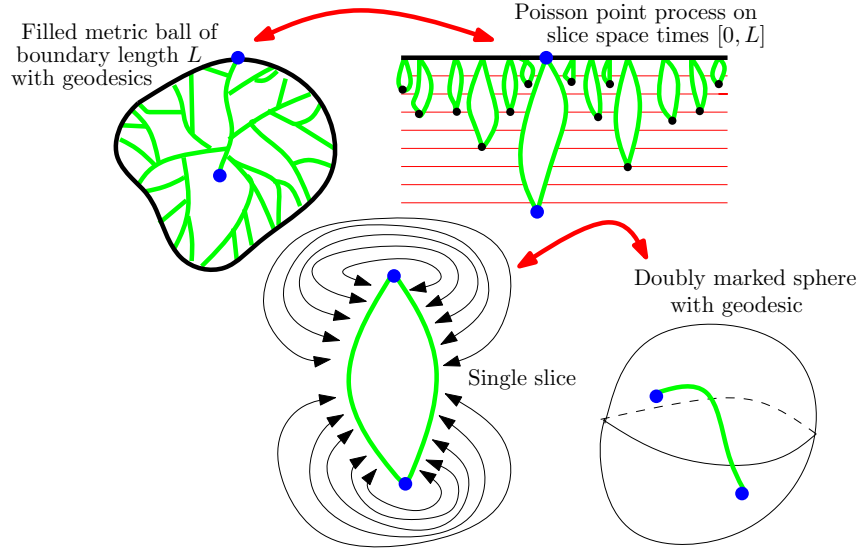


Figure 1.3: **Upper left:** A filled metric ball of the Brownian map (with boundary length  $L$ ) can be decomposed into “slices” by drawing geodesics from the center to the boundary. **Upper right:** the slices are embedded in the plane so that along the boundary of each slice, the geodesic distance from the black outer boundary (in the left figure) corresponds to the Euclidean distance below the black line (in the right figure). We may glue the slices back together by identifying points on same horizontal segment (leftmost and rightmost points on a given horizontal level are also identified) to recover the filled metric ball. **Bottom:** Lower figures explain the equivalence of the slice measure and  $\mu_{\text{SPH}}^2$ .

Before describing the next properties we expect  $\mu_{\text{SPH}}^2$  to have, let us define  $B^\bullet(x, r)$  to be the set of vertices  $z$  with the property that every path from  $z$  to  $y$  includes a point whose distance from  $x$  is less than or equal to  $r$ . This is the obvious discrete analog of the definition of  $B^\bullet(x, r)$  given earlier. Informally,  $B^\bullet(x, r)$  includes the radius  $r$  metric ball centered at  $x$  together with all of the components “cut off” from  $y$  by the metric ball. It is not hard to see that vertices on the boundary of such a ball, together with the edges between them, form a cycle; examples of such boundaries are shown as the red cycles in Figure 1.2.

Observe that if we condition on  $B^\bullet(x, r)$ , and on the event that  $d(x, y) > r$  (so that  $y \notin B^\bullet(x, r)$ ), then the  $\mu_{\text{TRI},k}^2$  conditional law of the remainder of the surface depends only on the boundary length of  $B^\bullet(x, r)$ , which we denote by  $L_r(x, y)$ , or simply  $L_r$  when the choice of  $x$  and  $y$  is understood. This conditional law can be understood as the standard Boltzmann measure on singly marked triangulations of the disk with boundary length  $L_r$ , where the probability of each triangulation of the disk with  $n$  triangles is proportional to  $(27/2)^{-n}$ . From this we conclude in particular that  $L_r$  evolves as a Markovian process, terminating when  $y$  is reached at step  $d(x, y)$ . This leads us to a

couple more properties one would expect the Brownian map to have, based on discrete considerations.

1. Fix a constant  $r > 0$  and consider the restriction of  $\mu_{\text{SPH}}^2$  to the event  $d(x, y) > r$ . (We expect the total  $\mu_{\text{SPH}}^2$  measure of this event to be finite.) Then once  $B^\bullet(x, r)$  is given, the conditional law of the singly marked surface comprising the complement of  $B^\bullet(x, r)$  is a law that depends only a single real number, a “boundary length” parameter associated to  $B^\bullet(x, r)$ , that we call  $L_r$ .
2. This law depends on  $L_r$  in a *scale invariant* way—that is, the random singly marked surface of boundary length  $L$  and the random singly marked surface of boundary length  $CL$  differ only in that distances and areas in the latter are each multiplied by some power of  $C$ . (We do not specify for now what power that is.) To partially justify this, note that is not hard to see that if one has a limit of the sort shown in Figure 1.1, then the right hand graph has to be a power law (since for every  $C$ , the graph must be preserved when one rescales horizontally by  $C$  and vertically by *some* value). Thus if the  $\mu_{\text{TRI},k}^2$  have a scaling limit of the form  $dM \otimes f(A)dA$  (as one would expect if the  $n$ -triangle triangulations, each rescaled to have area 1, have  $dM$  as a limit) then  $f(A)$  has to be a power law. A similar argument applies if one replaces the area parameter  $A$  with the diameter, or with the distance between  $x$  and  $y$  (in the doubly marked case).
3. The above properties also imply that the process  $L_r$  (or at least its restriction to a countable dense set) evolves as a Markov process, terminating at time  $d(x, y)$ , and that the  $\mu_{\text{SPH}}^2$  law of  $L_r$  is that of the (infinite) excursion measure associated to this Markov process.

The scale invariance assumptions described above do not specify the law of  $L_r$ . They suggest that  $\log L_r$  should be a time change of a Lévy process, but this still leaves an infinite dimensional family of possibilities. In order to draw further conclusions about this law, let us consider the time-reversal of  $L_r$ , which should also be an excursion of a Markov process. (This is easy to see on a discrete level; suppose we do not decide in advance the value of  $T = d(x, y)$ , but we observe  $L_{T-1}, L_{T-2}, \dots$  as a process that terminates after  $T$  steps. Then the conditional law of  $L_{T-k-1}$  given  $L_{T-k}$  is easily seen to depend only the value of  $L_{T-k}$ .) Given this reverse process up to a stopping time, what is the conditional law of the filled ball centered at  $y$  with the corresponding radius?

On the discrete level, this conditional law is clearly the uniform measure (weighted by  $(27/2)^{-n}$ , where  $n$  is the number of triangles, as usual) on triangulations of the boundary-length- $L$  disk in which there is a single fixed root and all points on the boundary are equidistant from that root. A sample from this law can be obtained by choosing  $L$  independent “slices” and gluing them together, see Figure 1.2. As illustrated in Figure 1.3, we expect to see a similar property in the continuum. Namely, that given

a boundary length parameter  $L$ , and a set of points along the boundary, the evolution of the lengths within each of the corresponding slices should be an independent process.

This suggests that the time-reversal of an  $L_r$  excursion should be an excursion of a so-called *continuous state branching process*, as we will discuss in Section 3.5. This property and scale invariance will determine the law of the  $L_r$  process up to a single parameter that we will call  $\alpha$ .

In addition to the spherical-surface measures  $\mu_{\text{SPH}}^k$  and  $\mu_{\text{SPH}}^{A=1}$  discussed earlier, we will in the coming sections consider a few additional measures on disk-homeomorphic measure-endowed metric spaces with a given fixed “boundary length” value  $L$ . (For now we give only informal definitions.)

1. A probability measure  $\mu_{\text{DISK}}^L$  on boundary length  $L$  surfaces that in some sense represents a “uniform” measure on all such surfaces — just as  $\mu_{\text{SPH}}^k$  in some sense represents a uniform measure on spheres with  $k$  marked points. It will be enough to define this for  $L = 1$ , as the other values can be obtained by rescaling. This  $L = 1$  measure is expected to be an  $m \rightarrow \infty$  scaling limit of the probability measure on discrete disk-homeomorphic triangulations with boundary length  $m$ , where the probability of an  $n$ -triangle triangulation is proportional to  $(27/2)^{-n}$ . (Note that for a given large  $m$  value, one may divide area, boundary length, and distance by factors of  $m^2$ ,  $m$ , and  $m^{1/2}$  respectively to obtain an approximation of  $\mu_{\text{DISK}}^L$  with  $L = 1$ .)
2. A measure  $\mu_{\text{DISK}}^{1,L}$  on marked disks obtained by weighting  $\mu_{\text{DISK}}^L$  by area and then choosing an interior marked point uniformly from that area. In the context of Theorem 1.1, this is the measure that should correspond to the conditional law of  $S \setminus B^\bullet(x, r)$  given that the boundary length of  $B^\bullet(x, r)$  is  $L$ .
3. A measure  $\mu_{\text{MET}}^L$  on disk-homeomorphic measure-endowed metric spaces with a given boundary length  $L$  and an interior “center point” such that all vertices on the boundary are equidistant from that point. In other words,  $\mu_{\text{MET}}^L$  is a probability measure on the sort of surfaces that arises as a filled metric ball. Again, it should correspond to a scaling limit of a uniform measure (except that as usual the probability of an  $n$ -triangle triangulation is proportional to  $(27/2)^{-n}$ ) on the set of all marked triangulations of a disk with a given boundary length and the property that all points on the boundary are equidistant from that marked point. This is the measure that satisfies the “slice independence” described at the end of the statement of Theorem 1.1.

Suppose we fix  $r > 0$  and restrict the measure  $\mu_{\text{SPH}}^2$  to the event that  $d(x, y) > r$ , so that  $\mu_{\text{SPH}}^2$  becomes a finite measure. Then one expects that given the filled metric ball of radius  $r$  centered at  $x$ , the conditional law of the component containing  $y$  is a sample from  $\mu_{\text{DISK}}^{1,L}$ , where  $L$  is a boundary length measure. Similarly, suppose one conditions

on the *outside* of the filled metric ball of radius  $d(x, y) - r$  centered at  $x$ . Then the conditional law of the filled metric ball itself should be  $\mu_{\text{MET}}^L$ . This is the measure that one expects (based on the intuition derived from Figure 1.2 and 1.3 above) to have the “slice independence” property.

## 2 Preliminaries

### 2.1 Metric measure spaces

A triple  $(S, d, \nu)$  is called a **metric measure space** (or **mm-space**) if  $(S, d)$  is a complete separable metric space and  $\nu$  is a measure on the Borel  $\sigma$ -algebra generated by the topology generated by  $d$ , with  $\nu(S) \in (0, \infty)$ . We remark that one can represent the same space by the quadruple  $(S, d, \tilde{\nu}, m)$ , where  $m = \nu(S)$  and  $\tilde{\nu} = m^{-1}\nu$  is a probability measure. This remark is important mainly because some of the literature on metric measure spaces requires  $\nu$  to be a probability measure. Relaxing this requirement amounts to adding an additional parameter  $m \in (0, \infty)$ .

Two metric measure spaces are considered equivalent if there is a measure-preserving isometry from a full measure subset of one to a full measure subset of the other. Let  $\mathcal{M}$  be the space of equivalence classes of this form. Note that when we are given an element of  $\mathcal{M}$ , we have no information about the behavior of  $S$  away from the support of  $\nu$ .

Next, recall that a measure on the Borel  $\sigma$ -algebra of a topological space is called **good** if it has no atoms and it assigns positive measure to every open set. Let  $\mathcal{M}_{\text{SPH}}$  be the space of geodesic metric measure spaces that can be represented by a triple  $(S, d, \nu)$  where  $(S, d)$  is a geodesic metric space homeomorphic to the sphere and  $\nu$  is a good measure on  $S$ .

Note that if  $(S_1, d_1, \nu_1)$  and  $(S_2, d_2, \nu_2)$  are two such representatives, then the a.e. defined measure-preserving isometry  $\phi: S_1 \rightarrow S_2$  is necessarily defined on a dense set, and hence can be extended to the completion of its support in a unique way so as to yield a continuous function defined on all of  $S_1$  (similarly for  $\phi^{-1}$ ). Thus  $\phi$  can be uniquely extended to an *everywhere* defined measure-preserving isometry. In other words, the metric space corresponding to an element of  $\mathcal{M}_{\text{SPH}}$  is uniquely defined, up to measure-preserving isometry.

As we are ultimately interested in probability measures on  $\mathcal{M}$ , we will need to describe a  $\sigma$ -algebra on  $\mathcal{M}$ . We will also show that  $\mathcal{M}_{\text{SPH}}$  belongs to that  $\sigma$ -algebra, so that in particular it makes sense to talk about measures on  $\mathcal{M}$  that are supported on  $\mathcal{M}_{\text{SPH}}$ . We would like to have a  $\sigma$ -algebra that can be generated by a complete separable metric, since this would allow us to define regular conditional probabilities for all subsets. We will introduce such a  $\sigma$ -algebra in Section 2.4. We first discuss some basic facts about metric spheres in Section 2.2.

## 2.2 Observations about metric spheres

Let  $\mathcal{M}_{\text{SPH}}^k$  be the space of elements of  $\mathcal{M}_{\text{SPH}}$  that come endowed with an ordered set of  $k$  marked points  $z_1, z_2, \dots, z_k$ . When  $j \leq k$  there is an obvious projection map from  $\mathcal{M}_{\text{SPH}}^k$  to  $\mathcal{M}_{\text{SPH}}^j$  that corresponds to “forgetting” the last  $k - j$  coordinates. We will be particularly interested in the set  $\mathcal{M}_{\text{SPH}}^2$  in this paper, and we often represent an element of  $\mathcal{M}_{\text{SPH}}^2$  by  $(S, d, \nu, x, y)$  where  $x$  and  $y$  are the two marked points. The following is a simple deterministic statement about geodesic metric spheres (i.e., it does not involve the measure  $\nu$ ).

**Proposition 2.1.** *Suppose that  $(S, d)$  is a geodesic metric space which is homeomorphic to  $\mathbf{S}^2$  and that  $x \in S$ . Then each of the components of  $S \setminus \overline{B(x, r)}$  has a boundary that is a simple closed curve in  $S$ , homeomorphic to the circle  $\mathbf{S}^1$ .*

*Proof.* Let  $U$  be one such component and consider the boundary set  $\Gamma = \partial U$ . We aim to show that  $\Gamma$  is homeomorphic to  $\mathbf{S}^1$ . Note that every point in  $\Gamma$  is of distance  $r$  from  $x$ .

Since  $U$  is connected and has connected complement, it must be homeomorphic to  $\mathbf{D}$ . We claim that the set  $S \setminus \Gamma$  contains only two components: the component  $U$  and another component that is also homeomorphic to  $\mathbf{D}$ . To see this, let us define  $\tilde{U}$  to be the component of  $S \setminus \Gamma$  containing  $x$ . By construction,  $\partial \tilde{U} \subseteq \Gamma$ , so every point on  $\partial \tilde{U}$  has distance  $r$  from  $x$ . A geodesic from any *other* point in  $\Gamma$  would have to pass through  $\partial \tilde{U}$ , and hence such a point would have to have distance greater than  $r$  from  $x$ . Since all points in  $\Gamma$  have distance  $r$  from  $x$ , we conclude that  $\partial \tilde{U} = \Gamma$ . Note that  $\tilde{U}$  has connected complement, and hence is also homeomorphic to  $\mathbf{D}$ .

The fact that  $\Gamma$  is the common boundary of two disjoint disks is not by itself enough to imply that  $\Gamma$  is homeomorphic to  $\mathbf{S}^1$ . There are still some strange counterexamples (topologist’s sine curves, exotic prime ends, etc.) To begin to rule out such things, our next step is show that  $\Gamma$  is locally connected.

Suppose for contradiction that  $\Gamma$  is not locally connected. This implies that there exists  $z \in \Gamma$  and  $s > 0$  such that for every sub-neighborhood  $V \subseteq B(z, s)$  containing  $z$  the set  $V \cap \Gamma$  is disconnected. Note that since  $\Gamma$  is connected the closure of every component of  $\Gamma \cap B(z, s)$  has non-empty intersection with  $\partial B(z, s)$ . Since these components are closed within  $B(z, s)$ , all but one of them must have positive distance from  $z$ . Moreover, for each  $\epsilon \in (0, s)$ , we claim that the number of such components which intersect  $B(z, \epsilon)$  must be infinite. Indeed, otherwise  $\Gamma$  would be locally connected at  $z$ , which would contradict our assumption that  $\Gamma$  is not locally connected at  $z$  (and this latter statement, the reader may recall, is the one we were assuming for the purpose of deriving a later contradiction).

Now (still assuming that  $\Gamma$  is not locally connected), the above discussion implies that there must be an annulus  $A$  (i.e., a difference between the disk-homeomorphic

complements of two concentric filled metric balls) centered at  $z$  such that  $A \cap \Gamma$  contains infinitely many connected components. Let  $\delta$  be equal to the width of  $A$  (i.e., the distance between the inside and outside boundaries of  $A$ ). It is not hard to see from this that both  $A \cap U$  and  $A \cap \tilde{U}$  contain infinitely many distinct components crossing  $A$ , each of diameter at least  $\delta$ .

Let  $A_I$  be the inner boundary of  $A$  and let  $A_M$  be the image of a simple loop in  $A$  which has positive distance from  $\partial A$  and surrounds  $A_I$ . Fix  $\epsilon > 0$ . Then the above implies that we can find  $w \in A_I \cap B(x, r)$  and points  $z_1, z_2 \in A_M \cap \partial \tilde{U}$  with  $d(z_1, z_2) < \epsilon$  such that a given geodesic  $\gamma$  which connects  $w$  and  $x$  necessarily crosses a given geodesic  $\eta$  which connects  $z_1$  and  $z_2$ . Since  $w \in B(x, r)$ , we have that  $\gamma$  is contained in  $B(x, r)$ . Let  $v$  be a point on  $\gamma \cap \eta$ . Then  $d(x, w) = d(x, v) + d(v, w)$ . We claim that  $d(v, w) < \epsilon$ . Indeed, if  $d(v, w) \geq \epsilon$  then as  $d(z_j, v) < \epsilon$  for  $j = 1, 2$  we would have that

$$d(x, z_j) \leq d(x, v) + d(v, z_j) < d(x, v) + \epsilon \leq d(x, v) + d(v, w) = d(x, w) < r.$$

This contradicts that  $z_1, z_2 \notin B(x, r)$ , which establishes the claim. Since  $d(v, w) < \epsilon$ , we therefore have that

$$d(z_j, w) \leq d(z_j, v) + d(v, w) < 2\epsilon.$$

Since  $\epsilon > 0$  was arbitrary and  $A_I, A_M$  are closed, we therefore have that  $A_M \cap A_I \neq \emptyset$ . This is a contradiction since we took  $A_M$  to be disjoint from  $A_I$ . Therefore  $\Gamma$  is locally connected.

Note that the image of  $\Gamma$  under a homeomorphism  $S \rightarrow \mathbf{S}^2$  must be locally connected as well. Moreover, there is a conformal map  $\varphi$  from  $\mathbf{D}$  to the image of  $\tilde{U}$ , and a standard result from complex analysis (see e.g. [Law05, Proposition 3.6]) states that since the image of  $\Gamma$  is locally connected, the map  $\varphi$  must extend continuously to its boundary. This tells us that  $\Gamma$  is given by the image of a continuous curve  $\psi: \mathbf{S}^1 \rightarrow S$ . It remains only to show  $\psi(z_1) \neq \psi(z_2)$  for all  $z_1, z_2 \in \mathbf{S}^1$ . This will complete the proof because then  $\psi$  is a simple curve which parameterizes  $\partial U$ .

Assume for contradiction that there exists  $z_1, z_2 \in \mathbf{S}^1$  distinct so that  $\psi(z_1) = \psi(z_2)$ . We write  $[z_1, z_2]$  for the counterclockwise segment of  $\mathbf{S}^1$  which connects  $z_1$  and  $z_2$ . Then we have that  $\psi$  restricted to each of  $[z_1, z_2]$  and  $\mathbf{S}^1 \setminus (z_1, z_2)$  is a loop and the two loops touch only at  $\psi(z_1) = \psi(z_2)$ . Therefore the loops are nested and only one of them separates  $U$  from  $x$ . We assume without loss of generality that  $\psi|_{\mathbf{S}^1 \setminus (z_1, z_2)}$  separates  $U$  from  $x$ . Fix  $w \in (z_1, z_2)$ , let  $\eta$  be a path from  $x$  to  $w$ , and let  $t_1$  (resp.  $t_2$ ) be the first time that  $\eta$  hits  $\partial U$  (resp.  $w$ ). Then we have that  $t_1 \neq t_2$ . Applying this to the particular case of a geodesic from  $x$  to  $w$ , we see that the distance of  $x$  to  $w$  is strictly larger than the distance of  $\partial U$  to  $w$ . This is a contradiction, which completes the proof.  $\square$

As mentioned earlier, given a doubly marked geodesic metric space  $(S, d, x, y)$  which is homeomorphic to  $\mathbf{S}^2$ , we let  $B^\bullet(x, r)$  denote the filled metric ball of radius  $r$  centered at

$x$ , as viewed from  $y$ . That is,  $B^\bullet(x, r)$  is the complement of the  $y$ -containing component of  $S \setminus \overline{B(x, r)}$ .

Fix some  $r$  with  $0 < r < d(x, y)$ , and a point  $z \in \partial B^\bullet(x, r)$ . Clearly, any geodesic from  $z$  to  $x$  is a path contained in  $B^\bullet(x, r)$ . In general there may be multiple such geodesics, but the following proposition gives us a way to single out a unique geodesic.

**Proposition 2.2.** *Suppose that  $(S, d, x, y)$  is a doubly marked geodesic metric space which is homeomorphic to  $\mathbf{S}^2$ , that  $0 < r < d(x, y)$ , and that  $B^\bullet(x, r)$  is the radius  $r$  filled ball centered at  $x$  and  $z \in \partial B^\bullet(x, r)$ . Assume that an orientation of  $\partial B^\bullet(x, r)$  is fixed (so that one can distinguish the “clockwise” and “counterclockwise” directions). Then there exists a unique geodesic from  $z$  to  $x$  that is leftmost viewed from  $x$  (i.e., furthest counterclockwise) when lifted and understood as an element of the universal cover of  $B^\bullet(x, r) \setminus \{x\}$ .*

*Proof.* Note that for each  $r' \in (0, r)$ , the lifting of  $\partial B^\bullet(x, r')$  to this universal cover is homeomorphic to  $\mathbf{R}$  (since  $\mathbf{R}$  is the lifting of the circle to its universal cover) and one can find the leftmost (i.e., furthest counterclockwise) point in this universal cover reachable by any geodesic. It is not hard to see that the union of such points (over all  $r'$ ) forms the desired leftmost geodesic.  $\square$

We next establish some “rigidity” results for metric spaces. Namely, we will first show that there is no non-trivial isometry of a geodesic closed-disk-homeomorphic metric space which fixes the boundary. We will then use this to show that the identity map is the only orientation-preserving isometry of a triply marked geodesic sphere that fixes all of the marked points. (Note that there can be many automorphisms of the unit sphere that fix two marked points if those points are on opposite poles.) We will note that it suffices to fix two points if one also fixes a distinguished geodesic between them.

**Proposition 2.3.** *Suppose that  $(S, d)$  is a geodesic metric space such that there exists a homeomorphism  $\varphi: \overline{\mathbf{D}} \rightarrow S$ . Suppose that  $\phi: S \rightarrow S$  is an isometry which fixes  $\partial S := \varphi(\partial \mathbf{D})$ . Then  $\phi(z) = z$  for all  $z \in S$ .*

*Proof.* Fix  $x_1, x_2, x_3 \in \partial S$  distinct. Then  $x_1, x_2, x_3$  determine an orientation of  $\partial S$ . Thus for  $x \in \partial S$  and  $z \in S$ , we have a well-defined leftmost geodesic  $\gamma$  connecting  $z$  to  $x$  with respect to this orientation. Since  $\phi$  fixes  $\partial S$ , it preserves the orientation of  $\partial S$ . In particular, if it is true that  $\phi(z) = z$  then it follows that  $\phi$  must fix  $\gamma$  (for otherwise we would have more than one leftmost geodesic from  $z$  to  $x$ ). We conclude that  $\{z : \phi(z) = z\}$  is connected and connected to the boundary, and hence its complement must have only simply connected components. Brouwer’s fixed point theorem implies that none of these components can be non-empty, since there would necessarily be a fixed point inside. This implies that  $\phi(z) = z$  for all  $z \in S$ .  $\square$

**Proposition 2.4.** *Suppose that  $(S, d, x_1, x_2, x_3)$  is a triply marked geodesic metric space which is topologically equivalent to  $\mathbf{S}^2$ . We assume that  $S$  is oriented so that we can distinguish the clockwise and counterclockwise directions of simple loops. Suppose that  $\phi: S \rightarrow S$  is an orientation-preserving isometry with  $\phi(x_j) = x_j$  for  $j = 1, 2, 3$ . Then  $\phi(z) = z$  for all  $z \in S$ . Similarly, if  $(S, d, x_1, x_2)$  is a doubly marked space and  $\gamma$  is a geodesic from  $x_1$  to  $x_2$ , then the identity is the only orientation-preserving isometry that fixes  $x_1$ ,  $x_2$ , and  $\gamma$ .*

*Proof.* The latter statement is immediate from Proposition 2.3 applied to the disk obtained by cutting the sphere along  $\gamma$ . To prove the former statement, we assume without loss of generality that  $R = d(x_1, x_2) \leq d(x_1, x_3)$ . Proposition 2.2 implies that there exists a unique leftmost geodesic  $\gamma$  from  $x_2$  to  $x_1$ . Since  $\phi$  fixes  $x_1$ , it follows that  $\phi(\partial B(x_1, R)) = \partial B(x_1, R)$ . Since  $\phi$  fixes  $x_2$ , it thus follows that  $\phi$  fixes  $\gamma$  and hence (by the latter proposition statement) all of  $S$ .  $\square$

We remark that the above argument implies that the identity is the only map that fixes  $x$  and the restriction of  $\gamma$  to *any* neighborhood about  $x$ . In other words, the identity is the only map that fixes  $x$  and the equivalence class of geodesics  $\gamma$  that end at  $x$ , where two geodesics considered equivalent if they agree in a neighborhood of  $x$ . This is analogous to the statement that a planar map on the sphere has no non-trivial automorphisms (as a map) once one fixes a single oriented edge. We next observe that Proposition 2.3 can be further strengthened.

**Proposition 2.5.** *In the context of Proposition 2.3, if the isometry  $\phi: S \rightarrow S$  is orientation preserving and fixes even one point  $x \in \partial S$  it must be the identity.*

*Proof.* By Proposition 2.3, it suffices to check that  $\phi$  fixes the circle  $\partial S$  pointwise (since  $\phi$  is a homeomorphism, it clearly fixes  $\partial S$  as a set). From Proposition 2.4, it suffices to show that  $\phi$  fixes three points on  $\partial S$  (since one can identify the boundaries of two copies of  $\partial S$  to obtain a sphere). Write  $f(y) = d(x, y)$ , and note that we must have  $f(y) = f \circ \phi(y)$  for all  $y \in \partial S$ . In particular, if  $y$  is the first point around the circle clockwise at which  $f$  obtains a certain value  $a$ , then  $\phi$  must fix that point. Choosing three values for  $a$  gives the result.  $\square$

We now return to our study of leftmost geodesics.

**Proposition 2.6.** *Suppose that we are in the setting of Proposition 2.2. Suppose that  $a \in \partial B^\bullet(x, r)$  and that  $(a_j)$  is a sequence of points in  $\partial B^\bullet(x, r)$  which approach  $a$  from the left. For each  $j$ , we let  $\gamma_j$  be the leftmost geodesic from  $a_j$  to  $x$  and  $\gamma$  the leftmost geodesic from  $a$  to  $x$ . Then we have that  $\gamma_j \rightarrow \gamma$  uniformly as  $j \rightarrow \infty$ . Moreover, for all but countably many values of  $a$  (which we will call **jump values**) the same is true when the  $a_j$  approach  $a$  from the right. If  $a$  is one of these jump values, then the limit of the geodesics from  $a_j$ , as the  $a_j$  approach  $a$  from the right, is a non-leftmost geodesic from  $a$  to  $x$ .*

*Proof.* Suppose that the  $(a_j)$  in  $\partial B^\bullet(x, r)$  approach  $a \in \partial B^\bullet(x, r)$  from the left and  $\gamma_j, \gamma$  are as in the statement. Suppose that  $(\gamma_{j_k})$  is a subsequence of  $(\gamma_j)$ . It suffices to show that  $(\gamma_{j_k})$  has a subsequence which converges uniformly to  $\gamma$ . The Arzelà-Ascoli theorem implies that  $(\gamma_{j_k})$  has a subsequence which converges uniformly to some limiting path  $\tilde{\gamma}$  connecting  $a$  to  $x$ . This path is easily seen to be a geodesic connecting  $a$  to  $x$  which is non-strictly to the left of  $\gamma$ . Since  $\gamma$  is leftmost, we conclude that  $\gamma = \tilde{\gamma}$ . This proves the first part of the proposition.

Suppose now that the  $(a_j)$  approach  $a$  from the right and let  $\gamma_j, \gamma$  be as in the previous paragraph. The Arzelà-Ascoli theorem implies that every subsequence of  $(\gamma_j)$  has a further subsequence which converges uniformly to a geodesic connecting  $a$  to  $x$ . That the limit does not depend on the subsequence follows by monotonicity.

To prove the second part of the proposition, note that each jump value  $a$  is associated with the non-empty open set  $J_a \subseteq B^\bullet(x, r)$  which is between the leftmost geodesic from  $a$  to  $x$  and the uniform limit of leftmost geodesics along any sequence  $(a_j)$  approaching  $a$  from the right. Moreover, for distinct jump values  $a, a'$  we must have that  $J_a \cap J_{a'} = \emptyset$ . Therefore the set of jump values is countable.  $\square$

As in the proof of Proposition 2.6, if  $a$  is a jump value, we let  $J_a$  denote the open set bounded between the (distinct) left and right limits described in Proposition 2.6, both of which are geodesics from  $a$  to  $x$ . Recall that if  $a, a'$  are distinct jump values then  $J_a, J_{a'}$  are disjoint. Moreover, observe that the union of the  $J_a$  (over all jump values  $a$ ) is the complement of the closure of the union of all leftmost geodesics. As the point  $a$  moves around the circle, the leftmost geodesic from  $a$  to  $x$  may vary continuously (as it does when  $(S, d)$  is a Euclidean sphere) but it may also have countably many times when it “jumps” over an open set  $J_a$  (as is a.s. the case when  $(S, d, \nu)$  is an instance of the Brownian map, see Section 4).

We next need to say a few words about “cutting” geodesic metric spheres along curves and/or “welding” closed geodesic metric disks together. Before we do this, let us consider the general question of what it means to take a quotient of a metric space w.r.t. an equivalence relation (see [BBI01, Chapter 3] for more discussion on this point). Given any metric space  $(S, d)$  and any equivalence relation  $\cong$ , one may define a distance function  $\bar{d}$  between equivalence classes of  $\cong$  as follows: if  $a$  and  $b$  are representatives of distinct equivalence classes, take  $\bar{d}(a, b)$  to be the infimum, over even-length sequences  $a = x_0, x_1, x_2, \dots, x_{2k} = b$  with the property that  $x_m \cong x_{m+1}$  for odd  $m$ , of the sum

$$\sum_{m=0}^{k-1} d(x_{2m}, x_{2m+1}).$$

This  $\bar{d}$  is *a priori* only a pseudometric on the set of equivalence classes of  $\cong$  (i.e., it may be zero for some distinct  $a$  and  $b$ ). However, it defines a metric on the set of equivalence classes of  $\cong^*$  where  $a \cong^* b$  whenever  $\bar{d}(a, b) = 0$ . It is not hard to see that  $\bar{d}$  is the

largest pseudometric such that  $\bar{d}(a, b) \leq d(a, b)$  for all  $a, b$  and  $d(a, b) = 0$  when  $a \cong b$ . The procedure described above is what we generally have in mind when we speaking of taking a quotient of a metric space w.r.t. an equivalence relation.

Now let us ask what happens if a geodesic metric sphere is *cut* along a simple loop  $\Gamma$ , to produce two disks. Note that on each disk, there is an *internal metric*, where the distance between points  $a$  and  $b$  is defined to be the length of the shortest path that stays entirely within the given disk. This distance is clearly finite when  $a$  and  $b$  are in the interior of the disk. (This can be deduced by taking a closed path from  $a$  to  $b$  bounded away from the disk boundary, covering it with open metric balls bounded away from the disk boundary, and taking a finite subcover.) However, when either  $a$  or  $b$  is on the boundary of the disk, it is not hard to see that (if the simple curve is windy enough) it could be infinite.

Let us now ask a converse question. What happens when we take the two metric disks and try to “glue them together” to recover the sphere? We can clearly recover the sphere as a topological space, but what about the metric? Before we address that point, note there is always *one* way to glue the disks back together to create a new metric space: namely, we may consider the disjoint union of the pair of disks to be a common metric space (with the distance between points on distinct disks formally set to be infinity) and then take a metric quotient (in the sense discussed above) w.r.t. the equivalence relation that identifies the boundary arcs. This can be understood as the largest metric compatible with the boundary identification. In this metric, the distance between  $a$  and  $b$  is the length (in the original metric) of the shortest path from  $a$  to  $b$  that only crosses  $\Gamma$  finitely many times. However, although we will not prove this here, it appears that one can actually construct a geodesic metric sphere with a closed curve  $\Gamma$  and points  $a$  and  $b$  such that the shortest path from  $a$  to  $b$  that crosses  $\Gamma$  finitely many times is *longer* than the shortest path overall. In other words, it appears that there may be situations where cutting a sphere into two disks and gluing the disks back together (using the quotient procedure described above) does not reproduce the original sphere.

On the other hand, it is easy to see that this type of pathology does not arise if  $\Gamma$  is a curve comprised of a finite number of geodesic arcs, since one can easily find a geodesic  $\gamma$  between any points  $a$  and  $b$  that crosses no geodesic arc of  $\Gamma$  more than once. (If it crosses an arc multiple times, one may replace the portion of  $\gamma$  between the first and last hitting times by a portion of the arc itself.) The same applies if one has a disk cut into two pieces using a finite sequence of geodesic arcs. This is an important point, since in this paper we will frequently need to glue together disk-homeomorphic “slices” whose boundaries are geodesic curves. The following proposition formalizes one example of such a statement.

**Proposition 2.7.** *Suppose that  $(S, d, x, y)$  is a doubly marked geodesic metric space which is homeomorphic to  $\mathbf{S}^2$ . Suppose that  $\gamma_1, \gamma_2$  are distinct geodesics which connect  $x$  to  $y$  and that  $S \setminus (\gamma_1 \cup \gamma_2)$  has two components  $U_1, U_2$ . For  $j = 1, 2$ , let  $x_j$  (resp.*

$y_j$ ) be the first (resp. last) point on  $\partial U_j$  visited by  $\gamma_1$  (or equivalently by  $\gamma_2$ ). We then let  $(U_j, d_j, x_j, y_j)$  be the doubly marked metric space where  $d_j$  is given by the internal metric induced by  $d$  on  $U_j$ . Let  $\tilde{S}$  be given by the disjoint union of  $\bar{U}_1$  and  $\bar{U}_2$  and let  $\tilde{d}$  be the distance on  $\tilde{S}$  which is defined by  $\tilde{d}(a, b) = d_j(a, b)$  if  $a, b \in \bar{U}_j$  for some  $j = 1, 2$ , otherwise  $\tilde{d}(a, b) = \infty$ . We then define an equivalence relation  $\cong$  on  $\tilde{S}$  by declaring that  $a \cong b$  if either  $a = b$  or if  $a \in \partial U_1$  corresponds to the same point  $b \in \partial U_2$  in  $S$ . Let  $\bar{d}$  be the largest metric compatible with  $\tilde{S}/\cong$ . Then  $\bar{d} = d$ . That is, the metric gluing of the  $(U_j, d_j, x_j, y_j)$  along their boundaries gives  $(S, d, x, y)$ .

For future reference, let us remark that another instance where this pathology will not arise is when  $(S, d, x)$  is an instance of a Brownian map with a marked point  $x$  and  $\Gamma$  is the boundary of a filled metric ball centered at  $x$ . In that case, the definition of  $d$  will imply that the length of the shortest path between points  $a$  and  $b$  is the infimum over the lengths of paths comprised of finitely many arcs, each of which is a segment a geodesic from some point to  $x$ . Such a path clearly only crosses  $\Gamma$  finitely many times. Note that the two situations discussed above (cutting along geodesics and along boundaries of filled metric balls) are precisely those that are needed to make sense of the statements in Theorem 1.1.

### 2.3 A consequence of slice independence/scale invariance

At the end of Section 1.5, the measure  $\mu_{\text{MET}}^L$  is informally described, along with a notion of “slice independence” one might expect such a measure to satisfy. Although we have not given a formal description of  $\mu_{\text{MET}}^L$  yet, we can observe now some properties we would expect this measure to have. For concreteness, let us assume that  $L = 1$  and that a point on the boundary is fixed, so that the boundary of a sample from  $\mu_{\text{MET}}^L$  can be identified with the interval  $[0, 1]$ . We “cut” along the geodesic from 0 to  $x$  and view a sample from  $\mu_{\text{MET}}^L$  as a “triangular slice” with one side identified with  $[0, 1]$  and the other two sides forming geodesics of the same length (one from 0 to  $x$  and one from 1 to  $x$ ).

We define  $\tilde{d}(a, b)$  to be the distance from the boundary at which the leftmost geodesic from  $a$  to  $x$  and the leftmost geodesic from  $b$  to  $x$  merge. Now, no matter what space and  $\sigma$ -algebra  $\mu_{\text{MET}}^L$  is defined on, we would expect that if we restrict to rational values of  $a$  and  $b$ , then the  $\tilde{d}(a, b)$  should be a countable collection of real-valued random variables. Before we even think about  $\sigma$ -algebras on  $\mathcal{M}$  or  $\mathcal{M}_{\text{SPH}}$ , we can answer a more basic question. What would “slice independence” and “scale invariance” assumptions tell us about the joint law of these random variables  $\tilde{d}(a, b)$ ? The following proposition formalizes what we mean by scale invariance and slice independence, and shows that in fact these properties characterize the joint law of the  $\tilde{d}(a, b)$  up to a single real parameter. As we will see in the proof of Theorem 1.1, this will allow us to deduce that the metric net associated with a space which satisfies the hypotheses of Theorem 1.1 is related to the so-called Lévy net introduced in Section 3 below.

**Proposition 2.8.** *Consider a random function  $\tilde{d}$  defined on all rational points in  $[0, 1] \times [0, 1]$  such that*

1.  $\tilde{d}(a, b) = \tilde{d}(b, a)$  for all  $a$  and  $b$  a.s.
2. If  $a < b$  and  $c < d$  then  $\tilde{d}(a, b)$  and  $\tilde{d}(c, d)$  are independent provided that  $(a, b)$  and  $(c, d)$  are disjoint.
3.  $\tilde{d}(a, a) = 0$  a.s. for all  $a$
4. If  $a < b < c$  then  $\tilde{d}(a, c) = \max(\tilde{d}(a, b), \tilde{d}(b, c))$ .
5. The law of  $\tilde{d}(a, b)$  depends only  $|b - a|$ . In fact, there is some  $\beta$  so that for any  $a$  and  $b$  the law of  $\tilde{d}(a, b)$  is equivalent to the law of  $|a - b|^\beta \tilde{d}(0, 1)$ .

Then the law of  $\tilde{d}(a, b)$  has a particular form. Precisely, one can construct a sample from this law as follows. First choose a collection of pairs  $(s, x)$  as a Poisson point process on  $[0, 1] \times \mathbf{R}_+$  with intensity  $ds \otimes x^\alpha dx$  where  $\alpha = -1/\beta - 1$  and  $ds$  (resp.  $dx$ ) denotes Lebesgue measure on  $[0, 1]$  (resp.  $\mathbf{R}_+$ ). Then define  $\tilde{d}(a, b)$  to be the largest value of  $x$  such that  $(s, x)$  is a point in this point process for some  $x \in (a, b)$ .

*Proof.* The lemma statement describes two ways of choosing a random  $\tilde{d}$  and asserts that the two laws agree. It is immediate from Lemma 2.9 (stated and proved just below) that the laws agree when one restricts attention to  $[0, 1/k, 2/k, \dots, 1]^2$ , for any  $k \in \mathbf{N}$ . Since this holds for all  $k$ , the result follows.  $\square$

**Lemma 2.9.** *Suppose for some  $\beta > 0$ , a real-valued random variable  $A$  has the following property. When  $A_1, A_2, \dots, A_k$  are i.i.d. copies of  $A$ , the law of  $k^{-\beta} \max_{1 \leq i \leq k} A_i$  is the same as the law of  $A$ . Then  $A$  agrees in law (up to some multiplicative constant) with the size of the maximum element of a Poisson point process chosen from the infinite measure  $x^\alpha dx$ , where  $\alpha = -1/\beta - 1$  and  $dx$  denotes Lebesgue measure on  $\mathbf{R}_+$ .*

*Proof.* Let  $F$  be the cumulative distribution function of  $A$ , so that  $F(s) = \mathbf{P}[A \leq s]$ . Then

$$F(s) = \mathbf{P}[A \leq s] = \mathbf{P}[k^{-\beta} A \leq s]^k = F(k^\beta s)^k.$$

Thus  $F(k^\beta s) = F(s)^{1/k}$ . Set  $r = k^\beta$  so that  $1/k = r^{-1/\beta}$ . Then when  $r$  has this form we have  $F(rs) = F(s)^{1/k} = F(s)^{r^{-1/\beta}}$ . Applying this twice allows us to draw the same conclusion when  $r = k_1^\beta/k_2^\beta$  for rational  $k = k_1/k_2$ , i.e., for all values  $r$  which are a  $\beta$ th power of a rational. Since this is a dense set, we can conclude that in general, if we set  $e^t = F(1)$ , we have

$$F(r) = e^{tr^{-1/\beta}}. \tag{2.1}$$

It is then straightforward to see that this implies that (up to a multiplicative constant)  $A$  has the same law as the Poisson point process maximum described in the lemma statement. (See, e.g., [Sat99, Exercise 22.4].)  $\square$

## 2.4 A $\sigma$ -algebra on the space of metric measure spaces

We present here a few general facts about measurability and metric spaces, following up on the discussion in Section 1.4. Most of the basic information we need about the Gromov-Prohorov metric and the Gromov-weak topology can be found in [GPW09]. Other related material can be found in the metric geometry text by Burago, Burago, and Ivanov [BBI01], as well as Villani’s book [Vil09, Chapters 27-28].

As in Section 1.4, let  $\mathcal{M}$  denote the space of metric measure spaces, defined modulo a.e. defined measure preserving isometry. Suppose that  $(S, d, \nu) \in \mathcal{M}$ . If we choose points  $x_1, x_2, \dots, x_k$  i.i.d. from  $\nu$ , then we obtain a  $k \times k$  matrix of distances  $d_{ij} = d(x_i, x_j)$  indexed by  $i, j \in \{1, 2, \dots, k\}$ . Denote this matrix by  $M_k = M_k(S, d, \nu)$ .

If  $\psi$  is any fixed bounded continuous function on  $\mathbf{R}^{k^2}$ , then the map

$$(S, d, \nu) \rightarrow \mathbf{E}_\nu[\psi(M_k)]$$

is a real-valued function on  $\mathcal{M}$ . The Gromov-weak topology is defined to be the weakest topology w.r.t. which the functions of this type are continuous. In other words, a sequence of elements of  $\mathcal{M}$  converge in this topology if and only if the laws of the corresponding  $M_k$  (understood as measures on  $\mathbf{R}^{k^2}$ ) converge weakly for each  $k$ . We denote by  $\mathcal{F}$  the Borel  $\sigma$ -algebra generated by this topology. Since we would like to be able to sample marked points from  $\nu$  and understand their distances from each other, we feel comfortable saying that  $\mathcal{F}$  is the weakest “reasonable”  $\sigma$ -algebra we could consider. We will sometimes abuse notation and use  $(\mathcal{M}_{\text{SPH}}, \mathcal{F})$  to denote a measure space, where in this context  $\mathcal{F}$  is understood to refer to the intersection of  $\mathcal{F}$  with the set of subsets of  $\mathcal{M}_{\text{SPH}}$ . (We will apply a similar notational abuse to the “marked” analogs  $\mathcal{M}^k$ ,  $\mathcal{M}_{\text{SPH}}^k$ , and  $\mathcal{F}^k$  introduced below.)

It turns out that the Gromov-weak topology can be generated by various natural metrics that make  $\mathcal{M}$  a complete separable metric space: the so-called Gromov-Prohorov metric and the Gromov- $\square_1$  metric [GPW09, Löh13]. Thus,  $(\mathcal{M}, \mathcal{F})$  is a *standard Borel space* (i.e., a measure space whose  $\sigma$ -algebra is the Borel  $\sigma$ -algebra of a topology generated by a metric that makes the space complete and metrizable). We do not need to discuss the details of these metrics here. We bring them up in order to show that  $(\mathcal{M}, \mathcal{F})$  is a standard Borel space. One useful consequence of the fact that  $(\mathcal{M}, \mathcal{F})$  is a standard Borel space is that if  $\mathcal{G}$  is any sub- $\sigma$ -algebra of  $\mathcal{F}$ , then the regular conditional probability of a random variable, conditioned on  $\mathcal{G}$ , is well defined [Dur10, Chapter 5.1.3].

We can also consider *marked* spaces; one may let  $\mathcal{M}^k$  denote the set of tuples of the form  $(S, d, \nu, x_1, x_2, \dots, x_k)$  where  $(S, d, \nu) \in \mathcal{M}$  and  $x_1, x_2, \dots, x_k$  are elements (“marked points”) of  $S$ . Given such a space, one may sample additional points  $x_{k+1}, x_{k+2}, \dots, x_m$  i.i.d. from  $\nu$  and consider the random matrix  $M_m$  of distances between the  $x_i$ . One may again define a Gromov-weak topology on the marked space to be the weakest topology w.r.t. which expectations of bounded continuous functions of  $M_m$  are continuous. We

let  $\mathcal{F}^k$  denote the Borel  $\sigma$ -algebra of the marked space. Clearly for any  $m > k$  one has a measurable map  $\mathcal{M}^m \rightarrow \mathcal{M}^k$  that corresponds to “forgetting” the last  $m - k$  points. One can similarly define  $\mathcal{F}^\infty$  to be the space of  $(S, d, \nu, x_1, x_2, \dots)$  with an  $x_j$  defined for all positive integer  $j$ . The argument that these spaces are standard Borel is essentially the same as in the case without marked points. One immediate consequence of the definition of the Gromov-weak topology is the following:

**Proposition 2.10.** *Fix  $(S, d, \nu) \in \mathcal{M}$  with  $\nu(S) = 1$ . Let  $x_1, x_2, \dots$  be i.i.d. samples from  $\nu$ . Let  $(S_k, d_k, \nu_k)$  be defined by taking  $S_k = \{x_1, x_2, \dots, x_k\}$  (where the  $x_k$  are i.i.d. from  $\nu$ ), letting  $d_k$  be the restriction of  $d$  to this set, and letting  $\nu_k$  assign mass  $1/k$  to each element of  $S_k$ . Then  $(S_k, d_k, \nu_k)$  converges to  $(S, d, \nu)$  a.s. in the Gromov-weak topology. A similar statement holds for marked spaces. If  $m < k$  and  $(S, d, \nu, x_1, x_2, \dots, x_m) \in \mathcal{M}^m$  then one may choose  $x_{m+1}, x_{m+2}, \dots, x_k$  i.i.d. and consider the discrete metric on  $\{x_1, \dots, x_k\}$  with uniform measure, and  $x_1, \dots, x_m$  marked. Then these approximations converge a.s. to  $(S, d, \nu, x_1, \dots, x_m)$  in the Gromov-weak topology on  $\mathcal{M}^m$ .*

Let  $\mathcal{N}$  be the space of all infinite-by-infinite matrices (entries indexed by  $\mathbf{N} \times \mathbf{N}$ ) with the usual product  $\sigma$ -algebra and let  $\widehat{\mathcal{N}}$  be the subset of  $\mathcal{N}$  consisting of those matrices with the property that for each  $k$ , the initial  $k \times k$  matrix of  $\mathcal{N}$  describes a distance function on  $k$  elements, and the limit of the corresponding  $k$ -element metric spaces (endowed with the uniform probability measure on the  $k$  elements) exists in  $\mathcal{M}$ . We refer to this limit as the *limit space* of the infinite-by-infinite matrix. It is a straightforward exercise to check that  $\widehat{\mathcal{N}}$  is a measurable subset of  $\mathcal{N}$ .

**Proposition 2.11.** *There is a one-to-one correspondence between*

1. *Real-valued  $\mathcal{F}$ -measurable functions  $\phi$  on  $\mathcal{M}$ , and*
2. *Real-valued measurable functions  $\tilde{\phi}$  on  $\widehat{\mathcal{N}}$  with the property that their value depends only on the limit space.*

*The relationship between the functions is the obvious one:*

1. *If we know  $\tilde{\phi}$ , then we define  $\phi$  by setting  $\phi((S, d, \nu))$  to be the a.s. value of  $\tilde{\phi}(M_\infty)$  when  $M_\infty$  is chosen via  $(S, d, \nu)$ .*
2. *If we know  $\phi$ , then  $\tilde{\phi}(M_\infty)$  is  $\phi$  of the limit space of  $M_\infty$ .*

Moreover, for each  $k \in \mathbf{N}$  the analogous correspondence holds with  $(\mathcal{M}^k, \mathcal{F}^k)$  in place of  $(\mathcal{M}, \mathcal{F})$ .

*Proof.* We will prove the result for  $(\mathcal{M}, \mathcal{F})$ ; the case of  $(\mathcal{M}^k, \mathcal{F}^k)$  for general  $k \in \mathbf{N}$  is analogous.

Suppose that  $\tilde{\phi}$  is a bounded, continuous function on  $\mathcal{N}$  which depends only on a finite number of coordinate entries. Then we know that  $(S, d, \nu) \mapsto \mathbf{E}_\nu[\tilde{\phi}(M_\infty)]$  is an  $\mathcal{F}$ -measurable function where  $M_\infty$  is the infinite matrix of distances associated with an i.i.d. sequence  $(x_i)$  chosen from  $\nu$ . It therefore follows that  $(S, d, \nu) \mapsto \mathbf{E}_\nu[\tilde{\phi}(M_\infty)]$  is  $\mathcal{F}$ -measurable for any bounded, measurable function on  $\mathcal{N}$ . In particular, this holds if  $\tilde{\phi}$  is a bounded, measurable function on  $\hat{\mathcal{N}}$  which depends only on the limit space. This proves one part of the correspondence.

On the other hand, suppose that  $\phi$  is an  $\mathcal{F}$ -measurable function of the form  $(S, d, \nu) \mapsto \mathbf{E}_\nu[\psi(M_k)]$  where  $\psi$  is a bounded, continuous function on  $\mathbf{R}^{k^2}$  and  $M_k$  is the matrix of distances associated with  $x_1, \dots, x_k$  chosen i.i.d. from  $\nu$ . Suppose that  $M_\infty \in \hat{\mathcal{N}}$ . For each  $k$ , we let  $(S_k, d_k, \nu_k)$  be the element of  $\mathcal{M}$  which corresponds to the  $k \times k$  submatrix  $M_k$  of  $M_\infty$ . Then the map which associates  $M_\infty$  with  $\phi((S_k, d_k, \nu_k))$  is continuous on  $\hat{\mathcal{N}}$ . Therefore the map which associates  $M_\infty$  with  $\phi((S, d, \nu))$  where  $(S, d, \nu)$  is the limit space of  $M_\infty$  is measurable as it is the limit of continuous maps. This proves the other part of the correspondence.  $\square$

We are now going to use Proposition 2.11 to show that certain subsets of  $\mathcal{M}$  are measurable. We begin by showing that the set of compact metric spaces in  $\mathcal{M}$  is measurable. Throughout, we let  $\hat{\mathcal{C}}$  consist of those elements of  $\hat{\mathcal{N}}$  whose limit space is compact.

**Proposition 2.12.** *The set of compact metric spaces in  $\mathcal{M}$  is measurable. More generally, for each  $k \in \mathbf{N}$  we have that the set of compact metric spaces in  $\mathcal{M}^k$  with  $k$  marked points is measurable.*

*Proof.* We are going to prove the first assertion of the proposition (i.e., the case  $k = 0$ ). The result for general values of  $k$  is analogous.

For each  $\epsilon > 0$  and  $n \in \mathbf{N}$ , we let  $\hat{\mathcal{N}}_{n,\epsilon}$  be those elements  $(d_{ij})$  in  $\hat{\mathcal{N}}$  such that for every  $j$  there exists  $1 \leq k \leq n$  such that  $d_{jk} \leq \epsilon$ . That is,  $(d_{ij})$  is in  $\hat{\mathcal{N}}_{n,\epsilon}$  provided the  $\epsilon$ -balls centered at points in the limit space which correspond to the first  $n$  rows (or columns) in  $(d_{ij})$  cover the entire space. As  $\hat{\mathcal{N}}_{n,\epsilon}$  is measurable, we have that both  $\hat{\mathcal{N}}_\epsilon = \cup_n \hat{\mathcal{N}}_{n,\epsilon}$  and  $\cap_{\epsilon \in \mathbf{Q}_+} \hat{\mathcal{N}}_\epsilon$  are measurable. By Proposition 2.11, it therefore suffices to show that  $\cap_{\epsilon \in \mathbf{Q}_+} \hat{\mathcal{N}}_\epsilon$  is equal to  $\hat{\mathcal{C}}$ .

Suppose that  $(d_{ij}) \in \hat{\mathcal{C}}$ . Fix  $\epsilon > 0$ . As the limit space associated with  $(d_{ij})$  is compact, it follows that there exists  $n \in \mathbf{N}$  such that the union of the  $\epsilon$ -balls centered at the points associated with the first  $n$  columns (or rows) of  $(d_{ij})$  covers the entire space. Therefore  $\hat{\mathcal{C}} \subseteq \cap_{\epsilon \in \mathbf{Q}_+} \hat{\mathcal{N}}_\epsilon$ , so we just need to establish the reverse inclusion. Suppose that  $(d_{ij}) \in \cap_{\epsilon \in \mathbf{Q}_+} \hat{\mathcal{N}}_\epsilon$ . We are going to show that  $(d_{ij}) \in \hat{\mathcal{C}}$  by showing that the limit space of  $(d_{ij})$  is sequentially compact. Suppose that  $(j_k)$  is any sequence in  $\mathbf{N}$ . It suffices to show that there exists a subsequence  $(\tilde{j}_k)$  of  $(j_k)$  such that  $d_{\tilde{j}_k, \tilde{j}_{k+1}} \leq 2^{-k}$  because this implies that the corresponding sequence in the limit space is Cauchy hence convergent

(recall that the limit space is complete). We construct this sequence diagonally from  $(j_k)$  as follows. By assumption, there exists  $n_1$  such that for every  $j$  there exists  $1 \leq k \leq n_1$  such that  $d_{jk} \leq 2^{-2}$ . Therefore there exists  $1 \leq k_1 \leq n_1$  such that  $d_{j_k k_1} \leq 2^{-2}$  for an infinite number of  $k$ . Let  $(j_k^1)$  be the subsequence of  $(j_k)$  with  $d_{j_k^1 k_1} \leq 2^{-2}$  for all  $k$ . Then we note that  $d_{j_k^1 j_\ell^1} \leq 2^{-1}$  for all  $k, \ell$ . Assume that we have defined subsequences  $(j_k^1), \dots, (j_k^m)$  of  $(j_k)$ . By assumption, there exists  $n_{m+1}$  such that for every  $j$  there exists  $1 \leq k \leq n_{m+1}$  such that  $d_{jk} \leq 2^{-m-2}$ . Let  $(j_k^{m+1})$  be a subsequence of  $(j_k^m)$  so that  $d_{j_k^{m+1} k_{m+1}} \leq 2^{-m-2}$  for some  $1 \leq k_{m+1} \leq n_{m+1}$  and all  $k$ . Then we have that  $d_{j_k^{m+1} j_{k+1}^{m+1}} \leq 2^{-m-1}$  for all  $k$ . Passing to a diagonal subsequence of the sequences  $(j_k^m)$  implies the result.  $\square$

To prove the measurability of certain sets in  $\mathcal{M}$ , we will find it useful first to show that they are measurable with respect to the Gromov-Hausdorff topology and then use that there is a natural map from  $\widehat{\mathcal{C}}$  into the Gromov-Hausdorff space which is measurable. In order to remind the reader of the Gromov-Hausdorff distance, we first need to remind the reader of the definition of the Hausdorff distance. Suppose that  $K_1, K_2$  are closed subsets of a metric space  $(S, d)$ . For each  $\epsilon > 0$ , we let  $K_j^\epsilon$  be the  $\epsilon$ -neighborhood of  $K_j$ . Recall that the **Hausdorff distance** between  $K_1, K_2$  is given by

$$d_H(K_1, K_2) = \inf\{\epsilon > 0 : K_1 \subseteq K_2^\epsilon, K_2 \subseteq K_1^\epsilon\}. \quad (2.2)$$

Suppose that  $(S_1, d_1), (S_2, d_2)$  are compact metric spaces. The **Gromov-Hausdorff distance** between  $(S_1, d_1)$  and  $(S_2, d_2)$  is given by

$$d_{GH}((S_1, d_1), (S_2, d_2)) = \inf \{d_H(\varphi_1(S_1), \varphi_2(S_2))\} \quad (2.3)$$

where the infimum is over all metric spaces  $(S, d)$  and isometries  $\varphi_j : S_j \rightarrow S$ . We let  $\mathcal{X}$  be the set of all compact metric spaces equipped with the Gromov-Hausdorff distance  $d_{GH}$ . More generally, for each  $k \in \mathbf{N}$ , we let  $\mathcal{X}^k$  be the set of all compact metric spaces  $(S, d)$  marked with  $k$  points  $x_1, \dots, x_k \in S$ . We equip  $\mathcal{X}^k$  with the distance function

$$\begin{aligned} & d_{GH}((S_1, d_1, x_{1,1}, \dots, x_{1,k}), (S_2, d_2, x_{2,1}, \dots, x_{2,k})) \\ &= \inf \left\{ d_H(\varphi_1(S_1), \varphi_2(S_2)) + \sum_{j=1}^k d(\varphi_1(x_{1,j}), \varphi_2(x_{2,j})) \right\}. \end{aligned} \quad (2.4)$$

where the infimum is as in (2.3). We refer the reader to [Vil09, Chapter 27] as well as [BBI01, Chapter 7] for more on the Hausdorff and Gromov-Hausdorff distances.

We remark that in (2.3), one may always take the ambient metric space to be  $\ell_\infty$ . Indeed, this follows because every compact metric space can be isometrically embedded into  $\ell_\infty$ . We will use this fact several times in what follows.

We also note that there is a natural projection  $\pi : \widehat{\mathcal{C}} \rightarrow \mathcal{X}$ . Moreover, if we equip  $\widehat{\mathcal{N}}$  with the  $\ell_\infty$  topology (in place of the product topology), then the projection  $\pi : \widehat{\mathcal{C}} \rightarrow \mathcal{X}$  is

continuous. Indeed, this can be seen by using the representation of  $d_{\text{GH}}$  in terms of the distortion of a so-called correspondence between metric spaces; see [Vil09, Chapter 27]. Since the product topology generates the same  $\sigma$ -algebra as the  $\ell_\infty$  topology on  $\widehat{\mathcal{N}}$ , it follows that  $\pi$  is measurable. This observation will be useful for us for proving that certain sets in  $\widehat{\mathcal{N}}$  are measurable. We record this fact in the follow proposition.

**Proposition 2.13.** *The projection  $\pi: \widehat{\mathcal{C}} \rightarrow \mathcal{X}$  is measurable.*

In the following proposition, we will combine Proposition 2.11 and Proposition 2.13 to show that the set of compact, geodesic metric spaces in  $\mathcal{M}$  is measurable.

**Proposition 2.14.** *The set of compact, geodesic spaces is measurable in  $\mathcal{M}$ .*

*Proof.* That the set of geodesic spaces is closed hence measurable in  $\mathcal{X}$  follows from [Vil09, Theorem 27.9]; see also the discussion in [BBI01, Chapter 7.5]. Therefore the result follows by combining Proposition 2.11 and Proposition 2.13.  $\square$

We note that it is also possible to give a short proof of Proposition 2.14 which does not rely on the measurability of the projection  $\pi: \widehat{\mathcal{C}} \rightarrow \mathcal{X}$ . The following proposition will imply that the set of good measure endowed geodesic spheres is measurable in  $\mathcal{M}$ .

**Proposition 2.15.** *For each  $k \in \mathbf{N}$  we have that  $\mathcal{M}_{\text{SPH}}^k$  is measurable in  $\mathcal{M}^k$ .*

We will prove Proposition 2.15 result in the case that  $k = 0$  (i.e., we do not have any extra marked points). The proof for general values of  $k$  is analogous. As in the proof of Proposition 2.14, it suffices to show that the set of geodesic metric spaces  $(S, d)$  which are homeomorphic to  $\mathbf{S}^2$  is measurable in  $\mathcal{X}$ . In order to prove this, we first need to prove the following lemma.

**Lemma 2.16.** *Suppose that  $(S, d)$  is a geodesic metric space homeomorphic to  $\mathbf{S}^2$  and suppose that  $\gamma$  is a non-space-filling curve on  $S$ . Let  $U$  be a connected component of  $S \setminus \gamma$  and let  $A = S \setminus U$ . For every  $\epsilon > 0$ ,  $\gamma$  is homotopic to a point inside of the  $\epsilon$ -neighborhood of  $A$ .*

*Proof.* Since  $\gamma$  is a continuous curve, it follows that  $U$  is topologically equivalent to  $\mathbf{D}$ . Let  $\varphi: \mathbf{D} \rightarrow U$  be a homeomorphism. Then there exists  $\delta > 0$  so that  $\Gamma = \varphi(\partial(1 - \delta)\mathbf{D})$  is contained in the  $\epsilon$ -neighborhood of  $A$ . Since  $\Gamma$  is a simple curve, it follows that there exists a homeomorphism  $\psi$  from  $\mathbf{D}$  to the component  $V$  of  $S \setminus \Gamma$  which contains  $\gamma$ . Let  $\tilde{\gamma} = \psi^{-1}(\gamma)$ . Then  $\tilde{\gamma}$  is clearly homotopic to 0 in  $\mathbf{D}$  hence  $\gamma$  is homotopic to  $\psi(0)$  in  $V$ , which implies the result.  $\square$

*Proof of Proposition 2.15.* We are going to prove the result by showing that the set  $\mathcal{Y}$  of geodesic metric spaces in  $\mathcal{X}$  which are homeomorphic to  $\mathbf{S}^2$  is measurable in  $\mathcal{X}$ . The result will then follow by invoking Proposition 2.11 and Proposition 2.13.

Let  $\bar{\mathcal{Y}}$  be the closure of  $\mathcal{Y}$  in  $\mathcal{X}$ . Suppose that  $(S, d)$  is in  $\mathcal{X}$ . Let  $\gamma$  be a path in  $(S, d)$  and let  $f(\gamma, (S, d))$  be the infimum of  $\text{diam}(A)$  over all  $A \subseteq S$  in which  $\gamma$  is homotopic in  $A$  to a point in  $S$  and  $S \setminus A$  is connected. Let  $f(\delta, (S, d))$  be equal to the supremum of  $f(\gamma, (S, d))$  over all paths  $\gamma$  in  $(S, d)$  with diameter at most  $\delta$ . Let  $\tilde{\mathcal{Y}}$  consist of those  $(S, d)$  in  $\mathcal{Y}$  such that for every  $\epsilon > 0$  there exists  $\delta > 0$  such that  $f(\delta, (S, d)) < \epsilon$ .

We are first going to show that  $\tilde{\mathcal{Y}} = \mathcal{Y}$ . We clearly have that  $\mathcal{Y} \subseteq \tilde{\mathcal{Y}}$ , so we just need to show that  $\tilde{\mathcal{Y}} \subseteq \mathcal{Y}$ . Suppose that  $(S, d)$  is in  $\tilde{\mathcal{Y}}$ . We assume without loss of generality that  $\text{diam}(S) = 1$ . Then there exists a sequence  $(S_n, d_n)$  in  $\mathcal{Y}$  which converges to  $(S, d)$  in  $\mathcal{X}$ . We note that we may assume without loss of generality that both  $S$  and the  $S_n$ 's are subsets of  $\ell_\infty$  such that  $d_H(S_n, S) \rightarrow 0$  as  $n \rightarrow \infty$  and that  $\text{diam}(S_n) = 1$  for all  $n$ .

Fix  $\epsilon > 0$ . It suffices to show that there exists  $\delta > 0$  such that  $f(\delta, (S_n, d_n)) < \epsilon$  for all  $n \in \mathbf{N}$ . Indeed, this implies that the  $(S_n, d_n)$  converge to  $(S, d)$  in  $\mathcal{X}$  *regularly* which, by [Beg44], implies that  $(S, d)$  is in  $\mathcal{Y}$ .

Fix  $\delta > 0$  such that  $f(\delta, (S, d)) < \epsilon$ . We assume that  $n_0 \in \mathbf{N}$  is sufficiently large so that

$$d_H(S_n, S) \leq \frac{\delta}{16} \quad \text{for all } n \geq n_0. \quad (2.5)$$

We note that for each  $1 \leq n \leq n_0$  there exists  $\delta_n > 0$  such that  $f(\delta_n, (S_n, d_n)) < \epsilon$ . We set  $\delta_0 = \min_{1 \leq n \leq n_0} \delta_n$ . We are now going to show that there exists  $\hat{\delta} > 0$  such that  $f(\hat{\delta}, (S_n, d_n)) < \epsilon$  for all  $n \geq n_0$ . Upon showing this, we will have that with  $\tilde{\delta} = \delta_0 \wedge \hat{\delta}$  we have  $f(\tilde{\delta}, (S_n, d_n)) < \epsilon$  for all  $n$ .

Fix  $n \geq n_0$  and suppose that  $\gamma_n: \mathbf{S}^1 \rightarrow S_n$  is a path in  $S_n$  with  $\text{diam}(\gamma_n) \leq \delta/4$ . Then we can construct a path  $\gamma$  in  $S$  as follows. We pick times  $0 \leq t_0^n < \dots < t_j^n \leq 2\pi$  such that with  $x_i^n = \gamma_n(t_i^n)$  we have

$$\|x_{i-1}^n - x_i^n\|_{\ell_\infty} \leq \frac{\delta}{16} \quad \text{for all } 1 \leq i \leq j. \quad (2.6)$$

By (2.5), for each  $1 \leq i \leq j$  there exists  $x_i \in S \subseteq \ell_\infty$  such that  $\|x_i^n - x_i\|_{\ell_\infty} \leq \delta/16$ . We then take  $\gamma$  to be the path  $\mathbf{S}^1 \rightarrow S$  which is given by successively concatenating geodesics from  $x_{i-1}$  to  $x_i$  for each  $1 \leq i \leq j+1$  where we take  $x_{j+1} = x_0$ . Suppose that  $a, b \in \gamma$ . Then there exists  $i_q$  such that  $\|q - x_{i_q}\|_{\ell_\infty} \leq 3\delta/16$  for  $q \in \{a, b\}$  as  $\|x_{i-1} - x_i\|_{\ell_\infty} \leq 3\delta/16$  for each  $1 \leq i \leq j+1$ . Consequently, by (2.5) and (2.6) we have that

$$\begin{aligned} \|a - b\|_{\ell_\infty} &\leq \|a - x_{i_a}\|_{\ell_\infty} + \|x_{i_a} - x_{i_b}\|_{\ell_\infty} + \|x_{i_b} - b\|_{\ell_\infty} \\ &\leq \frac{3}{8}\delta + \|x_{i_a} - x_{i_a}^n\|_{\ell_\infty} + \|x_{i_a}^n - x_{i_b}^n\|_{\ell_\infty} + \|x_{i_b}^n - x_{i_b}\|_{\ell_\infty} \end{aligned}$$

$$\leq \frac{9}{16}\delta + \text{diam}(\gamma^n) < \delta.$$

This implies that  $\text{diam}(\gamma) < \delta$ . Moreover, we have that the  $d_H$ -distance between the ranges of  $\gamma^n$  and  $\gamma$  is at most  $\delta/2$ .

By assumption, we can contract  $\gamma$  to a point in  $S$  inside of a set  $A \subseteq S$  of diameter at most  $\epsilon$  such that  $B = S \setminus A$  is connected. Pick  $x \in B$ . Since

$$1 = \text{diam}(S) \leq \text{diam}(A) + \text{diam}(B) \leq \epsilon + \text{diam}(B)$$

we have that  $\text{diam}(B) \geq 1 - \epsilon$ .

Fix  $x_n \in S_n$  with  $\|x - x_n\|_{\ell_\infty} \leq \delta/16$ . We claim that the component  $B_n$  of  $S_n \setminus \gamma_n$  containing  $x_n$  has diameter at least  $1 - \epsilon - \delta$ . Indeed, suppose that  $u, v \in S$  are such that there exists a path  $\eta$  connecting  $u, v$  which has distance at least  $\delta/2$  from  $\gamma$ . Arguing as above, we can find a path  $\eta_n$  in  $S_n$  whose range has Hausdorff distance at most  $\delta/2$  from the range of  $\eta$  so that the range of  $\eta_n$  is disjoint from the range of  $\gamma_n$ . This proves the claim.

Thus as  $\text{diam}(S_n) = 1$ , with  $A_n = S_n \setminus B_n$  we have that  $A_n$  is contained in the  $(\epsilon + \delta)$ -neighborhood of  $B_n$ . Moreover, we have that  $\text{diam}(\partial B_n) \leq \text{diam}(\gamma_n) \leq \delta/2$ . Therefore

$$\text{diam}(A_n) \leq \text{diam}(\partial B_n) + (\epsilon + \delta) \leq \epsilon + \frac{3\delta}{2}.$$

Therefore  $f(\delta, (S_n, d_n)) \leq \epsilon + \frac{3\delta}{2}$  for all  $n \geq n_0$ . This finishes the proof that  $\mathcal{Y} = \tilde{\mathcal{Y}}$ .

To finish proving the result, we will show that  $\tilde{\mathcal{Y}}$  (hence  $\mathcal{Y}$ ) can be written as an intersection of sets which are relatively open in the closure of geodesic spheres in  $\mathcal{X}$ , hence is measurable. It follows from the argument given just above that, for each fixed  $\delta > 0$ , the map  $(S, d) \mapsto f(\delta, (S, d))$  is uniformly continuous on  $\mathcal{Y}$ . This implies that  $(S, d) \mapsto f(\delta, (S, d))$  extends to a continuous map on  $\bar{\mathcal{Y}}$ . It therefore follows that, for each  $\epsilon > 0$ , we have that

$$\bar{\mathcal{Y}}_{\epsilon, \delta} = \{(S, d) \in \bar{\mathcal{Y}} : f(\delta, (S, d)) < \epsilon\}$$

is relatively open in  $\bar{\mathcal{Y}}$ . Therefore with  $\mathbf{Q}_+ = \mathbf{Q} \cap (0, \infty)$  we have that

$$\bigcap_{\epsilon \in \mathbf{Q}_+} \bigcup_{\delta \in \mathbf{Q}_+} \bar{\mathcal{Y}}_{\epsilon, \delta}$$

is a Borel set in  $\mathcal{X}$ . The result follows since this set is equal to  $\tilde{\mathcal{Y}}$ .  $\square$

**Proposition 2.17.** *Fix a constant  $r > 0$  and let  $\mathcal{M}_{\text{SPH}, r}^2$  be the set of elements  $(S, d, \nu, x, y) \in \mathcal{M}_{\text{SPH}}^2$  such that  $R = d(x, y) - r > 0$  (and note that this is a measurable subset of  $\mathcal{M}_{\text{SPH}}^2$ ). Then the space which corresponds to  $B^\bullet(x, R)$  (with its internal metric) is in  $\mathcal{M}^1$ . The function  $\mathcal{M}_{\text{SPH}, r}^2 \rightarrow \mathcal{M}^1$  given by associating  $(S, d, \nu, x, y)$*

to this space is measurable. Moreover, if we have a measurable way of choosing  $z_1, z_2, \dots, z_k \in \partial B^\bullet(x, R)$  and an orientation of  $\partial B^\bullet(x, R)$  that only requires us to look at  $S \setminus B^\bullet(x, R)$ , then the map to the set of  $k$  slices (i.e., the metric measure spaces which correspond to the regions between the leftmost geodesics from each  $z_j$  to  $x$ ) is measurable as a map  $\mathcal{M}_{\text{SPH}, r}^2 \rightarrow (\mathcal{M}^3)^k$ . (The three marked points in the  $j$ th slice are given by  $z_j$ ,  $z_{j+1}$ , and the point where the leftmost geodesics from  $z_j$  and  $z_{j+1}$  to  $x$  first meet.)

One example of a function which associates  $S \setminus B^\bullet(x, R)$  with points  $z_1, \dots, z_k$  is as follows. Assume that we have a measurable way of measuring “boundary length” on  $\partial B^\bullet(x, R)$ . Then we take  $z_1, \dots, z_k \in \partial B^\bullet(x, R)$  to be equally spaced points according to boundary length with  $z_1$  given by the point on  $B^\bullet(x, R)$  which is first visited by the leftmost geodesic from  $z$  to  $x$  (relative to  $y$ ).

*Proof of Proposition 2.17.* That the space which corresponds to  $B^\bullet(x, R)$  is an element of  $\mathcal{M}^1$  is obvious.

We are now going to argue that the map which associates  $(S, d, \nu, x, y) \in \mathcal{M}_r^2$  with the metric measure space associated with  $B^\bullet(x, R)$  is measurable. To see this, we note that a point  $w$  is in  $S \setminus B^\bullet(x, R)$  if and only if there exists  $\epsilon > 0$  and points  $y_1, \dots, y_\ell \in S$  such that the following hold:

1.  $d(y_j, x) \geq R + \epsilon$  for each  $1 \leq j \leq \ell$ ,
2.  $y \in B(y_1, \epsilon)$  and  $w \in B(y_\ell, \epsilon)$ , and
3.  $B(y_j, \epsilon)$  has non-empty intersection with both  $B(y_{j-1}, \epsilon)$  and  $B(y_{j+1}, \epsilon)$  for each  $2 \leq j \leq \ell - 1$ .

Suppose that  $x_1 = x$ ,  $x_2 = y$ , and  $x_3, x_4, \dots$  is an i.i.d. sequence chosen from  $\nu$  and suppose that  $d_{ij} = d(x_i, x_j)$ . The above tells us how to determine those indices  $j$  such that  $x_j \in S \setminus B^\bullet(x, R)$ . In particular, it is clear from the above that the event that  $x_i \in B^\bullet(x, R)$  is a measurable function of  $(d_{ij})$  viewed as an element of  $\widehat{\mathcal{N}}$ . Suppose that we are on the event that  $x_i, x_j \in B^\bullet(x, R)$  for  $i, j$  distinct. Then the event that  $d_{ij} < \delta$  is equivalent to the event that there exists  $\epsilon > 0$  and indices  $j_1 = i, j_2, \dots, j_{k-1}, j_k = j$  such that  $d_{j_\ell j_{\ell+1}} < \epsilon$  for each  $1 \leq \ell \leq k - 1$ ,  $(k - 1)\epsilon < \delta$ , and  $x_{j_\ell} \in B^\bullet(x, R)$  for each  $1 \leq \ell \leq k$  (which we can determine using the recipe above). Thus it is easy to see that the element of  $\widehat{\mathcal{N}}$  which corresponds to the matrix of distances between the  $(x_i)$  which are in  $B^\bullet(x, R)$  with the internal metric is measurable. Thus the measurability of the metric measure space corresponding  $B^\bullet(x, R)$  viewed as an element of  $\mathcal{M}^1$  follows by applying Proposition 2.11.

To see the final claim of the proposition, we note that we can tell that a point  $w$  is in one of the geodesic slices if and only if there exists  $\epsilon > 0$  and points  $y_1, \dots, y_\ell$  with  $d(y_j, x) \leq R$  such that

1.  $B(y_1, \epsilon)$  has non-empty intersection with  $\partial B^\bullet(x, R)$ ,
2.  $B(y_j, \epsilon)$  has non-empty intersection with  $B(y_{j-1}, \epsilon)$  and  $B(y_{j+1}, \epsilon)$  for each  $2 \leq j \leq \ell - 1$
3. No geodesic from  $z_{i+1}$  to  $x$  passes through the  $\overline{B(y_j, \epsilon)}$
4. No geodesic from a point on  $\partial B^\bullet(x, R)$  which is infinitesimally to the left of  $z_i$  to  $x$  passes through the  $B(y_j, \epsilon)$ .

The third property holds if and only if

$$\min_{1 \leq j \leq k} \inf \{d(x, y) + d(y, z_{i+1}) : y \in B(y_j, \epsilon)\} > d(x, z_{i+1}).$$

The last property can be checked in an analogous way, so the result thus follows in view of Proposition 2.11 and the argument described in the previous paragraph.  $\square$

**Proposition 2.18.** *Let  $\psi$  be the map that sends an element  $(S, d, \nu, x, y)$  of  $\mathcal{M}_{\text{SPH}}^2$  to the element of  $\mathcal{X}^2$  that represents the metric net from  $x$  to  $y$ . Then  $\psi$  is a measurable map from  $\mathcal{M}_{\text{SPH}}^2$  to  $\mathcal{X}^2$ .*

*Proof.* We are going to prove the result by showing that the map from the set of doubly marked geodesic spheres in  $\mathcal{X}^2$  to itself which associates  $(S, d, x, y)$  with the metric net from  $x$  to  $y$  is continuous. This, in turn, implies the result by combining with Proposition 2.11 and Proposition 2.13.

Fix  $\epsilon > 0$  and suppose for  $i = 1, 2$  that  $(S_i, d_i, x_i, y_i)$  is an element of  $\mathcal{X}^2$  which is a geodesic sphere and that the  $d_{\text{GH}}$ -distance between the two spaces is at most  $\epsilon/2$ . Then we may assume without loss of generality that  $(S_1, d_1)$  and  $(S_2, d_2)$  are isometrically embedded into  $\ell_\infty$  such that  $d_{\text{H}}(S_1, S_2) < \epsilon$ ,  $\|x_1 - x_2\|_{\ell_\infty} < \epsilon$ , and  $\|y_1 - y_2\|_{\ell_\infty} < \epsilon$ . For each  $r > 0$  and  $i = 1, 2$  we let  $U_{i,r}$  be the component of  $S_i \setminus B(x_i, r)$  which contains  $y_i$ . We are going to show that for each  $2\epsilon < r < d(x, y) - 2\epsilon$  we have that  $\partial U_{1,r}$  is contained in the  $7\epsilon$ -neighborhood of  $\partial U_{2,r-2\epsilon}$  and vice-versa. This, in turn, implies that the  $d_{\text{H}}$ -distance of the metric net in  $(S_1, d_1)$  from  $x_1$  to  $y_1$  from the metric net in  $(S_2, d_2)$  from  $x_2$  to  $y_2$  is at most  $7\epsilon$ , so the same is also true for the  $d_{\text{GH}}$ -distance.

Fix  $2\epsilon < r < d(x_1, y_1) - 2\epsilon$  and suppose that  $v_1 \in \partial U_{1,r}$ . Then there exists  $u_1 \in U_{1,r}$  with  $d_1(u_1, v_1) < \epsilon$ . Let  $\gamma_1$  be a path in  $U_{1,r}$  connecting  $u_1$  and  $y_1$ . Arguing as in the proof of Proposition 2.15, there exists a path  $\gamma_2$  in  $S_2$  terminating at  $y_2$  such that the  $d_{\text{H}}$ -distance between the range of  $\gamma_1$  and  $\gamma_2$  (viewed as paths in  $\ell_\infty$ ) is at most  $\epsilon$  and  $\|u_1 - u_2\|_{\ell_\infty} < \epsilon$  where  $u_2 = \gamma_2(0)$ . In particular, the distance between any point on  $\gamma_2$  and  $x_2$  is at least  $r - 2\epsilon$ . It thus follows that  $\gamma_2$  is in  $U_{2,r-2\epsilon}$ . In particular,  $u_2 \in U_{2,r-2\epsilon}$ . Moreover,

$$d_2(x_2, u_2) \leq \|x_2 - x_1\|_{\ell_\infty} + \|x_1 - v_1\|_{\ell_\infty} + \|v_1 - u_1\|_{\ell_\infty} + \|u_1 - u_2\|_{\ell_\infty} \leq r + 3\epsilon.$$

Therefore  $u_2$  is in the  $5\epsilon$ -neighborhood of  $\partial U_{2,r-2\epsilon}$ . Thus since

$$\|v_1 - u_2\|_{\ell_\infty} \leq \|v_1 - u_1\|_{\ell_\infty} + \|u_1 - u_2\|_{\ell_\infty} < 2\epsilon$$

we have that  $v_1$  is in the  $7\epsilon$ -neighborhood of  $\partial U_{2,r-2\epsilon}$ , as desired.  $\square$

### 3 Tree gluing and the Lévy net

Section 3.1 and Section 3.2 briefly recall two tree-mating constructions developed in [DMS14], one involving a pair of continuum random trees, and the other involving a pair of  $\alpha$ -stable looptrees. These sections provide some motivation and context for Section 3.3, which describes how to construct the  $\alpha$ -Lévy net by gluing an  $\alpha$ -stable looptree to itself (equivalently, by gluing an  $\alpha$ -stable looptree to a certain related real tree derived from the  $\alpha$ -stable looptree — the geodesic tree of the Lévy net). We then give a similar but related construction in Section 3.4. Next, we give a review of continuous state branching processes in Section 3.5, then give a breadth-first construction of the Lévy net in Section 3.6, and finally prove the topological equivalence of the Lévy net constructions in Section 3.7. We end this section by showing in Section 3.8 that the embedding of the Lévy net into  $\mathbf{S}^2$  is determined up to homeomorphism by the geodesic tree and its associated equivalence relation in the Lévy net.

#### 3.1 Gluing together pair of continuum random trees

There are various ways to “glue together” two continuum trees to produce a sphere decorated by a space-filling path (describing the “interface” between the two trees). One approach, which is explained in [DMS14, Section 1.1], is the following: let  $X_t$  and  $Y_t$  be independent Brownian excursions, both indexed by  $t \in [0, T]$ . Thus  $X_0 = X_T = 0$  and  $X_t > 0$  for  $t \in (0, T)$  (and similarly for  $Y_t$ ). Once  $X_t$  and  $Y_t$  are chosen, choose  $C$  large enough so that the graphs of  $X_t$  and  $C - Y_t$  do not intersect. (The precise value of  $C$  does not matter.) Write  $R = [0, T] \times [0, C]$ , viewed as a Euclidean metric space.

Let  $\cong$  denote the smallest equivalence relation on  $R$  that makes two points equivalent if they lie on the same vertical line segment with endpoints on the graphs of  $X_t$  and  $C - Y_t$ , or they lie on the same horizontal line segment that never goes above the graph of  $X_t$  (or never goes below the graph of  $C - Y_t$ ). Maximal segments of this type are shown in Figure 3.1. As explained in [DMS14, Section 1.1], if one begins with the Euclidean rectangle and then takes the topological quotient w.r.t. this equivalence relation, one obtains a topological sphere, and the path obtained by going through the vertical lines in left-to-right order is a continuous space-filling path on the sphere, which intuitively describes the “interface” between the two identified trees. In fact, this remains true more generally when  $X_t$  and  $Y_t$  are not independent, and the pair  $(X_t, Y_t)$  is instead an excursion of a correlated two dimensional Brownian motion into the positive quadrant (starting and ending at the origin), as explained in detail in [DMS14, MS15a].

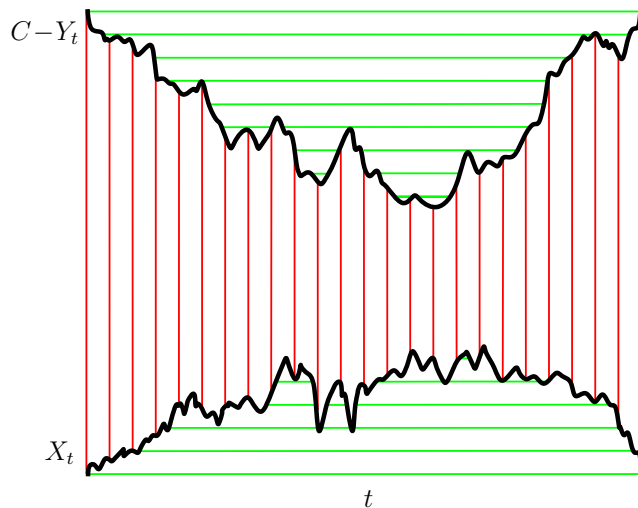


Figure 3.1: *Gluing continuum random trees to each other.* Here  $X_t$  and  $Y_t$  are Brownian excursions and  $C$  is a constant chosen so that the two graphs shown do not intersect. Points on the same vertical (or horizontal) line segment are declared to be equivalent. The space of equivalence classes (endowed with the quotient topology) can be shown to be homeomorphic to the sphere [DMS14, Section 1.1].

### 3.2 Gluing together pair of stable looptrees

Also discussed in [DMS14, Section 1.3] is a method of obtaining a sphere by gluing together two stable looptrees (with the disk in the interior of each loop included), as illustrated in Figure 3.3. In the setting discussed there, each of the grey disks surrounded by a loop is given a conformal structure (that of a “quantum disk”), and this is shown to determine a conformal structure of the sphere obtained by gluing the trees together; given this structure, the interface between the trees in Figure 3.3 is shown to be an  $\text{SLE}_{\kappa'}$  process for  $\kappa' = 16/\gamma^2 \in (4, 8)$ . In a closely related construction, the interface between the trees in Figure 3.1 is shown to be a space-filling form of  $\text{SLE}_{\kappa'}$  in which the path “goes inside and fills up” each loop after it is created. As explained in [DMS14], one obtains a range different values of  $\kappa'$  by taking the trees to be correlated with each other and varying the correlation coefficient.

### 3.3 Gluing stable looptree to itself to obtain the Lévy net

Figure 3.4 illustrates a procedure for generating a sphere from a single stable looptree, which in turn is generated from the time-reversal of a Lévy excursion with only upward jumps. Precisely, Proposition 3.3 below will show that the topological quotient of the rectangle, w.r.t. the equivalence relation illustrated, actually is a.s. homeomorphic to the sphere. The process  $Y_t$  illustrated there is sometimes known as the *height process*

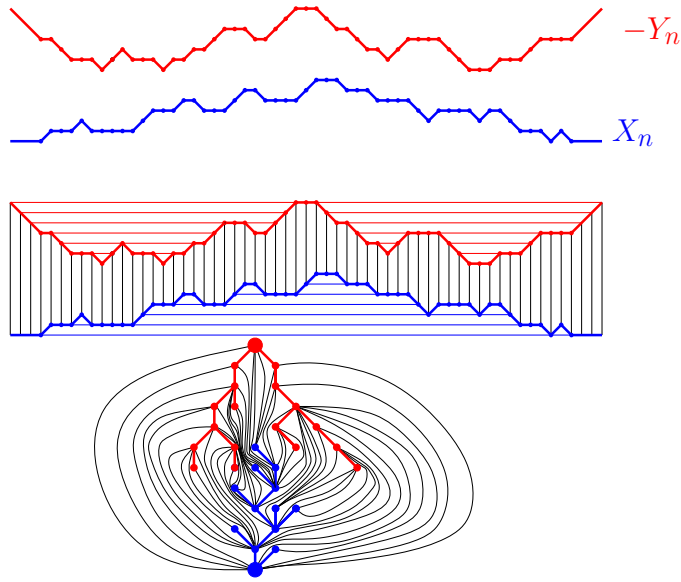


Figure 3.2: *Gluing discrete trees to each other.* There is a standard discrete analog of the construction shown in Figure 3.1 that produces a planar triangulation (with distinguished tree and dual tree) from a finite walk  $(X_n, Y_n)$  in  $\mathbf{Z}_+^2$  that starts and ends at  $(0, 0)$ . The bottom figure is obtained by collapsing the horizontal red and blue lines to produce two trees, connected to each other by black edges. See [Mul67, Ber07, She11] for details.

of the  $\alpha$ -stable process  $X_t$  (or, more precisely, its time reversal). The fact that this  $Y_t$  is well defined and a.s. has a continuous modification (along with Hölder continuity and the exact Hölder exponent) is established for example in [DLG05, Theorems 1.4.3 and 1.4.4] (see also [LGLJ98]).

In this construction the upper tree in the figure is not independent of the lower tree (with holes); in fact, it is strictly determined by the Lévy excursion below, as explained in the figure caption. Note that every jump in the Lévy excursion (corresponding to a bubble) comes with a “height” which is encoded in the upper tree. If one removes from the constructed sphere the grey interiors of the disks shown, one obtains a closed subset of the sphere; this set, together with its topological structure, can also be obtained directly without reference to the sphere (simply take the quotient topology on the set of equivalence classes in the complement of the grey regions in Figure 3.4). It is important to note that after a given time  $t$ , the set of *record infima* achieved after time  $t$  looks locally like the range of a stable subordinator with index  $\alpha - 1$  [Ber96, Chapter VIII, Lemma 1], and that in particular it a.s. has a well-defined Minkowski measure [FT83], which also corresponds to the time parameter of the stable subordinator.<sup>6</sup>

<sup>6</sup>For an  $\alpha$ -stable process with no *negative* jumps ( $\beta = 1$  in language of [Ber96]) the statement in [Ber96, Chapter VIII, Lemma 1] is that the set of *record maxima* (the range of the so-called “ladder

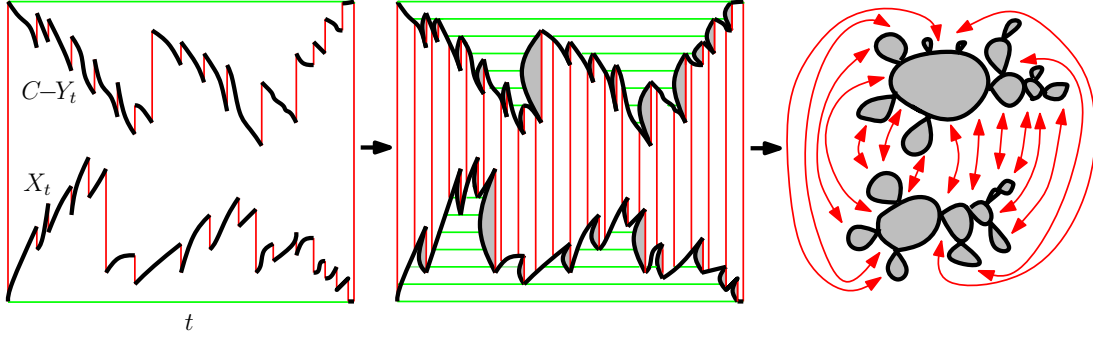


Figure 3.3: *Gluing stable looptrees to each other.* **Left:**  $X_t$  and  $Y_t$  are i.i.d. Lévy excursions, each with only negative jumps. Graphs of  $X_t$  and  $C - Y_t$  are sketched; red segments indicate jumps. **Middle:** Add a black curve to the left of each jump, connecting its two endpoints; the precise form of the curve does not matter (as we care only about topology for now) but we insist that it intersect each horizontal line at most once and stay below the graph of  $X_t$  (or above the graph of  $C - Y_t$ ) except at its endpoints. We also draw the vertical segments that connect one graph to another, as in Figure 3.1, declaring two points equivalent if they lie on the same such segment (or on the same jump segment). Shaded regions (one for each jump) are topological disks. **Right:** By collapsing green segments and red jump segments, one obtains two trees of disks with outer boundaries identified.

**Proposition 3.1.** *It is a.s. the case that there exists no time  $t$  such that the height process  $Y_t$  has a decrease time—i.e., a time  $t_0$  and  $h > 0$  such that  $Y_s \geq Y_{t_0}$  for all  $s \in (t_0 - h, t_0)$  and  $Y_s \leq Y_{t_0}$  for  $s \in (t_0, t_0 + h)$ .*

*Proof.* See Figure 3.5 for an illustration and additional explanation of the proof. This amounts to saying that there is no point from which there are simultaneously two distinct paths in the geodesic tree and two distinct paths in the dual tree; if there were, then all geodesics in between the dual paths would have to merge into this point, and hence one would not have geodesic uniqueness for a positive measure of points. This is a contradiction in view of Lemma 3.18 (stated and proved below).  $\square$

**Proposition 3.2.** *It is a.s. the case that  $Y_t$  has countably many local maxima, and each of these local maxima occurs at a distinct height (and hence in particular each local maximum is isolated).*

---

height” process) has the law of the range of a stable subordinator of index  $\alpha\rho$  where

$$\rho = \frac{1}{2} + (\pi\alpha)^{-1} \arctan(\tan(\pi\alpha/2)) = \frac{1}{2} + (\pi\alpha)^{-1}(\pi\alpha/2 - \pi) = 1 - 1/\alpha.$$

(Recall that for  $x \in (\pi/2, \pi)$  we have  $\arctan(\tan(x)) = x - \pi$ .) Thus in this case the index of the stable subordinator is  $\alpha\rho = \alpha - 1$ . This value varies between 0 and 1 as  $\alpha$  varies between 1 and 2. The dimension of the range is given by the index  $\alpha - 1$  (a special case of [Ber96, Chapter III, Theorem 15].

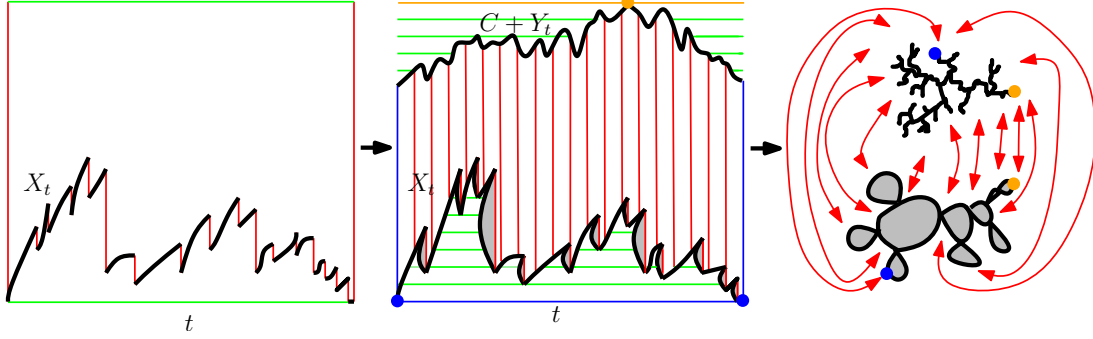


Figure 3.4: *Gluing a stable looptree to itself.* **Left:**  $X_t$  is the time-reversal of an  $\alpha$ -stable Lévy excursion with only positive jumps. **Middle:** Extra arcs are added to the lower graph as in Figure 3.3.  $Y_t$  is the Minkowski measure of the set of record infimum values obtained by  $X|_{[t,T]}$ . (This quantity corresponds to a “distance” to the dual root, in the sense of [DLG02].) Red and green lines indicate equivalences. Note that whenever the lower endpoints of two vertical red segments are connected to one another by a green segment, it must be the case that the upper endpoints have the same height (which may be hard to recognize from this hand-drawn figure). **Right:** Once the green lines are collapsed, one has a tree and a tree of loops (which we will refer to as either the dual tree or looptree). The tree above is the geodesic tree. The orange dot is the root of that tree. The blue dot is a “dual root” (a second marked point). The horizontal green lines above the graph of  $Y_t$  “wrap around” from one side of the rectangle to the other; these lines correspond to the points on the geodesic tree arc from the orange dot to the blue dot.

*Proof.* This is established in the first assertion in the proof of [DLG05, Theorem 4.4] See also [DLG02, Lemma 2.5.3] for a related result.  $\square$

**Proposition 3.3.** *The quotient of the rectangle shown in Figure 3.4, w.r.t. the equivalence relation induced by the horizontal and vertical lines as illustrated, is topologically equivalent to  $\mathbf{S}^2$ .*

We will prove Proposition 3.3 using Moore’s theorem [Moo25], which for the convenience of the reader we restate here. Recall that an equivalence relation  $\cong$  on  $\mathbf{S}^2$  is said to be *topologically closed* if and only if whenever  $(x_n)$  and  $(y_n)$  are two sequences in  $\mathbf{S}^2$  with  $x_n \cong y_n$  for all  $n$ ,  $x_n \rightarrow x$  and  $y_n \rightarrow y$  as  $n \rightarrow \infty$ , then  $x \cong y$ . Equivalently,  $\cong$  is topologically closed if the graph  $\{(x, y) : x \cong y\}$  is closed as a subset of  $\mathbf{S}^2 \times \mathbf{S}^2$ . The *topological closure* of a relation  $\cong$  is the relation whose graph is the closure of the graph of  $\cong$ . (Note that it is not true in general that the topological closure of an equivalence relation is an equivalence relation.) The following statement of Moore’s theorem is taken from [Mil04].

**Proposition 3.4.** *Let  $\cong$  be any topologically closed equivalence relation on  $\mathbf{S}^2$ . Assume that each equivalence class is connected and not equal to all of  $\mathbf{S}^2$ . Then the quotient*

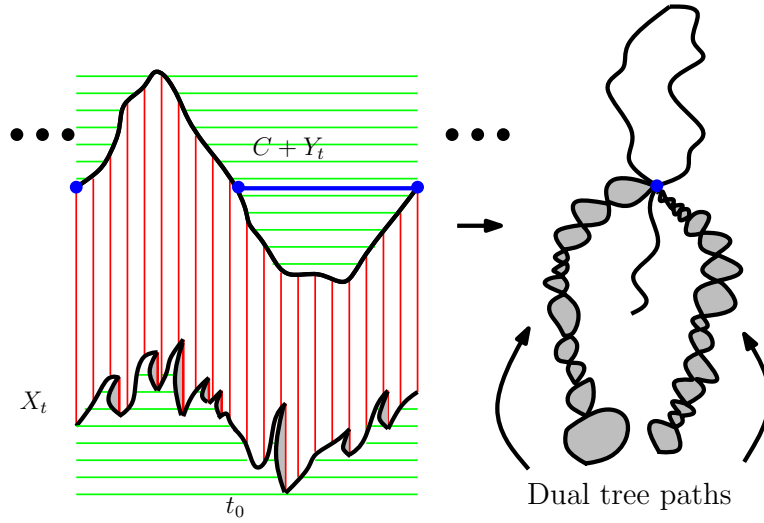


Figure 3.5: Illustration of the proof of Proposition 3.1, which states that  $Y_t$  cannot have a decrease time, i.e., there cannot be a time  $t_0$  and  $h > 0$  such that  $Y_s \geq Y_{t_0}$  for all  $s \in (t_0 - h, t_0)$  and  $Y_s \leq Y_{t_0}$  for all  $s \in (t_0, t_0 + h)$ . Shown is the behavior of the geodesic tree and dual tree if  $Y$  did have a decrease time  $t_0$ . The middle blue line on the graph of  $C + Y_t$  corresponds to the decrease time and the blue dots to its left and right are points which are all glued together by the Lévy net equivalence relation. Observe that every point in the Lévy net which corresponds to a point in the graph of  $C + Y_t$  which lies below the blue line would have more than one geodesic back to the root. This is a contradiction in view of Lemma 3.18, because then we would have a positive measure of points from which there is more than one geodesic to the root.

*space  $\mathbf{S}^2 / \cong$  is itself homeomorphic to  $\mathbf{S}^2$  if and only if no equivalence class separates  $\mathbf{S}^2$  into two or more connected components.*

*Proof of Proposition 3.3.* Proposition 3.1 implies that no vertical line segment in Figure 3.4 has an endpoint on two distinct (non-zero-length) horizontal green segments. Thus no equivalence class contains a non-empty horizontal chord of both the upper and lower graphs. The equivalence classes can thus be classified as:

- Type I: Those containing neither upper nor lower chords. These are isolated points (on the boundaries of the grey regions) or single vertical lines connecting one graph to the other.
- Type II: Those containing an upper (but not lower) chord. By Proposition 3.2, such a chord can hit the graph of  $Y_t$  either two or three times, but not more. Thus these equivalence classes consist of a horizontal line segment attached to either two or three vertical chords.

Type III: Those containing a lower (but not upper) chord. Since stable Lévy processes with only downward jumps have a countable collection of unique local minima, such a chord must hit the black curves in either two or three places. In the (a.s. countable) set of places where the latter occurs, it is not hard to see that the rightmost point is a.s. in the interior of one of the boundaries of the grey regions. (One can see from this that the path tracing the boundary of the looptree hits no point more than twice.) Thus the number of vertical line segments is either one (if one of the two endpoints lies on the boundary of a grey region) or two (if neither endpoint lies on the boundary of a grey region).

From this description, it is obvious that all equivalence classes are connected, fail to disconnect the space, and do not contain the entire space. It only remains to check that the equivalence relation is topologically closed. To do this we use essentially the same argument as the one given in [DMS14, Section 1.1]. Suppose that  $x_i$  and  $y_i$  are sequences with  $x_i \rightarrow x$  and  $y_i \rightarrow y$ , and  $x_i \cong y_i$  for all  $i$ . Then we can find a subsequence of  $i$  values along which the equivalence classes of  $x_i$  and  $y_i$  all have the same type (of the types enumerated above). By compactness, we can then find a further subsequence and such that the collection of segment endpoints converges to a limit. It is not hard to see that the resulting limit is a necessarily a collection of vertical chords and horizontal chords (each of which is an equivalence class) that are adjacent at endpoints; since  $x$  and  $y$  are both in this limit we must have  $x \cong y$ .  $\square$

*Definition 3.5.* The **( $\alpha$ -stable) Lévy net** is the random doubly marked compact topological space described in Figure 3.4. As described in the caption of Figure 3.4, the orange dot is the *root* of the geodesic tree, and the blue dot is a *root* of the looptree (a.k.a. dual tree) shown in the lower part of the figure. The Lévy net comes naturally endowed with a map from a “geodesic tree” (the quotient one obtains from the upper graph using only the equivalence classes from the horizontal chords above graph) to the space itself. Although *a priori* we do not put a full metric space structure on the Lévy net, we define a “distance from the root” of a point in the Lévy net to be the distance inherited from the geodesic tree. Also, from every point in the of the Lévy net, one has either one or two distinguished “geodesics” from that point to the root, which correspond to paths in the geodesic tree. When there are two, we refer to them as a *left geodesic* and a *right geodesic*.

We next briefly remark that the Lévy net can be endowed with a metric space structure in various ways. One approach is use the distance inherited from the leftmost-geodesic tree; given any two points  $x$  and  $y$ , one may draw their leftmost geodesic until they merge at a point  $z$  and define the distance to be the sum of geodesic arc lengths from  $x$  to  $z$  and from  $y$  to  $z$ . Another is to consider the geodesic tree (as described by  $Y_t$ ) with its intrinsic metric structure and then take the quotient (as in Section 2.2) w.r.t. the equivalence relation induced by the gluing with the looptree. Note that when two points in the upper tree are equivalent, their distance from the root is always the same;

thus, the distance between any point and the root is the same in the quotient metric space as it is in the tree itself. This implies that this metric space quotient defined this way is not completely degenerate — i.e., it is not the case that *all* points become identified with each other when one takes the metric space quotient in this way. It would be natural to try to prove a stronger form of non-degeneracy for this metric structure: namely, one would like to show that a.s. *no* two distinct points in the Lévy net have distance zero from each other in this quotient metric. This is not something that we will prove for general  $\alpha$  in this paper; however, in the case that  $\alpha = 3/2$ , it will be derived in Section 4 as a consequence of the proof of our main theorem.

We will see in Section 3.8 that given the structure described in Definition 3.5, one can recover additional structure: namely an embedding in the sphere (unique up to homeomorphism of the sphere), a cyclic ordering of the points around each metric ball boundary (which is homeomorphic to either a circle or a figure 8) with a distinguished point where the geodesic from  $x$  to  $y$  intersects the metric ball boundary, and a boundary length measure on each such boundary.

### 3.4 A second approach to the Lévy net quotient

The next proposition suggests an arguably simpler way to understand Figure 3.4, which only involves the upper graph  $C + Y_t$  (or equivalently just  $Y_t$ ). The implications of this are discussed further in the caption to Figure 3.6.

**Proposition 3.6.** *It is a.s. the case that two distinct points on the graph of  $C + Y_t$  in Figure 3.4 are equivalent in  $\cong$  if and only if one of the following holds.*

1. *There is a horizontal chord above or below the graph that connects those two points and intersects the graph of  $C + Y_t$  only at its endpoints.*
2. *There is a horizontal chord above the graph that intersects the graph of  $C + Y_t$  at exactly one location, in addition to its two endpoints.*
3. *The two points are the left and right endpoints of the (uncountable) set of local minima of a given height corresponding to a jump time for  $X_t$ .*

*Proof.* This is immediate from the proof of Proposition 3.3. □

The right hand side of Figure 3.6 illustrates an alternate way to represent the topological sphere shown in Figure 3.4. On the left hand side of Figure 3.6, two distinct points are considered to be equivalent if and only if either:

Case 1: The line segment connecting them is horizontal and intersects the graph of  $Y_t$  in at most finitely many points. (Recall that it is a.s. the case that there can be at

most three such intersection points, counting the endpoints themselves; and if one of these points is in the interior of the segment, it must be a local maximum of  $Y_t$ .)

Case 2: They are a pair representing the leftmost and rightmost local minima of a given height (which in turn corresponds to a jump in the Lévy process).

It is interesting because at first glance it looks like any two points of the same horizontal line in Figure 3.6 should be equivalent. But of course, this is not the case if the segment between them intersects the graph of  $Y_t$  infinitely often.<sup>7</sup>

It is straightforward to verify that the right side of Figure 3.6 (modulo the given equivalence relation) is homeomorphic to the middle image of Figure 3.6 (modulo the given equivalence relation). We remark that it is also straightforward to check directly that the relation on the right hand side of Figure 3.6 satisfies the conditions of Moore's theorem (Proposition 3.4), since each of the equivalence classes is a single point, a single line segment (horizontal or vertical), a solid rectangle, or the union of the left, right, and lower sides of a grey rectangle. One can thus define the Lévy net using Figure 3.6 in place of Figure 3.4.

### 3.5 Characterizing continuous state branching processes

To study the Lévy net in more detail, we will need to recall some basic facts about *continuous state branching processes*, which were introduced by Jiřina and Lamperti several decades ago [Jiř58, Lam67a, Lam67b] (see also the more recent overview in [LG99] as well as [Kyp06, Chapter 10]). A Markov process  $(Y_t, t \geq 0)$  with values in  $\mathbf{R}_+$ , whose sample paths are càdlàg (right continuous with left limits) is said to be a continuous state branching process (CSBP for short) if the transition kernels  $P_t(x, dy)$  of  $Y$  satisfy the additivity property:

$$P_t(x + x', \cdot) = P_t(x, \cdot) * P_t(x', \cdot). \quad (3.1)$$

*Remark 3.7.* Note that (3.1) implies that the law of a CSBP at a *fixed* time is infinitely divisible. In particular, this implies that for each fixed  $t$  there exists a subordinator (i.e., a non-decreasing process with stationary, independent increments)  $A^t$  with  $A_0^t = 0$  such that  $A_t^t \stackrel{d}{=} Y_t$ . (We emphasize though that  $Y$  does not *evolve* as a subordinator in  $t$ .) We will make use of this fact several times.

---

<sup>7</sup>If one begins with the tree obtained by gluing along horizontal chords above the graph (the tree we call the geodesic tree) then each of the two types of equivalence classes described above produces an equivalence relation on this tree in which each equivalence class has exactly one or two elements. The smaller equivalence class obtained by focusing on either one of these two cases is a dense subset in the full equivalence relation; so the full relation can be understood as the topological closure of either of these two smaller relations.

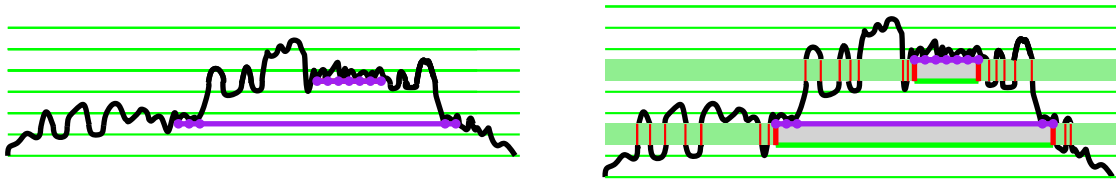


Figure 3.6: **Left:** Graph of  $Y_t$  together with all horizontal lines, both above and below the graph, drawn as chords. The points on a horizontal chord that lies strictly above or below the graph (*except* for its two endpoints) are considered to be equivalent. The equivalence class corresponding to a given chord is either the chord itself or a pair of such chords above the graph with a common endpoint (a local maximum). The two horizontal purple segments correspond to sets of local minima of the same height each indicated with a purple dot, which in turn correspond to jumps of the Lévy process. Only two such segments are drawn, but in fact there are infinitely many; the endpoints of such segments occupy a dense set of points on the graph of  $Y_t$ . Each such segment contains an uncountable collection of equivalence classes, including uncountably many single points (purple dots), countably many closed chords that lie strictly under the graph except at endpoints, and the pair of endpoints of the whole black segment (which is its own equivalence class). Each purple segment becomes a circle in the topological quotient. **Right:** Same graph with a horizontal stripe of “extra space” inserted at each purple segment. The height of the stripe can be chosen so that the sum of the heights of all of the (countably many) stripes is finite. At each of the (uncountably many) places where  $Y_t$  intersects the purple segment, a corresponding red vertical “bridge” is added crossing the green stripe; points on the same bridge are considered equivalent. Points on the closure of the same green rectangle (bounded between successive bridges) are also considered equivalent. The bottom, left, and right edges of each grey rectangle together constitute a single equivalence class, so that the topological quotient of each grey rectangle’s boundary is a circle (as in the left figure).

The Lamperti representation theorem states that there is simple time-change procedure that gives a one-to-one correspondence between CSBPs and non-negative Lévy processes without negative jumps (stopped when they reach zero), where each is a time-change of the other. The statement of the theorem we present below is lifted from a recent expository treatment of this result [CLUB09].

Consider the space  $\mathcal{D}$  of càdlàg functions  $f: [0, \infty] \rightarrow [0, \infty]$  such that  $\lim_{t \rightarrow \infty} f(t)$  exists in  $[0, \infty]$  and  $f(t) = 0$  (resp.  $f(t) = \infty$ ) implies  $f(t + s) = 0$  (resp.  $f(t + s) = \infty$ ) for all  $s \geq 0$ . For any  $f \in \mathcal{D}$ , let  $\theta_t := \int_0^t f(s) ds \in [0, \infty]$ , and let  $\kappa$  denote the right-continuous inverse of  $\theta$ , so  $\kappa_t := \inf\{u \geq 0 : \theta_u > t\} \in [0, \infty]$ , using the convention  $\inf \emptyset = \infty$ . The *Lamperti transformation* is given by  $L(f) = f \circ \kappa$ . The following is the Lamperti representation theorem, which applies to  $[0, \infty]$ -valued processes indexed by  $[0, \infty]$ .

**Theorem 3.8.** *The Lamperti transformation is a bijection between CSBPs and Lévy*

processes with no negative jumps stopped when reaching zero. In other words, for any CSBP  $Y$ ,  $L(Y)$  is a Lévy process with no negative jumps stopped whenever reaching zero; and for any Lévy process  $X$  with no negative jumps stopped when reaching zero,  $L^{-1}(X)$  is a CSBP.

Informally, the CSBP is just like the Lévy process it corresponds to except that its speed (the rate at which jumps appear) is given by a constant times its current value (instead of being independent of its current value). The following is now immediate from Theorem 3.8 and the definitions above:

**Proposition 3.9.** *Suppose that  $X_t$  is a Lévy process with non-negative jumps that is strictly  $\alpha$ -stable in the sense that for each  $C > 0$ , the rescaled process  $X_{C^\alpha t}$  agrees in law with  $CX_t$  (up to a change of starting point). Let  $Y = L^{-1}(X)$ . Then  $Y$  is a CSBP with the property that  $Y_{C^{\alpha-1}t}$  agrees in law with  $CY_t$  (up to a change of starting point). The converse is also true. Namely, if  $Y$  is a CSBP with the property that  $Y_{C^{\alpha-1}t}$  agrees in law with  $CY_t$  (up to a change of starting point) then  $Y$  is the CSBP obtained as a time-change of the  $\alpha$ -stable Lévy process with non-negative jumps.*

Proposition 3.9 will be useful on occasions when we want to prove that a given process  $Y$  is the CSBP obtained as a time change of the  $\alpha$ -stable Lévy process with non-negative jumps. (We refer to this CSBP as the  $\alpha$ -stable CSBP for short.<sup>8</sup>) It shows that it suffices in those settings to prove that  $Y$  is a CSBP and that it has the scaling symmetry mentioned in the proposition statement. To avoid dealing with uncountably many points, we will actually often use the following slight strengthening of Proposition 3.9:

**Proposition 3.10.** *Suppose that  $Y$  is a Markovian process indexed by the dyadic rationals that satisfies the CSBP property (3.1) and that  $Y_{C^{\alpha-1}t}$  agrees in law with  $CY_t$  (up to a change of starting point) when  $C^{\alpha-1}$  is a power of 2. Assume that  $Y$  is not trivially equal to 0 for all positive time, or equal to  $\infty$  for all positive time. Then  $Y$  is the restriction (to the dyadic rationals) of an  $\alpha$ -stable CSBP.*

*Proof.* By the CSBP property 3.1, the law of  $Y_1$ , assuming  $Y_0 = a > 0$ , is infinitely divisible and equivalent to the law of the value  $A_a$  where  $A$  is a subordinator and  $A_0 = 0$  (recall Remark 3.7). Fix  $k \in \mathbf{N}$  and pick  $C > 0$  such that  $C^{1-\alpha} = 2^{-k}$ . Similarly, by scaling, we have that  $Y_{C^{1-\alpha}} \stackrel{d}{=} C^{-1}A_{Ca}$ . By the law of large numbers, this law is concentrated on  $a\mathbf{E}[A_1]$  when  $k$  is large; we observe that  $\mathbf{E}[A_1] = 1$  since otherwise (by taking the  $k \rightarrow \infty$  limit) one could show that  $Y$  is equal to 0 (if  $\mathbf{E}[A_1] < 1$ ) or  $\infty$  (if  $\mathbf{E}[A_1] > 1$ ) for all positive time.

From this we deduce that  $Y$  is a martingale, and the standard upcrossing lemma allows us to conclude that almost surely  $Y$  has only finitely many upcrossings across the

---

<sup>8</sup>This process is also referred to as a  $\psi$ -CSBP with “branching mechanism”  $\psi(u) = u^\alpha$  in other work in the literature, for example [DLG02].

interval  $(x, x + \epsilon)$  for any  $x$  and  $\epsilon$ , and that  $Y$  a.s. is bounded above. This in turn guarantees, for all  $t \geq 0$ , the existence of left and right limits of  $Y_{t+s}$  as  $s \rightarrow 0$ . It implies that  $Y$  is a.s. the restriction to the dyadic rationals of a càdlàg process; and there is a unique way to extend  $Y$  to a càdlàg process defined for all  $t \geq 0$ . Since left limits exist almost surely at any fixed time, it is straightforward to verify that the hypotheses of Proposition 3.9 apply to  $Y$ .  $\square$

CSBPs are often introduced in terms of their Laplace transform [LG99], [Kyp06, Chapter 10] and Proposition 3.9 is also immediate from this perspective. We will give a brief review of this here, since this perspective will also be useful in this article. In the case of an  $\alpha$ -stable CSBP  $Y_t$ , this Laplace transform is explicitly given by

$$\mathbf{E}[\exp(-\lambda Y_t) | Y_s] = \exp(-Y_s u_{t-s}(\lambda)) \quad \text{for all } t > s \geq 0 \quad (3.2)$$

where

$$u_t(\lambda) = (\lambda^{1-\alpha} + (\alpha - 1)t)^{1/(1-\alpha)}. \quad (3.3)$$

More generally, CSBPs are characterized by the property that they are Markov processes on  $\mathbf{R}_+$  such that their Laplace transform has the form given in (3.2) where  $u_t(\lambda)$ ,  $t \geq 0$ , is the non-negative solution to the differential equation

$$\frac{\partial u_t}{\partial t}(\lambda) = -\psi(u_t(\lambda)) \quad \text{for } u_0(\lambda) = \lambda. \quad (3.4)$$

The function  $\psi$  is the so-called *branching mechanism* for the CSBP and corresponds to the Laplace exponent of the Lévy process associated with the CSBP via the Lamperti transform (Theorem 3.8). In this language, an  $\alpha$ -stable CSBP is called a “CSBP with branching mechanism  $\psi(u) = u^\alpha$ .”

One of the uses of (3.2) is that it provides an easy derivation of the law of the extinction time of a CSBP, which we record in the following lemma.

**Lemma 3.11.** *Suppose that  $Y$  is an  $\alpha$ -stable CSBP and let  $\zeta = \inf\{t \geq 0 : Y_t = 0\}$  be the extinction time of  $Y$ . Then we have that*

$$\mathbf{P}[\zeta > t] = 1 - \exp(-c_\alpha t^{1/(1-\alpha)} Y_0) \quad \text{where } c_\alpha = (\alpha - 1)^{1/(1-\alpha)}. \quad (3.5)$$

*Proof.* Note that  $\{\zeta > t\} = \{Y_t > 0\}$ . Consequently,

$$\mathbf{P}[\zeta > t] = \mathbf{P}[Y_t > 0] = 1 - \lim_{\lambda \rightarrow \infty} \mathbf{E}[e^{-\lambda Y_t}] = 1 - \exp(-c_\alpha t^{1/(1-\alpha)} Y_0),$$

which proves (3.5).  $\square$

As we will see in Section 3.6 just below, it turns out that the boundary length of the segment in a ball boundary between two geodesics in the Lévy net evolves as a CSBP as one decreases the size of the ball. The merging time for the geodesics corresponds to when this CSBP reaches 0. Thus Proposition 2.8 together with Lemma 3.11 allows us to relate the structure of geodesics in a space which satisfies the hypotheses of Theorem 1.1 with the Lévy net.

### 3.6 A breadth-first approach to the Lévy net quotient

Now, we would like to consider an alternative approach to the Lévy net in which we observe loops in the order of their distance from the root of the tree of loops (instead of in the order in which they are completed when tracing the boundary of the stable looptree). Consider a line at some height  $C + s$  as depicted in Figure 3.7. As explained in the figure caption, we would like to define  $Z_s$  to be in some sense the “fractal measure” of the set of points at which this line intersects the graph (which should be understood as some sort of local time) and then understand how  $Z_s$  evolves as  $s$  changes. A detailed account of the construction and properties of  $Z_s$ , along with Proposition 3.12 (stated and proved below), appears in [DLG05]. We give a brief sketch here.

First of all, in what sense is  $Z_s$  defined? Note that if we fix  $s$ , then we may define the set  $E_t = \{t : Y_t > s\}$ . Observe that within each open interval of  $E_t$  the process  $X_t$  evolves as an  $\alpha$ -stable Lévy process, which obtains the same value at its endpoints and is strictly larger than that value in the interim. In other words, the restriction of  $X_t$  to that interval is (a translation of) an  $\alpha$ -stable Lévy excursion. If we condition on the number  $N_\epsilon$  of excursions of this type that reach height at least  $\epsilon$  above their endpoint height, then it is not hard to see that the conditional law of the set of excursions is that of an i.i.d. collection of samples from the Lévy excursion measure (restricted to the positive and finite measure set of excursions which achieve height at least  $\epsilon$ ). The ordered collection of Lévy excursions agree in law with the ordered collection one would obtain by considering the “reflected  $\alpha$ -stable Lévy process” (with positive jumps) obtained by replacing an  $\alpha$ -stable Lévy process  $R_t$  by  $\tilde{R}_t = R_t - \inf\{R_s : 0 \leq s \leq t\}$ . (See [Ber96] for a more thorough treatment of local times and reflected processes.) The process  $\tilde{R}_t$  then has a *local time* describing the amount of time it spends at zero; this time is given precisely by  $\tilde{R}_t - R_t$ . The set of excursions of  $\tilde{R}_t$  explored during the local time interval  $[0, Q]$  (i.e., during the time before  $\tilde{R}_t - R_t$  first reaches  $Q$ ) can be understood as a Poisson point process corresponding to the product of the Lebesgue measure  $[0, Q]$  and the (infinite) Lévy excursion measure. In particular, one can deduce from this that as  $\epsilon$  tends to zero (and  $\beta$  is the appropriate constant) the quantity  $N_\epsilon/\epsilon^\beta$  a.s. tends to the local time; this can then be taken as the definition of  $Z_s$ .

Note that the discussion above in principle only allows us to define  $Z_s$  for almost all  $s$ , or for a fixed countable dense set of  $s$  values. We have not ruled out the possibility that there exist exceptional  $s$  values for which the limit that defines  $Z_s$  is undefined. To be concrete, we may use the above definition of  $Z_s$  for all dyadic rational times and extend to other times by requiring the process to be càdlàg (noting that this definition is almost surely equal to the original definition of  $Z_s$  for almost all  $s$  values, and for any fixed  $s$  value; alternatively see [DLG05] for more discussion of the local time definition). This allows us to use Proposition 3.10 to derive the following, which is referred to in [DLG05, Theorem 1.4.1] as the Ray-Knight theorem (see also the Lévy tree level set discussion in [DLG02, DLG05]):

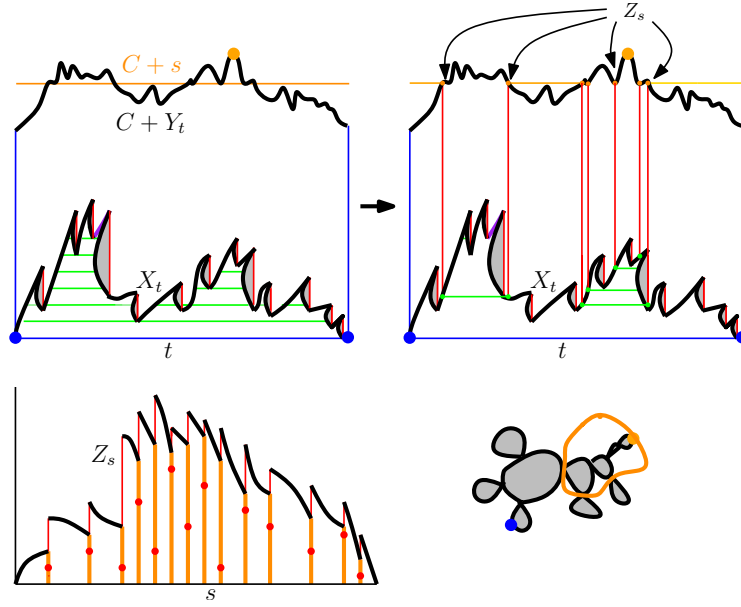


Figure 3.7: **Upper left:** An orange line is drawn at height  $C + s$  for some  $s$ . **Upper right:** If  $a$  and  $b$  are the endpoints of an excursion of the black path above the orange line, then  $a$  and  $b$  are identified (via a red line) to points on the lower graph that are identified (via a green horizontal line). **Lower left:** As the height of the orange segment in the upper graphs increases (i.e.,  $s$  increases),  $Z_s$  measures the local time of the intersection between that segment and the graph of  $C + Y_t$ . When the rising orange line encounters a point  $(t, s)$  on the upper graph such that  $X$  has a jump at time  $t$ , there is a corresponding upward jump in  $Z_s$  of the same magnitude. This is due to the fact (not obvious in this illustration) that all points on the corresponding looptree are identified with points on the upward graph of the same height; the local time of this set of points is the magnitude of the jump. The amount of this local time in the orange/black intersection that lies to the *right* of the point  $(t, s)$  is a quantity that lies strictly between 0 and the height of  $X$  at the lower end of that jump (see [DLG05, Proposition 1.3.3]); this quantity is encoded by the height of the red dot (one for each of the countably many jumps) shown in the center graph. Another perspective is that the jumps in  $Z_s$  correspond to loops observed in the tree on the right as one explores them in order of their distance from the boundary, where the distance between two macroscopic loops is the measure of the set of cut points between those loops. The orange circle on the right encloses the set of loops explored up until time  $s$ . Each red dot in the middle graph indicates *where* along the boundary a new loop is attached to the already-explored looptree structure, as defined relative to the branch in the geodesic tree connecting the root and dual root. Conditioned on  $Z_s$ , the vertical locations of the red dots are independent and uniform.

**Proposition 3.12.** *The process  $Z$  illustrated in Figure 3.7 has the law of an  $\alpha$ -stable CSBP.*

*Proof.* The CSBP property (3.1) is immediate from the derivation above, and the scale invariance required by Proposition 3.10 is immediate from the scale invariance of the overall pair of graphs in Figure 3.7.  $\square$

Related to Proposition 3.12 is the following correspondence between the jumps of the  $Z$  and  $X$  processes shown in Figure 3.7.

**Proposition 3.13.** *The (countably many) jumps in the process  $Z$  illustrated in Figure 3.7 are a.s. in one-to-one correspondence with the (countably many) jumps in the process  $X$  in Figure 3.7. Namely: it is a.s. the case that whenever a jump in  $Z$  occurs at a time  $s$  we have  $s = Y_t$  for some  $t$  value at which the process  $X$  has a jump, and vice-versa; in this case, the corresponding jumps have the same magnitude.*

*Proof.* When a jump occurs in  $Z_s$ , the graph of  $C + s$  intersects that of  $C + Y_t$  at all points at which  $X_t$  (run from right to left) reaches a record minimum following the jump, up until  $X_t$  (run from right to left) again reaches the value on the lower side of the jump. Using the description of local time above (in terms of  $\tilde{R}$  and  $R$ ), we see that the amount of local time added due to the appearance of the jump is precisely the height of the  $X_t$  jump.  $\square$

Next, we make a simple observation:

**Proposition 3.14.** *Suppose that  $A_s$  is a subordinator with  $A_0 = 0$  and  $\mathbf{P}[A_1 > 0] = 1$ . Suppose also that  $\tilde{A}_s$  is an independent instance of the same process. Then for any fixed values  $a$  and  $b$  we have*

$$\mathbf{E} \left[ \frac{A_a}{A_a + \tilde{A}_b} \right] = \frac{a}{a + b}. \quad (3.6)$$

*Proof.* First, suppose that  $a = m\delta$  and  $b = n\delta$  for some small  $\delta > 0$  and  $m, n \in \mathbf{N}$ . Then  $A_a$  is the sum of  $m$  i.i.d. copies  $X_1, \dots, X_m$  of a random variable and  $\tilde{A}_b$  is the sum of  $n$  such copies  $X_{m+1}, \dots, X_{m+n}$ .

Imagine that we sample  $X_1, \dots, X_{m+n}$  in two steps:

1. Condition on the sequence of  $m + n$  values  $P = (X_1, \dots, X_{m+n})$ ; and then
2. Randomly decide which of the elements of  $P$  contribute to  $A_a$  (as opposed to  $\tilde{A}_b$ ).

Note that  $P$  determines  $Q = A_a + \tilde{A}_b = X_1 + \dots + X_{m+n}$ . Moreover, given  $P$ , we have that the conditional probability that a given element of  $P$  is part of the sum that makes up  $A_a$  is

$$\frac{m}{m + n} = \frac{a}{a + b}.$$

In particular,

$$\mathbf{E} \left[ \frac{A_a}{A_a + \tilde{A}_b} \mid P \right] = \frac{1}{Q} \sum_{i=1}^{m+n} \frac{m}{m+n} X_i = \frac{a}{a+b}.$$

This proves (3.6) in the special case that  $a = m\delta$  and  $b = n\delta$ .

The general statement of (3.6) is easily obtained by sandwiching the expectation between two approximating rationals. (Note that rounding  $a$  down to the nearest multiple of  $\delta$  and  $b$  up to the nearest multiple of  $\delta$  only decreases the expectation; rounding  $a$  up to the nearest multiple of  $\delta$  and  $b$  down to the nearest multiple of  $\delta$  only increases the expectation.)  $\square$

Proposition 3.14 now implies another simple but interesting observation, which we record as Proposition 3.15 below (and which is related to the standard “confluence-of-geodesics” story). See Figure 3.8 and Figure 3.9 for relevant illustrations.

In the statement of Proposition 3.15, we will make use of the following setup. Let  $Z_s$  be defined as in Figure 3.7, and let  $[0, D]$  denote the interval on which it is defined. Let  $\partial U_s$  be the set of points which have distance equal to  $D - s$  from the root (so that  $\partial U_s$  corresponds to a horizontal line in Figure 3.8). In view of Figure 3.7, we note that if  $x, y \in \partial U_s$  then it makes sense to talk about the clockwise (resp. counterclockwise) segments of  $\partial U_s$  which connect  $x$  and  $y$ . Fix  $r, t > 0$  and assume that we are working on the event that  $D > t$  and  $Z_t \geq r$ . Let  $\gamma$  be the branch of the geodesic tree which connects the root and the dual root. We can then describe each point  $x \in \partial U_s$  in terms of the length of the counterclockwise segment of  $\partial U_s$  which connects  $x$  and the point  $x_s$  on  $\partial U_s$  which is visited by  $\gamma$ . We let  $\eta$  be the geodesic starting from the point on  $\partial U_t$  such that the length of the counterclockwise segment of  $\partial U_t$  to  $x_t$  is equal to  $r$ . For each  $s \geq t$ , we let  $A_s$  (resp.  $B_s$ ) be the length of the counterclockwise (resp. clockwise) segment of  $\partial U_s$  which connects  $\eta \cap \partial U_s$  to  $x_s$ . Note that  $A_t = r$ ,  $B_t = Z_t - r$ , and  $A_s + B_s = Z_s$  for all  $s \in [t, D]$ .

**Proposition 3.15.** *When the processes  $A$ ,  $B$ , and  $Z$  and the values  $t$  and  $D$  are as defined just above, the following holds for the restrictions of these processes to the interval  $s \in [t, D]$ .*

1. *The processes  $A_s$  and  $B_s$  are independent  $\alpha$ -stable CSBPs.*
2. *The process  $A_s/Z_s = A_s/(A_s + B_s)$  is a martingale. (This corresponds to the horizontal location in the trajectory illustrated in Figure 3.9 when parameterized using distance).*
3. *The process  $A_s/Z_s$  almost surely hits 0 or 1 before time  $D$ .*

*Proof.* The first point is immediate from the construction; recall the proof of Proposition 3.12. Given the first point, the second point is immediate from Proposition 3.14

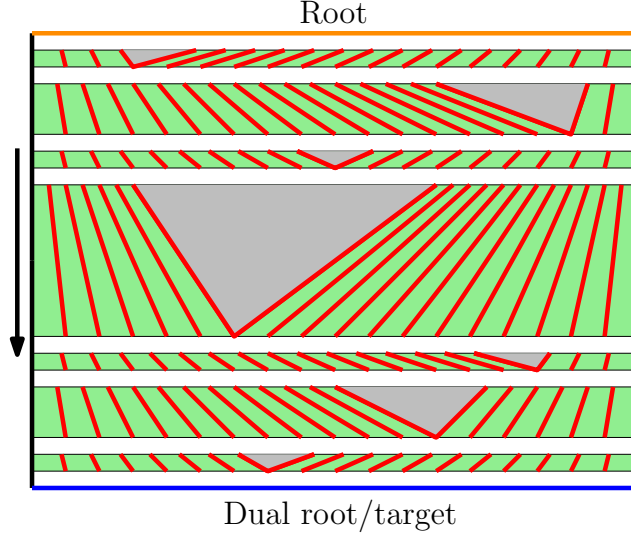


Figure 3.8: *Recovering topological structure from bubbles*: Shown is a representation of a Lévy net using a width-1 rectangle  $R$ . The top (resp. bottom) line represents the root (resp. dual root/target). The left and right sides of  $R$  are identified with each other and represent the branch  $\gamma$  in the geodesic tree connecting the root and dual root. If  $r$  is *not* one of the countably many values at which a jump in boundary length occurs, then each point  $z$  on the Lévy tree of distance  $r$  from the root is mapped to the point in the rectangle whose horizontal location is the length of the counterclockwise radius- $r$ -ball boundary segment from  $\gamma$  to  $z$  divided by the total length of the radius- $r$ -ball boundary; the vertical distance from the top of the rectangle is the sum of the squares of the boundary-length jumps that occur as the radius varies from 0 and  $r$ . Each of the green stripes represents the set of points whose distance from the root is a value  $r$  at which a jump *does* occur. Every red line (going from the top to the bottom of a stripe) is an equivalence class that encodes one of these points. The height of each green stripe is equal to the square of the jump in the boundary length corresponding to the grey triangle (the sum of these squares is a.s. finite since the sum of the squares of the jumps of an  $\alpha$ -stable Lévy process is a.s. finite; see, e.g., [Ber96, Chapter I]). The top (resp. bottom) of each green stripe represents the outer boundary of the metric ball infinitesimally before (resp. after) the boundary length of the metric ball jumps. Each red line is a single closed equivalence class (except that when two red lines share an end vertex, their union forms a single closed equivalence class). The uppermost horizontal orange line is also a single closed equivalence class. Also, each pair of left and right boundary points of the rectangle (with the same vertical coordinate) is a closed equivalence class. Any point that does not belong to one of these classes is in its own class.

(recall Remark 3.7). The fact that the martingale reaches 0 or 1 a.s. before reaching the

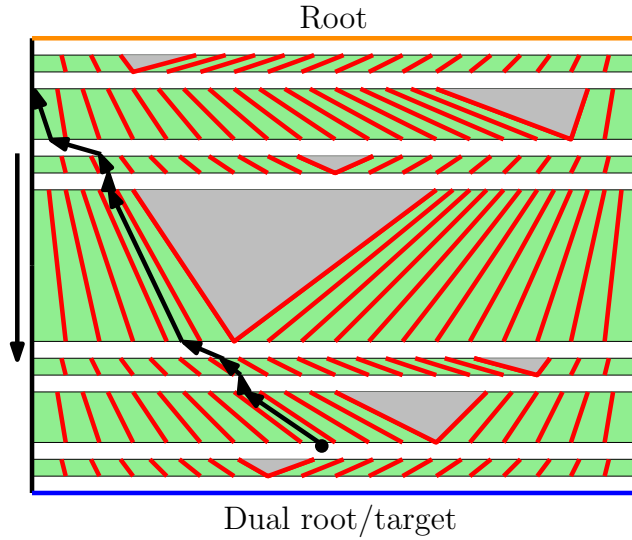


Figure 3.9: *Plotting a geodesic trajectory:* The black sequence of arrows represents a branch  $\eta$  in the geodesic tree in the Lévy net. We have drawn  $\eta$  beginning on one of the horizontal lines of the figure which, as explained in Figure 3.8, represents the boundary of the metric ball starting from the root. As shown in Proposition 3.15,  $\eta$  eventually merges with the left boundary of the rectangle (both left and right rectangle boundaries correspond to the root-to-target branch in the geodesic tree) just before getting back to the root vertex (represented by the uppermost orange line). Geodesics started at distinct points can “merge” with each other.

upper end of the rectangle is reached simply follows from the fact that two independent CSBPs, both started at positive values, almost surely do not reach zero at exactly the same time.  $\square$

**Lemma 3.16.** *In the bottom left of Figure 3.7, given the process  $Z$ , the locations of each of the red dots are conditionally independent and uniform on each of the vertical orange lines.*

*Proof.* This follows because the CSBP property (3.1) implies that for each fixed  $s$  we can write  $Z_{s+t}$  for  $t \geq 0$  as a sum  $n$  independent  $\alpha$ -stable CSBPs each starting from  $Z_s/n$  and the probability that any one of them has a jump in  $\epsilon > 0$  units of time is equal.  $\square$

**Theorem 3.17.** *The information encoded by the second graph in Figure 3.7 a.s. determines the information encoded by the first graph. That is, the procedure described in the caption of Figure 3.7 yields an a.e.-defined one-to-one measure-preserving correspondence between*

1.  $\alpha$ -stable Lévy excursions

2.  $\alpha$ -stable Lévy excursions (which are naturally reparameterized and viewed as CSBP excursions) that come equipped with a way of assigning to each jump a distinguished point between zero and the lower endpoint of that jump (as shown in the second graph of Figure 3.7).

Before we give the proof of Theorem 3.17, we first need the following lemma.

**Lemma 3.18.** *Let  $W_t$  be a process that starts at  $W_0 = \epsilon$ , then evolves as an  $\alpha$ -stable CSBP until it reaches 0, then jumps to  $\epsilon$  and continues to evolve as an  $\alpha$ -stable CSBP until again reaching zero, and so forth. Then as  $\epsilon$  tends to zero, the process  $W_t$  converges to zero in probability.*

*Proof.* Since  $W_t$  evolves as a martingale away from the times that it hits zero, we expect to have order  $\epsilon^{-1}$  of these jumps before  $W_t$  reaches 1. However, by scaling, on the event that the process reaches zero before reaching  $2\epsilon$ , the law of the time is a random constant times  $\epsilon^{\alpha-1}$ . Since  $\alpha \in (1, 2)$ , we have that  $\epsilon^{-1}\epsilon^{\alpha-1}$  tends to infinity as  $\epsilon \rightarrow 0$ , which implies that as  $\epsilon \rightarrow 0$ , the amount of time until  $W_t$  first goes above any fixed positive constant tends to infinity; from this the proposition follows.  $\square$

*Proof of Theorem 3.17.* We claim that the trajectory  $\eta$  considered in Proposition 3.15 is a.s. uniquely determined by the information in the decorated graph  $Z_s$ , as shown in the second graph of Figure 3.7. Upon showing this, we will have shown that the geodesic tree is almost surely determined by the decorated graph  $Z_s$  which in turn implies that the entire  $\alpha$ -stable Lévy net is almost surely determined.

To prove the claim, we choose two such trajectories  $\eta$  and  $\tilde{\eta}$  conditionally independently, given the decorated graph of  $Z_s$ , and show that they are almost surely equal.

We begin by noting that the length of the segment which is to the left of  $\eta$  evolves as an  $\alpha$ -stable CSBP and the length which is to the right of  $\eta$  evolves as an independent  $\alpha$ -stable CSBP. The same is also true for  $\tilde{\eta}$ . It follows from this that in the intervals of time in which  $\eta$  is not hitting  $\tilde{\eta}$  we have that the length  $A_s$  (resp.  $C_s$ ) of the segment which is to the left (resp. right) of both trajectories evolve as independent  $\alpha$ -stable CSBPs. Our aim now is to show that  $B_s$  also evolves as an  $\alpha$ -stable CSBP in these intervals of time.

Fix an interval of time  $I = [a, b]$  in which  $\eta$  does not collide with  $\tilde{\eta}$ . Then we know that both  $A|_I$  and  $C|_I$  can be a.s. deduced from the ordered set of jumps they have experienced in  $I$  along with their initial values  $A_a, C_a$  (since this is true for  $\alpha$ -stable CSBPs and  $\alpha$ -stable Lévy processes). That is, if we fix  $s \in I$  and let  $J_s^\epsilon$  be the sum of the jumps made by  $A|_{[a,s]}$  with size at least  $\epsilon$  then  $A_s$  is almost surely equal to  $A_a + \lim_{\epsilon \rightarrow 0} (J_s^\epsilon - \mathbf{E}[J_s^\epsilon])$  and the analogous fact is likewise true for  $C|_I$ . Since this is also true for  $(A + B + C)|_I$  as it is an  $\alpha$ -stable CSBP (Proposition 3.12), we see that  $B|_I$  is almost surely determined by the jumps made by  $B|_I$  and  $B_a$  in the same way.

To finish showing that  $B|_I$  evolves as an  $\alpha$ -stable CSBP, we need to show that the law of the jumps that it has made in  $I$  has the correct form. Lemma 3.16 implies that each time a new bubble comes along, we may sample which of the three regions it is glued to (with probability of each region proportional to each length). This implies that the jump law for  $B|_I$  is that of an  $\alpha$ -stable CSBP which implies that  $B|_I$  is in fact an  $\alpha$ -stable CSBP.

The argument is completed by applying Lemma 3.18 to deduce that since  $B_s$  starts at zero and evolves as an  $\alpha$ -stable CSBP away from time zero, it cannot achieve any positive value in finite time. We have now shown that it is possible to recover the first graph in Figure 3.7 from the second almost surely and (since we have already shown how to construct the second from the first) this completes the proof.  $\square$

We will later also need the following lemma, which gives an explicit description of the time-reversal of the Lévy process whose corresponding CSBP is used to generate a Lévy net.

**Lemma 3.19.** *Suppose that  $\alpha \in (1, 2)$  and  $W_t$  is an  $\alpha$ -stable Lévy excursion with positive jumps (indexed by  $t \in [0, T]$  for some  $T$ ). That is,  $W_t$  is chosen from the natural infinite measure on excursions of this type. Then the law  $W_{T-t}$  is also an infinite measure, and corresponds to an excursion of a Markov process that has only negative jumps. When the process value is  $c$ , the jump law for this Markov process is given by a constant times  $a^{-\alpha-1}(1 - a/c)^{\alpha-2}$ .*

*Proof.* This is a relatively standard sort of calculation about time-reversals of Lévy excursions. The Lévy excursion can be understood as a limit of measures obtained by starting an ordinary  $\alpha$ -stable Lévy process with negative jumps at  $\epsilon$ , and renormalizing the measure by a constant so that the probability of exceeding 1 before reaching zero is of constant order.

The conditional law of the time-reversal, given the process up to a stopping time, is (roughly speaking) that of an  $\alpha$ -stable Lévy process with negative jumps *conditioned* to have a record minimum of value zero (i.e., not to “jump past” zero first). Intuitively, this means that when considering the probability of a negative jump of magnitude  $a$ , one has to weight by the probability an  $\alpha$ -stable Lévy process from the new location, i.e. from  $c - a$ , will have a record minimum at exactly zero. Of course this probability is zero, but one may instead consider the probability that it has a record minimum within  $(0, \epsilon)$  and compare the rate of scaling as  $\epsilon \rightarrow 0$ .

The dimension of the record minima range for an unconstrained  $\alpha$ -stable process with negative jumps is given by the index  $\alpha - 1$  (see [Ber96] and the footnote in Section 3.3). Essentially we are conditioning on the event that this process includes zero, which we approximate by the probability that it includes a point in  $[0, \epsilon]$ . If we start at height  $(c - a)$  then the probability of this scales like  $(\frac{\epsilon}{c-a})^{2-\alpha}$ . (Note that for a random fractal

subset of  $[0, 1]$  of dimension  $d$ , we would expect the probability that it intersects an  $\epsilon$ -length interval to scale like  $\epsilon^{1-d}$ .) This is an  $\epsilon$ -dependent factor times  $(c - a)^{\alpha-2}$ , which is precisely the extra factor that appears in the statement of Lemma 3.19.  $\square$

### 3.7 Topological equivalence of Lévy net constructions

We have so far given three different descriptions of the Lévy net quotient, namely in Figure 3.4, Figure 3.6, and Figure 3.8. Moreover, we explained in Section 3.4 that the quotients in Figure 3.4 and Figure 3.6 yield an equivalent topology. The purpose of this section is show that the topology of the quotient constructed in Figure 3.8 is equivalent to the topology constructed in Figure 3.4.

**Proposition 3.20.** *The topology of the Lévy net quotient constructed in Figure 3.4 is equivalent to the topology of the quotient constructed in Figure 3.8. In particular, the quotient constructed in Figure 3.8 is a.s. homeomorphic to  $\mathbf{S}^2$ .*

We remark that it is also possible to give a short, direct proof that the quotient described in Figure 3.8 is a.s. homeomorphic to  $\mathbf{S}^2$  using Moore's theorem (Proposition 3.4), though we will not do so in view of Proposition 3.20.

For each  $r > 0$ , we let  $Z_s^r$  be the local time of the intersection of  $Y$  with the line of height  $s$  and width  $r$  (i.e., the line connecting  $(0, s)$  with  $(r, s)$ ). Note that  $Z_s = Z_s^T$  where  $T$  is the length of the Lévy excursion. In order to show that the topology of the breadth first construction of the Lévy quotient described in Figure 3.8 is equivalent to that associated with the constructions described in Figure 3.4 and Figure 3.6, we first need to construct a modification of  $Z_s^r$  which has certain continuity properties. We will then use this modification to construct the map which takes the construction described in Figure 3.6 to the breadth first construction.

**Proposition 3.21.** *The process  $(r, s) \mapsto Z_s^r$  has a jointly measurable modification which almost surely satisfies the following two properties (for all  $r, s$  simultaneously).*

1. *The map  $r \mapsto Z_s^r$  is continuous with respect to the uniform topology.*
2. *The map  $s \mapsto Z_s^r$  is càdlàg with respect to the uniform topology.*

See [DLG02, Proposition 1.3.3] for a related result. We note that the modification obtained in Proposition 3.21 has stronger continuity properties than given in [DLG02, Proposition 1.3.3].

We need to collect several intermediate lemmas before we give the proof of Proposition 3.21. We begin with two elementary estimates for  $\alpha$ -stable CSBPs.

**Lemma 3.22.** *Suppose that  $W$  is an  $\alpha$ -stable CSBP with  $W_0 > 0$  and let  $W^* = \sup_{s \geq 0} W_s$ . There exists constants  $c_0, \beta > 0$  depending only on  $\alpha$  such that*

$$\mathbf{P}[W^* \geq u] \leq c_0 \left( \frac{u}{W_0} \right)^{-\beta} \quad \text{for each } u \geq W_0. \quad (3.7)$$

*Proof.* Assume that  $W_0 = 1$ . By the Lamperti transform (Theorem 3.8), it suffices to prove the result in the case of an  $\alpha$ -stable Lévy process with only upward jumps starting from 1 and stopped upon first hitting 0 in place of  $W$ . Let  $S_t$  (resp.  $I_t$ ) be the running supremum (resp. infimum) of the Lévy process. Then we in particular have for each  $T \geq 0$  that

$$\mathbf{P}[W^* \geq u] \leq \mathbf{P}[S_T \geq u] + \mathbf{P}[I_T \geq 0]. \quad (3.8)$$

By [Ber96, Chapter VIII, Proposition 2], there exists a constant  $c_1 > 0$  such that

$$\mathbf{P}[I_T \geq 0] \leq c_1 T^{-1/\alpha}. \quad (3.9)$$

Moreover, [Ber96, Chapter VIII, Proposition 4] implies that there exists a constant  $c_2 > 0$  such that

$$\mathbf{P}[S_T \geq u] \leq c_2 T u^{-\alpha}. \quad (3.10)$$

Combining (3.8) with (3.9) and (3.10) and optimizing over  $T$  implies that there exists a constant  $c_3 > 0$  such that

$$\mathbf{P}[W^* \geq u] \leq c_3 u^{-\alpha/(1+\alpha)}. \quad (3.11)$$

This gives (3.7) for  $W_0 = 1$ . Scaling gives the result for general values of  $W_0 > 0$ .  $\square$

**Lemma 3.23.** *Suppose that  $W$  is an  $\alpha$ -stable CSBP. There exists a constant  $c_0 > 0$  depending only on  $\alpha$  such that*

$$\mathbf{P}[W_t \leq \delta] \leq \exp(-(\delta - c_0 W_0) t^{1/(1-\alpha)}) \quad \text{for all } \delta > 0.$$

*Proof.* Using the representation of the Laplace transform of an  $\alpha$ -stable CSBP given in (3.2), (3.3), we have for  $\lambda > 0$  that

$$\mathbf{P}[W_t \leq \delta] = \mathbf{P}[e^{-\lambda W_t} \geq e^{-\lambda \delta}] \leq e^{\lambda \delta} \mathbf{E}[e^{-\lambda W_t}] = e^{\lambda \delta - u_t(\lambda) W_0}.$$

where  $u_t(\lambda) = (\lambda^{1-\alpha} + (\alpha - 1)t)^{1/(1-\alpha)}$ . Taking  $\lambda = t^{1/(1-\alpha)}$  yields the result.  $\square$

For each  $s, u \geq 0$ , we let  $T_s^u$  be the smallest value of  $r$  that  $Z_s^r \geq u$ . On the event that  $T_s^u < \infty$ , we note that the same argument used to prove Proposition 3.12 implies that  $Z_t^{T_s^u}$  evolves as an  $\alpha$ -stable CSBP for  $t \geq s$  with initial value  $u$ .

**Lemma 3.24.** *There exists a constant  $c_0 > 0$  such that the following is true. Fix  $s > 0$ . For each  $u \geq 0$  and  $w, v > 0$  we have that*

$$\mathbf{P}[T_s^{u+v} - T_s^u \leq t \mid Z_s > w] \leq \exp(-c_0 v t^{-1/\alpha}). \quad (3.12)$$

*Proof.* Let  $\mathbf{n}$  be the excursion measure associated with an  $\alpha$ -stable Lévy process with only upward jumps from its running infimum. As explained in [Ber96, Chapter VIII.4], there exists a constant  $c_\alpha > 0$  depending only on  $\alpha$  such that  $\mathbf{n}[\zeta \geq t] = c_\alpha t^{-1/\alpha}$  where  $\zeta$  denotes the length of the excursion. This implies that in  $v$  units of local time, the number  $N$  of excursions with length at least  $t$  is distributed as a Poisson random variable with mean  $c_\alpha v t^{-1/\alpha}$ . Note that on the event that we have at least one such excursion, it is necessarily the case that  $T_s^{u+v} - T_s^u \geq t$ . Consequently, (3.12) follows from the explicit formula for the probability mass distribution for a Poisson random variable evaluated at 0.  $\square$

We turn to describe the setup for the proof of Proposition 3.21. We first assume that we have taken a modification of  $Z_s^r$  so that  $Z_t^{T_s^u}$  is càdlàg for every  $u, s \in \mathbf{Q}_+$  and  $t \geq s$ . Such a modification exists because each  $Z_t^{T_s^u}$  evolves as an  $\alpha$ -stable CSBP.

Fix  $s_0 > 0$ . Then we know that  $Z_t$  for  $t \geq s_0$  evolves as an  $\alpha$ -stable CSBP starting from  $Z_{s_0}$ . Fix  $\delta > 0$ . We inductively define stopping times as follows. First, we let  $n_1 = \lceil 4\delta^{-1}Z_{s_0} \rceil$ ,  $\delta_1 = Z_{s_0}/n_1$ , and let  $Z_t^{1,j} = Z_t^{T_{s_0}^{j\delta_1}} - Z_t^{T_{s_0}^{(j-1)\delta_1}}$  so that the  $Z^{1,j}$  for  $1 \leq j \leq n_1$  are independent  $\alpha$ -stable CSBPs defined on the time-interval  $[s_0, \infty)$  all with initial value  $\delta/5 \leq \delta_1 \leq \delta/4$  (unless  $n_1 = 1$ ). We then let

$$\tau_1 = \inf \left\{ t \geq s_0 : \max_{1 \leq j \leq n_1} Z_t^{1,j} \geq \delta/2 \right\}.$$

Assume that stopping times  $\tau_1, \dots, \tau_k$  and CSBPs  $Z^{j,1}, \dots, Z^{j,n_j}$  have been defined for  $1 \leq j \leq k$ . We then  $n_{k+1} = \lceil 4\delta^{-1}Z_{\tau_k} \rceil$ ,  $\delta_{k+1} = Z_{\tau_k}/n_{k+1}$ , and  $Z_t^{k+1,j} = Z_t^{T_{\tau_k}^{j\delta_{k+1}}} - Z_t^{T_{\tau_k}^{(j-1)\delta_{k+1}}}$ . Then the  $Z_t^{k+1,j}$  are independent  $\alpha$ -stable CSBPs defined on the time-interval  $[\tau_k, \infty)$  all with initial value  $\delta/5 \leq \delta_{k+1} \leq \delta/4$  (unless  $n_{k+1} = 1$ ). We then let

$$\tau_{k+1} = \inf \left\{ t \geq \tau_k : \max_{1 \leq j \leq n_{k+1}} Z_t^{k+1,j} \geq \delta/2 \right\}.$$

By further modifying  $Z$  if necessary, we may also assume that the processes  $Z_t^{k,j}$  are càdlàg.

We note that

$$n^* := \sup_j n_j \leq 1 + \frac{4}{\delta} \sup_{t \geq s_0} Z_t. \quad (3.13)$$

Combining (3.13) and Lemma 3.22, we see for constants  $c_0, \beta > 0$  that on the event  $\{Z_{s_0} \geq \delta\}$  we have

$$\mathbf{P}[n^* \geq M \mid Z_{s_0}] \leq c_0 \left( \frac{\delta M}{Z_{s_0}} \right)^{-\beta}. \quad (3.14)$$

**Lemma 3.25.** *For each  $\delta > 0$  and  $\delta < a < b < \infty$  there exists a constant  $c_0 > 0$  and a universal constant  $\beta > 0$  such that on the event  $\{Z_{s_0} \in [a, b]\}$  we have that*

$$\mathbf{P}[\tau_n \leq 1 \mid Z_{s_0}] \leq c_0 n^{-\beta}. \quad (3.15)$$

*Proof.* Throughout, we shall assume that we are working on the event  $\{Z_{s_0} \in [a, b]\}$ . By (3.14), we know that there exists constants  $c_0, \beta > 0$  such that

$$\mathbf{P}[\tau_n \leq 1 \mid Z_{s_0}] \leq \mathbf{P}[\tau_n \leq 1, n^* \leq M \mid Z_{s_0}] + c_0 \left( \frac{\delta M}{Z_{s_0}} \right)^{-\beta}. \quad (3.16)$$

We take  $M = n^{1/2} Z_{s_0} / \delta$  so that the error term on the right hand side of (3.16) is at most a constant times  $n^{-\beta/2}$ .

Let  $\mathcal{F}_t$  be the  $\sigma$ -algebra generated by  $Z_r^{T_s^u}$  for all  $s \leq r \leq t$  with  $u, s, r \in \mathbf{Q}_+$ . We claim that, given  $\mathcal{F}_{\tau_k}$ , we have that  $\tau_{k+1} - \tau_k$  is stochastically dominated from below by a random variable  $\xi_k$  such that the probability that  $\xi_k$  is at least  $1/n_{k+1}$  is at least some constant  $p_0 > 0$  (which may depend on  $\delta$  but not  $n$ ). Upon showing this, (3.15) will follow by combining (3.16) with binomial concentration. We note that the claim is clear in the case that  $n_{k+1} = 1$ , so we now assume that  $n_{k+1} \geq 2$  and we let

$$\sigma_{k+1} = \inf \left\{ t \geq \tau_k : \min_{1 \leq j \leq n_{k+1}} Z_t^{k+1,j} \leq \delta/8 \right\} \quad \text{and} \quad \tilde{\tau}_{k+1} = \tau_{k+1} \wedge \sigma_{k+1}.$$

Since  $\tilde{\tau}_{k+1} \leq \tau_{k+1}$ , it suffices to prove the stochastic domination result for  $\tilde{\tau}_{k+1} - \tau_k$  in place of  $\tau_{k+1} - \tau_k$ .

By the Lamperti transform (Theorem 3.8), it suffices to show that the probability that  $n_{k+1}$  independent  $\alpha$ -stable Lévy processes, each starting from a common value in  $[\delta/5, \delta/4]$  and run for time  $8(\delta n_{k+1})^{-1}$ , all do not leave the interval  $[\delta/8, \delta/2]$  is at least some  $p_0 > 0$ . This, in turn, follows from [Ber96, Chapter VII, Corollary 2] and [Ber96, Chapter VIII, Proposition 4].  $\square$

*Proof of Proposition 3.21.* We assume that we are working with the modification of  $Z_s^r$  as defined just after the statement of Lemma 3.23. We will prove the result by showing that  $r \mapsto Z_r^r$  for  $r \in \mathbf{Q}_+$  is almost surely uniformly continuous with respect to the uniform topology. Throughout, we assume that  $s_0, \delta_0, \delta > 0$  are fixed and we let  $H_{s_0, \delta_0} = \{Z_{s_0} \in [\delta_0/2, \delta_0]\}$ . Also,  $c_j > 0$  will denote a constant (which can depend on  $s_0, \delta_0, \delta$ ).

For each  $\ell \in \mathbf{N}$  and  $\Delta > 0$  we let

$$F_{\ell, \Delta}^\delta = \bigcap_k \left\{ T_{s_0 + \ell\Delta}^{k\delta^2} - T_{s_0 + \ell\Delta}^{(k-1)\delta^2} \geq \Delta^\alpha \delta^{3\alpha} \right\}.$$

Lemma 3.22 and Lemma 3.24 together imply that

$$\mathbf{P}[(F_{\ell,\Delta}^\delta)^c \mid H_{s_0,\delta_0}] \leq c_0 M^{-\beta} + \frac{M}{\delta^2} \exp(-c_1 \Delta^{-1} \delta^{-1}). \quad (3.17)$$

By optimizing over  $M$ , it follows from (3.17) that

$$\mathbf{P}[(F_{\ell,\Delta}^\delta)^c \mid H_{s_0,\delta_0}] \leq \exp(-c_2 \Delta^{-1} \delta^{-1}). \quad (3.18)$$

Let  $\zeta = \inf\{s > 0 : Z_s = 0\}$ . By performing a union bound over  $\ell$  values, from (3.18) and Lemma 3.11 we have with  $F_\Delta^\delta = \cap_\ell F_{\ell,\Delta}^\delta$  that

$$\mathbf{P}[(F_\Delta^\delta)^c \mid H_{s_0,\delta_0}] \leq \frac{T}{\Delta} \exp(-c_3 \Delta^{-1} \delta^{-1}) + c_4 T^{1/(1-\alpha)}. \quad (3.19)$$

Optimizing (3.19) over  $T$  values implies that

$$\mathbf{P}[(F_\Delta^\delta)^c \mid H_{s_0,\delta_0}] \leq \exp(-c_5 \Delta^{-1} \delta^{-1}). \quad (3.20)$$

Therefore the Borel-Cantelli lemma implies that with  $\Delta = e^{-j}$ , for each  $\delta > 0$  there almost surely exists  $j_F^\delta \in \mathbf{N}$  (random) such that  $j \geq j_F^\delta$  implies that  $F_\Delta^\delta$  occurs.

We also let  $G_{\ell,\Delta}^\delta$  be the event that for every  $s \in \mathbf{Q}$  with  $s \in [s_0 + (\ell - 1)\Delta, s_0 + \ell\Delta]$  and  $t_1, t_2 \in \mathbf{Q}_+$  with  $t_2 \geq t_1$  such that  $Z_s^{t_2} - Z_s^{t_1} \geq \delta$  we have that  $Z_{s_0+\ell\Delta}^{t_2} - Z_{s_0+\ell\Delta}^{t_1} \geq 2\delta^2$ . We claim that it suffices to show that

$$\mathbf{P}[(G_{\ell,\Delta}^\delta)^c \mid H_{s_0,\delta_0}] \leq \exp(-c_6 \delta \Delta^{1/(1-\alpha)}). \quad (3.21)$$

Letting  $G_\Delta^\delta = \cap_\ell G_{\ell,\Delta}^\delta$ , we have from (3.21) by performing a union bound over  $\ell$  values (and applying Lemma 3.11 as in the argument to prove (3.20)) that

$$\mathbf{P}[(G_\Delta^\delta)^c \mid H_{s_0,\delta_0}] \leq \exp(-c_7 \delta \Delta^{1/(1-\alpha)}).$$

Thus the Borel-Cantelli lemma implies that with  $\Delta = e^{-j}$ , for each  $\delta > 0$  there almost surely exists  $j_G^\delta \in \mathbf{N}$  (random) such that  $j \geq j_G^\delta$  implies that  $G_\Delta^\delta$  occurs. In particular, this implies that for every  $s \geq s_0$  with  $s \in \mathbf{Q}$  and  $t_1, t_2$  such that  $Z_s^{t_2} - Z_s^{t_1} \geq \delta$  we have that  $Z_{s_0+\ell\Delta}^{t_2} - Z_{s_0+\ell\Delta}^{t_1} \geq 2\delta^2$  where

$$\ell = \lceil (s - s_0)/\Delta \rceil \quad (3.22)$$

for  $\Delta = e^{-j}$  and  $j \geq j_G^\delta$ .

Assume that  $j \geq j_F^\delta \vee j_G^\delta$  so that with  $\Delta = e^{-j}$  we have that both  $F_\Delta^\delta$  and  $G_\Delta^\delta$  occur. Suppose that  $t_1, t_2, s$  are such that  $Z_s^{t_2} - Z_s^{t_1} \geq \delta$ . With  $\ell$  as in (3.22), it must be true that  $Z_{s_0+\ell\Delta}^{t_2} - Z_{s_0+\ell\Delta}^{t_1} \geq 2\delta^2$ . This implies that there exists  $k$  such that

$$T_{s_0+\ell\Delta}^{k\delta^2} \leq t_2 \quad \text{and} \quad T_{s_0+\ell\Delta}^{(k-1)\delta^2} \geq t_1. \quad (3.23)$$

Rearranging (3.23), we thus have that

$$t_2 - t_1 \geq T_{s_0+\ell\Delta}^{k\delta^2} - T_{s_0+\ell\Delta}^{(k-1)\delta^2} \geq \Delta^\alpha \delta^{3\alpha}. \quad (3.24)$$

This implies that  $r \mapsto Z^r|_{[s_0, \infty)}$  for  $r \in \mathbf{Q}_+$  has a certain modulus of continuity with respect to the uniform topology. In particular,  $r \mapsto Z^r|_{[s_0, \infty)}$  for  $r \in \mathbf{Q}_+$  is uniformly continuous with respect to the uniform topology hence extends continuously. The result then follows (assuming (3.21)) since  $s_0, \delta_0, \delta > 0$  were arbitrary.

To finish the proof, we need to establish (3.21). For each  $j$ , we let

$$E_j = \{\tau_j \geq s_0 + \Delta\} \cup \left( \bigcap_{k=1}^{n_j} \{Z_{s_0+\Delta}^{j,k} \geq 2\delta^2\} \right).$$

We first claim that  $G_{1,\Delta}^\delta \supseteq \bigcap_{j=1}^n E_j$ . To see this, fix a value of  $s \in [s_0, s_0 + \Delta]$  and suppose that  $Z_s^{t_2} - Z_s^{t_1} \geq \delta$ . Let  $j$  be such that  $\tau_j \leq s < \tau_{j+1}$  and let  $k$  be the first index so that  $Z_s^{j,1} + \dots + Z_s^{j,k} \geq Z_s^{t_1}$ . Since  $Z_s^{j,i} \leq \delta/2$  for all  $i$ , it follows that  $Z_s^{j,1} + \dots + Z_s^{j,k+1} \leq Z_s^{t_2}$ . Consequently,  $Z_{s_0+\Delta}^{t_2} - Z_{s_0+\Delta}^{t_1} \geq Z_{s_0+\Delta}^{j,k+1}$ . The claim follows because we have that  $Z_{s_0+\Delta}^{j,k+1} \geq 2\delta^2$  on  $\bigcap_j E_j$ .

Thus to finish the proof, it suffices to show that

$$\mathbf{P}[\bigcup_{j=1}^n E_j^c \mid H_{s_0, \delta_0}] \leq \exp(-c_8 \delta \Delta^{1/(1-\alpha)}) \quad (3.25)$$

(as the same analysis leads to the same upper bound for  $\mathbf{P}[(G_{\ell,\Delta}^\delta)^c \mid H_{s_0, \delta_0}]$  for other  $\ell$  values). To this end, Lemma 3.23 implies that

$$\mathbf{P}[E_j^c, Z^* \leq \delta M/4 \mid H_{s_0, \delta_0}] \leq M \exp(-c_9 \delta \Delta^{1/(1-\alpha)}). \quad (3.26)$$

Thus applying a union bound together with (3.26) in the second step below, we have for each  $n \in \mathbf{N}$  that

$$\begin{aligned} & \mathbf{P}[\bigcup_j E_j^c, Z^* \leq \delta M/4 \mid H_{s_0, \delta_0}] \\ &= \mathbf{P}[\bigcup_j E_j^c, Z^* \leq \delta M/4, \tau_n \geq \Delta \mid H_{s_0, \delta_0}] + \mathbf{P}[\tau_n \leq \Delta \mid H_{s_0, \delta_0}] \\ &\leq nM \exp(-c_{10} \delta \Delta^{1/(1-\alpha)}) + c_{11} n^{-\beta} \quad (\text{by Lemma 3.25}) \end{aligned} \quad (3.27)$$

Applying Lemma 3.22, we therefore have that

$$\mathbf{P}[\bigcup_j E_j^c \mid H_{s_0, \delta_0}] \leq nM \exp(-c_{12} \delta \Delta^{1/(1-\alpha)}) + c_{13} n^{-\beta} + c_{14} (\delta M)^{-\beta}. \quad (3.28)$$

Optimizing over  $n$  and  $M$  values implies (3.25).  $\square$

*Proof of Proposition 3.20.* As we remarked earlier, it suffices to show the equivalence of the quotient topology described in Figure 3.6 with the quotient topology described in Figure 3.8. We will show this by arguing that  $Z_s^r$  induces a continuous map  $\tilde{Z}_s^r$  from Figure 3.6 to Figure 3.8 which takes equivalence classes to equivalence classes in a

bijjective manner. This will prove the result because this map then induces a bijection which is continuous from the space which arises after quotienting as in Figure 3.6 to the space which arises after quotienting as in Figure 3.8 and the fact that bijections which are continuous from one compact space to another are homeomorphisms.

Fix a height  $s$  as in Figure 3.6 and let  $t$  be corresponding height as in Figure 3.4. If  $t$  is not a jump height for  $Z$ , then we take  $\tilde{Z}_s^r = Z_t^r/Z_t$ . Suppose that  $t$  is a jump height for  $Z$ . If  $s$  is the  $y$ -coordinate of the top (resp. bottom) of the corresponding rectangle, we take  $\tilde{Z}_s^r = \lim_{q \downarrow t} Z_q^r/Z_q$  (resp.  $\tilde{Z}_s^r = \lim_{q \uparrow t} Z_q^r/Z_q$ ). Suppose that  $s$  is between the bottom and the top of the corresponding rectangle. If  $(s, r)$  is outside of the interior of the rectangle, then we take  $\tilde{Z}_s^r = Z_t^r/Z_t$ . Note that in this case we have that the limit  $\lim_{q \rightarrow t} Z_q^r/Z_q$  exists and is equal to  $Z_t^r/Z_t$ . Let  $s_1$  (resp.  $s_2$ ) be the  $y$ -coordinate of the bottom (resp. top) of the rectangle. If  $(s, r)$  is in the rectangle, then we take  $\tilde{Z}_s^r$  to be given by linearly interpolating between the values of  $\tilde{Z}_{s_1}^r$  and  $\tilde{Z}_{s_2}^r$ . That is,

$$\tilde{Z}_s^r = \frac{s_2 - s}{s_2 - s_1} \tilde{Z}_{s_1}^r + \frac{s - s_1}{s_2 - s_1} \tilde{Z}_{s_2}^r.$$

By the continuity properties of  $Z$  given in Proposition 3.21 and the construction of  $\tilde{Z}$ , we have that the map  $(s, r) \mapsto \tilde{Z}_s^r$  is continuous.

Observe that  $\tilde{Z}$  is constant on the equivalence classes as defined in Figure 3.6. This implies that  $\tilde{Z}$  induces a continuous map from the topological space one obtains after quotienting by the equivalence relation as in Figure 3.6 into Figure 3.8 (not yet quotiented). As  $\tilde{Z}$  bijectively takes equivalence classes as in Figure 3.6 to equivalence classes as in Figure 3.8, it follows that  $\tilde{Z}$  in fact induces a bijection which is continuous from the quotient space as in Figure 3.6 to the quotient space as in Figure 3.8. The result follows because, as we mentioned earlier, a bijection which is continuous from one compact space to another is a homeomorphism.  $\square$

### 3.8 Recovering embedding from geodesic tree quotient

We now turn to show that the embedding of the Lévy net into  $\mathbf{S}^2$  is unique up to a homeomorphism of  $\mathbf{S}^2$ . Recall that a set is called *essentially 3-connected* if deleting two points always produces either a connected set, a set with two components one of which is an open arc, or a set with three components which are all open arcs. In particular, every 3-connected set is essentially 3-connected. Suppose that a compact topological space  $K$  can be embedded into  $\mathbf{S}^2$  and that  $\phi_1: K \rightarrow \mathbf{S}^2$  is such an embedding. It is then proved in [RT02] that  $K$  is essentially 3-connected if and only if for every embedding  $\phi: K \rightarrow \mathbf{S}^2$ , there is a homeomorphism  $h: \mathbf{S}^2 \rightarrow \mathbf{S}^2$  such that  $\phi = h \circ \phi_1$ .<sup>9</sup>

<sup>9</sup>It is clear from our construction that when  $K$  is a Lévy net there exists at least one embedding of  $K$  into  $\mathbf{S}^2$ . More generally, it is shown in [RRT14] that a compact and locally connected set  $K$  is homeomorphic to a subset of  $\mathbf{S}^2$  if and only if it contains no homeomorph of  $K_{3,3}$  or  $K_5$ .

**Proposition 3.26.** *For each  $\alpha \in (1, 2)$ , the Lévy net is a.s. 3-connected. Hence by [RT02] it can a.s. be embedded in  $\mathbf{S}^2$  in a unique way (up to a homeomorphism).*

*Proof.* Suppose that  $W$  is an instance of the Lévy net and assume for contradiction that  $W$  is not 3-connected. Then there exists distinct points  $x, y \in W$  such that  $W \setminus \{x, y\}$  is not connected. This implies that we can write  $W \setminus \{x, y\} = A \cup B$  for  $A, B \subseteq W$  disjoint and  $A, B \neq \emptyset$ . We assume that  $W$  has been embedded into  $\mathbf{S}^2$ . Let  $\tilde{A}$  (resp.  $\tilde{B}$ ) be given by  $A$  (resp.  $B$ ) together with all of the components of  $\mathbf{S}^2 \setminus W$  whose boundary is entirely contained in  $A$  (resp.  $B$ ). Then  $\tilde{A}, \tilde{B}$  are disjoint and we can write  $\mathbf{S}^2$  as a disjoint union of  $\tilde{A}, \tilde{B}, \{x\}, \{y\}$ , and the components of  $\mathbf{S}^2 \setminus W$  whose boundary has non-empty intersection with both  $A$  and  $B$ . Suppose that  $C$  is such a component. Then there exists a point  $w \in \partial C$  which is not in  $\tilde{A}$  or  $\tilde{B}$ . That is, either  $x \in \partial C$  or  $y \in \partial C$ .

Note that  $\mathbf{S}^2 \setminus (\tilde{A} \cup \tilde{B} \cup \{x, y\})$  must have at least two distinct components  $C_1, C_2$  (for otherwise  $\tilde{A}, \tilde{B}$  would not be disjoint). If either  $x$  or  $y$  is in  $\partial C_1 \cap \partial C_2$  then we have a contradiction because the distance of both  $\partial C_1$  and  $\partial C_2$  to the root of  $W$  must be the same but (in view of Figure 3.8) we know that the metric exploration from the root to the dual root in  $W$  does not separate more than one component from the dual root at any given time. If  $\partial C_1 \cap \partial C_2$  does not contain either  $x$  or  $y$ , then there must be a third component  $C_3$  of  $\mathbf{S}^2 \setminus (\tilde{A} \cup \tilde{B} \cup \{x, y\})$ . This leads to a contradiction because then (by the pigeon hole principle) either  $\partial C_1 \cap \partial C_3$  or  $\partial C_2 \cap \partial C_3$  contains either  $x$  or  $y$ .  $\square$

We are now going to use that the Lévy net a.s. has a unique embedding into  $\mathbf{S}^2$  up to homeomorphism to show that the Lévy net almost surely determines the Lévy excursion  $X$  used to generate it.

**Proposition 3.27.** *For each  $\alpha \in (1, 2)$ , the  $\alpha$ -stable Lévy excursion  $X$  used in the construction of the Lévy net is a.s. determined by the Lévy net together with an orientation.*

*Proof.* By Proposition 3.26, we know that the embedding of the Lévy net into  $\mathbf{S}^2$  is a.s. determined up to homeomorphism; we assume throughout that we have fixed an orientation so that the embedding is determined up to orientation preserving homeomorphism. Recall that the jumps of  $Z_s$  are in correspondence with those made by  $X_t$ . Thus, if we can show that the jumps of  $Z$  are determined by the Lévy net, then we will get that the jumps of  $X$  are determined by the Lévy net. More generally, if we can show that the processes  $Z_t^{T_s^u}$  are determined by the Lévy net, then we will be able to determine the jumps of  $X$  and their ordering. This will imply the result because  $X$  is a.s. determined by its jumps and the order in which they are made. For simplicity, we will just show that  $Z_s$  is a.s. determined by the Lévy net. The proof that  $Z_t^{T_s^u}$  is a.s. determined follows from the same argument.

Let  $x$  (resp.  $y$ ) denote the root (resp. dual root) of the Lévy net. Fix  $r > 0$  and condition on  $R = d(x, y) - r > 0$ . We let  $\partial B(x, R)$  be the boundary of the ball of radius

$R$  centered at  $x$  in the geodesic tree in the Lévy net. Fix  $\epsilon > 0$ . We then fix points  $z_1, \dots, z_{N_\epsilon} \in \partial B(x, R)$  as follows. We let  $z_1$  be the unique point on  $\partial B(x, R)$  which is visited by the unique geodesic from  $x$  to  $y$ . For  $j \geq 2$  we inductively let  $z_j$  be the first clockwise point on  $\partial B(x, R)$  (recall that we have assumed that the Lévy net has an orientation) such that the geodesic from  $z_j$  to  $x$  merges with the geodesic from  $z_{j-1}$  to  $x$  at distance  $\epsilon$ . As the embedding of the Lévy net into  $\mathbf{S}^2$  is a.s. determined up to (orientation preserving) homeomorphism, it follows that  $z_1, \dots, z_{N_\epsilon}$  is a.s. determined by the Lévy net.

Conditional on the boundary length  $L_r$  of  $\partial B(x, R)$ , we claim that  $N_\epsilon$  is distributed as a Poisson random variable  $Z_\epsilon$  with mean  $m_\epsilon^{-1} L_r$  where  $m_\epsilon = ((\alpha - 1)\epsilon)^{1/(\alpha-1)}$ . The desired result will follow upon showing this because then

$$\mathbf{E}[m_\epsilon Z_\epsilon \mid L_r] = L_r \quad \text{and} \quad \text{var}[m_\epsilon Z_\epsilon \mid L_r] = m_\epsilon L_r \rightarrow 0 \quad \text{as} \quad \epsilon \rightarrow 0.$$

To compute the conditional distribution of  $N_\epsilon$  given  $L_r$ , it suffices to show that the boundary length of the spacings are given by i.i.d. exponential random variables with mean  $m_\epsilon$  given  $L_r$ . We will establish this by using that  $L_r$  evolves as an  $\alpha$ -stable CSBP as  $r$  varies. Fix  $\delta > 0$  and let  $(Z_j^\delta)$  be a sequence of i.i.d.  $\alpha$ -stable CSBPs, each starting from  $\delta$ . Then the CSBP property (3.1) implies that the process  $s \mapsto L_{r+s}$  is equal in distribution to  $Z_1^\delta + \dots + Z_n^\delta + \tilde{Z}^\delta$  where  $n = \lfloor L_r/\delta \rfloor$  and  $\tilde{Z}^\delta$  is an independent  $\alpha$ -stable CSBP starting from  $L_r - \delta n < \delta$ . We then define indices  $(j_k^\delta)$  inductively as follows. We let  $j_1^\delta$  be the first index  $j$  such that the amount of time it takes the  $\alpha$ -stable CSBP  $Z_1^\delta + \dots + Z_j^\delta$  (which starts from  $j\delta$ ) to reach 0 is at least  $\epsilon$ . Assuming that  $j_1^\delta, \dots, j_k^\delta$  have been defined, we take  $j_{k+1}^\delta$  to be the first index  $j$  such that the amount of time that it takes the  $\alpha$ -stable CSBP  $Z_{j_k^\delta+1}^\delta + \dots + Z_j^\delta$  (which starts from  $\delta(j - (j_k^\delta + 1))$ ) to reach 0 is at least  $\epsilon$ .

Note that the random variables

$$Z_k^\delta = Z_{j_{k-1}^\delta+1}^\delta + \dots + Z_{j_k^\delta}^\delta$$

are i.i.d. We claim that the law of  $Z_1^\delta$  converges in distribution as  $\delta \rightarrow 0$  to that of an exponential random variable with mean  $m_\epsilon$ . To see this, we fix  $u > 0$ , let  $\tilde{u} = \delta \lfloor u/\delta \rfloor$ , and let  $W$  be an  $\alpha$ -stable CSBP starting from  $\tilde{u}$ . Then we have that

$$\mathbf{P}[Z_1^\delta \geq u] = \mathbf{P}[W_\epsilon = 0] = \lim_{\lambda \rightarrow \infty} \mathbf{E}[\exp(-\lambda W_\epsilon)]. \quad (3.29)$$

As in the proof of Lemma 3.23, using the representation of the Laplace transform of an  $\alpha$ -stable CSBP given in (3.2), (3.3), the Laplace transform on the right hand side of (3.29) is given by

$$\exp(-(\lambda^{1-\alpha} + ((\alpha - 1)\epsilon)^{1/(1-\alpha)} \tilde{u})).$$

Therefore the limit on the right hand side of (3.29) is given by  $\exp(-m_\epsilon^{-1} \tilde{u})$ . This, in turn, converges to  $\exp(-m_\epsilon^{-1} u)$  as  $\delta \rightarrow 0$ , which proves the result.  $\square$

## 4 Tree gluing and the Brownian map

### 4.1 Gluing trees given by Brownian-snake-head trajectory

We now briefly review the standard construction of the Brownian map (see e.g. [Le 14, Section 3.4]). Our first task is to identify the measures  $\mu_{\text{SPH}}^1$  and  $\mu_{\text{SPH}}^2$  discussed in Section 1.5 with certain Brownian snake excursion measures. In fact, this is the way  $\mu_{\text{SPH}}^1$  and  $\mu_{\text{SPH}}^2$  are formally constructed and defined.

Let  $\mathcal{S}$  be the set of all finite paths in  $\mathbf{R}$  beginning at 0. An element of  $\mathcal{S}$  is a continuous map  $w: [0, \zeta] \rightarrow \mathbf{R}$  for some value  $\zeta = \zeta(w) \geq 0$  that depends on  $w$ . We refer to  $\mathcal{S}$  as the *snake space* and visualize an element of  $\mathcal{S}$  as the ( $y$ -to- $x$  coordinate) graph  $\{(w(y), y) : y \in [0, \zeta]\}$ . As illustrated in Figure 4.1, such a graph may be viewed as a “snake” with a body beginning at  $(0, 0)$  and ending at the “head,” which is located at  $(w(\zeta), \zeta)$ . From this perspective,  $\zeta = \zeta(w)$  is the *height* of the snake, which is also the *vertical head coordinate*, and  $w(\zeta)$  is the *horizontal head coordinate*.

A distance on  $\mathcal{S}$  is given by

$$d(w, w') = |\zeta(w) - \zeta(w')| + \sup_{t \geq 0} |w(t \wedge \zeta(w)) - w'(t \wedge \zeta(w'))|. \quad (4.1)$$

There is a natural way to create an excursion into  $\mathcal{S}$  beginning and ending at the zero snake. To do so, let  $Y_t$  be a Brownian excursion into  $[0, \infty)$  (starting and ending at zero). Then  $Y_t$  encodes a continuum random tree (CRT)  $\mathcal{T}$  [Ald91a, Ald91b, Ald93], together with a map  $\phi: [0, T] \rightarrow \mathcal{T}$  that traces the boundary of  $\mathcal{T}$  in order. Once one is given the  $Y_t$  process, one may construct a Brownian process  $Z_\tau$  indexed by  $\tau \in \mathcal{T}$  and write  $X_t = Z_{\phi(t)}$ . Precisely, we take  $X_t$  to be the Gaussian process for which  $X_0 = 0$  and

$$\text{Cov}(X_s, X_t) = \inf \{Y_r : r \in [s, t]\}. \quad (4.2)$$

An application of the Kolmogorov-Centsov theorem implies that  $X$  has a Hölder continuous modification; see, e.g. [Le 14, Section 3.4]. The RHS of (4.2) describes the length of the intersection of the two tree branches that begin at  $\phi(0)$  and end at  $\phi(s)$  or  $\phi(t)$ . Given the  $(X_t, Y_t)$  process, it is easy to draw the body of the snake in Figure 4.1 for any fixed time  $t \in [0, T]$ . To do so, for each value  $b < Y_t$ , one plots the point  $(X_s, b)$  where  $s$  is the last time before  $t$  at which the  $Y$  process reached height  $s$ . Note also that if one takes  $s'$  to be the first time after  $t$  when the  $Y$  process reaches  $b$ , then we must have  $X_{s'} = X_s$ . Intuitively speaking, as  $Y_t$  goes down, the snake head retraces the snake body; as  $Y_t$  goes up, new randomness determines the left-right fluctuations; see the discrete analog in Figure 4.2. As discussed in the captions of Figure 4.1 and Figure 4.2, this evolution can be understood as a diffusion process on  $\mathcal{S}$ .

We now consider two natural infinite measures on the space of excursions into  $\mathcal{S}$ . The first is the measure described informally in the caption to Figure 4.1. To construct this,

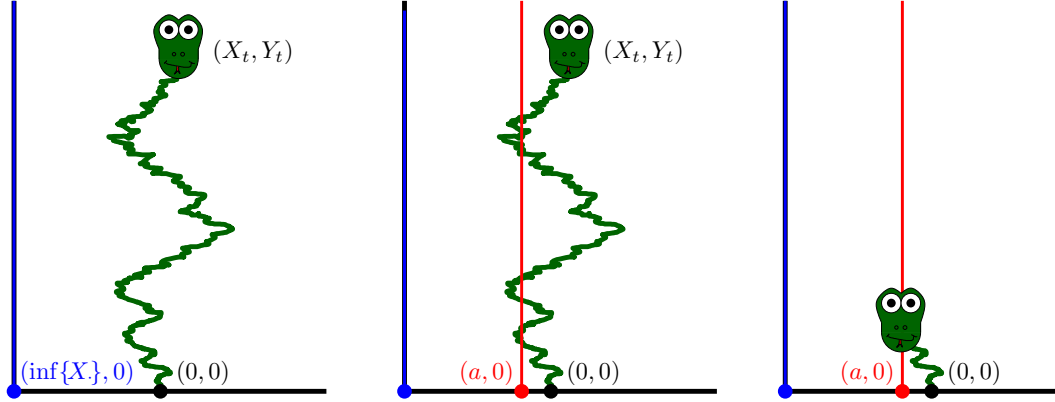


Figure 4.1: *Gluing an asymmetric pair of trees.* The doubly marked Brownian map construction is the same as the construction in Figure 3.1 except that the pair  $(X_t, Y_t)$  is produced from a Brownian snake excursion instead of a Brownian excursion. In this setup  $Y_t$  is chosen from the (infinite) Brownian excursion measure and  $X_t$  is a Brownian motion indexed by the corresponding CRT. The process  $(X_t, Y_t)$  determines a trajectory in the snake space  $\mathcal{S}$ . **Left:** At a given time  $t$ , the “snake” has a body that looks like the graph of a Brownian motion (rotated 90 degrees). The blue vertical line represents the leftmost point reached by the process  $(X_t, Y_t)$ . The (single) time at which the blue line is hit corresponds to the Brownian map root. At all other times, distance from the blue line represents distance from the root in the Brownian map metric. **Middle:** Suppose  $\inf\{X\} < a < 0$  and consider the vertical line through  $(a, 0)$ . This divides the snake space  $\mathcal{S}$  into the subspace  $\mathcal{S}_{>a}$  of snakes not hit by the red line (except at the origin if  $a = 0$ ) and the complementary subspace  $\mathcal{S}_{\leq a} = \mathcal{S} \setminus \mathcal{S}_{>a}$  of snakes that *are* hit. **Right:** If a snake is hit by the red line, then it has a unique “ancestor snake” whose body lies entirely to the right of the red line and whose head lies on the red line. A snake lies on the boundary of  $\mathcal{S}_{>a}$  if and only if it has this form. The distance from a snake in  $\mathcal{S}_{\leq a}$  to  $\mathcal{S}_{>a}$  (in terms of the metric on  $\mathcal{S}$ , not the Brownian map metric) is the difference in head height between itself and this ancestor. This distance evolves as a Brownian motion in the snake space diffusion.

first we define  $\mathbf{n}$  to be the natural Brownian excursion measure (see [RY99, Chapter XII] for more detail on the construction of  $\mathbf{n}$ ). Each such excursion comes with a terminal time  $T$  such that  $Y_0 = Y_T = 0$ ,  $Y_t > 0$  for  $t \in (0, T)$ , and  $Y_t = 0$  for all  $t \geq T$ . We recall that the excursion measure is an infinite measure that can be constructed as follows. Define  $\mathbf{n}_\epsilon$  to be  $\epsilon^{-1}$  times the probability measure on one-dimensional Brownian paths started at  $\epsilon$ , stopped the first time they hit zero. Note that this measure assigns unit mass to the set of paths that reach 1 before hitting zero. The measure  $\mathbf{n}$  is obtained by taking the weak limit of the  $\mathbf{n}_\epsilon$  measures as  $\epsilon \rightarrow 0$  (using the topology of uniform convergence of paths, say). Note that for each  $a > 0$  the  $\mathbf{n}$  measure of the set of paths that reach level  $a$  is exactly  $a^{-1}$ . Moreover, if one normalizes  $\mathbf{n}$  to make it a probability

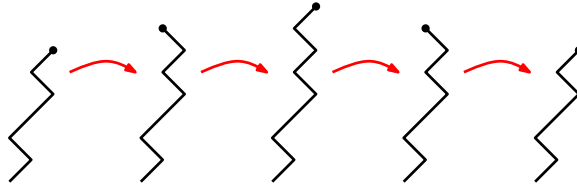


Figure 4.2: A discrete analog of the snake space diffusion process. In this model one tosses a fair coin at each step to decide whether the snake shrinks (we delete the top edge) or grows (an independent fair coin to decide whether we add a left or right directed edge to the top). A number of planar map models are known to be encoded by close variants of the discrete snake shown here. The microscopic rules depend on the model (triangulations, quadrangulations, etc.) but the scaling limit is the snake space diffusion in each case.

on this set of paths, then one finds that the law of the path after the first time it hits  $a$  is simply that of an ordinary Brownian motion stopped when it hits zero. Now that we have defined  $\mathbf{n}$ , we define  $\Pi$  to be a measure on excursions into  $\mathcal{S}$  such that the induced measure on  $Y_t$  trajectories is  $\mathbf{n}$ , and given the  $Y_t$  trajectory, the conditional law of  $X_t$  is that of the Brownian process indexed by the CRT encoded by  $Y_t$  (i.e., with covariance as in (4.2)).

Given a sample from  $\Pi$ , the tree encoded by  $X_t$  is the tree of geodesics drawn from all points to a fixed **root**, which is the value of  $\phi$  at the point  $t$  that minimizes  $X_t$ . The tree  $\mathcal{T}$  described by  $Y_t$  (the dual tree) has the law of a CRT, and  $Y_t$  describes the distance in  $\mathcal{T}$  from the dual root (which corresponds to time 0 or equivalently time  $T$ , which is the time when  $Y_t$  is minimal).

Note that for any time  $t$ , we can define the *snake* to be the graph of the function from  $y \in [0, Y_t]$  to  $x$  that sends a point  $y$  to the value of the Brownian process at the point on  $\mathcal{T}$  that is  $y$  units along the branch in  $\mathcal{T}$  from  $\phi(0)$  to  $\phi(t)$ .

As in Figure 4.1, for each  $a$  we let  $\mathcal{S}_{>a}$  be the subspace of  $\mathcal{S}$  which consists of those snakes  $w$  such that  $w(t) > a$  for all  $t \in [0, \zeta]$ . That is,  $w \in \mathcal{S}_{>a}$  if and only if its body lies to the right of the vertical line through  $(a, 0)$ . We also let  $\mathcal{S}_{\leq a} = \mathcal{S} \setminus \mathcal{S}_{>a}$ .

Now that we have defined  $\Pi$ , we define a related measure  $\Pi_+$  on the set of excursions into  $\mathcal{S}_{>0}$ , i.e., into the space of snakes whose bodies lie completely right of the vertical line through zero, except at their base point  $(0, 0)$ . This can be constructed in two ways: one is to consider a sample from  $\mathbf{n}$ , find the location on the corresponding CRT at which the  $X_t$  value is minimal, and then re-root the tree at that point. The other way is to consider the measure  $\mathbf{n}$  restricted to those excursions for which the minimum value of  $X_t$  is obtained within  $\epsilon$  time units of zero, and then take a limit (appropriately normalized) as  $\epsilon \rightarrow 0$ . The reader may check that these two approaches are equivalent as an exercise.

We next proceed to remind the reader how to associate an  $(X, Y)$  pair with a metric measure space structure. This will allow us to think of  $\Pi$  and  $\Pi_+$  as measures on  $\mathcal{M}$ . Roughly speaking, the procedure described in Figure 3.1 already tells us how to obtain a sphere from the pair  $(X, Y)$ . The points on the sphere are the equivalence classes from Figure 3.1. The tree described by  $X$  alone (the quotient of the graph of  $X$  w.r.t. the equivalence given by the chords under the graph) can be understood as a geodesic tree (which comes with a metric space structure), and we may construct the overall metric space as a quotient of this metric space (as defined in Section 2.2) w.r.t. the extra equivalence relations induced by  $Y$ , just as we did when defining the Lévy net (although in that case  $Y$  was used to describe the geodesic tree instead of  $X$ ).

An equivalent way to define the Brownian map is to first consider the CRT  $\mathcal{T}$  described by  $Y$ , and then define a metric and a quotient using  $X$  as the second step. This is the approach usually used in the Brownian map literature (see e.g. [Le 14, Section 3]) and we give a quick review of that construction here. Consider the function  $d^\circ$  on  $[0, T]$  defined by:

$$d^\circ(s, t) = X_s + X_t - 2 \max \left( \min_{r \in [s, t]} X_r, \min_{r \in [t, s]} X_r \right). \quad (4.3)$$

Here, we assume without loss of generality that  $s < t$  and define  $[t, s] = [0, s] \cup [t, T]$ . For  $a, b \in \mathcal{T}$ , we then set

$$d_{\mathcal{T}}^\circ(a, b) = \min \{ d^\circ(s, t) : \rho(s) = a, \rho(t) = b \} \quad (4.4)$$

where  $\rho: [0, T] \rightarrow \mathcal{T}$  is the natural projection map. Finally, for  $a, b \in \mathcal{T}$ , we set

$$d(a, b) = \inf \left\{ \sum_{j=1}^k d_{\mathcal{T}}^\circ(a_{j-1}, a_j) \right\} \quad (4.5)$$

where the infimum is over all  $k \in \mathbf{N}$  and  $a_0 = a, a_1, \dots, a_k = b$  in  $\mathcal{T}$ . We get a metric space structure by quotienting by the equivalence relation  $\cong$  defined by  $a \cong b$  if and only if  $d(a, b) = 0$  and we get a measure on the quotient space by taking the projection of Lebesgue measure on  $[0, T]$ . As mentioned in the introduction, it was shown by Le Gall and Paulin [LGP08] (see also [Mie08]) that the resulting metric space is a.s. homeomorphic to  $\mathbf{S}^2$  and that two times  $a$  and  $b$  are identified if and only if vertical red lines in Figure 3.1 (where  $X_t$  and  $Y_t$  are Brownian snake coordinates) belong to the same equivalence class as described in Figure 3.1. Thus the topological quotient described in Figure 3.1 is in natural bijection with the metric space quotient described above.

Given a sample from  $\Pi$ , the corresponding sphere comes with two special points corresponding to a snake whose head is at the leftmost possible value (the root), and the origin snake (the dual root). Indeed, if we let  $S$  denote the set of points on the sphere,  $\nu$  the measure,  $x$  the root, and  $y$  the dual root, then we obtain a doubly marked metric measure space  $(S, d, \nu, x, y)$  of the sort described in Section 2.4. We note that

by construction  $\Pi_+$  is supported on those snakes such that these two points coincide; in this case the sphere induced by a sample from  $\Pi_+$  comes with only a single marked point  $x$

In fact, we claim that  $\Pi$  induces a measure on  $(\mathcal{M}_{\text{SPH}}^2, \mathcal{F}^2)$ , and  $\Pi_+$  induces a measure on  $(\mathcal{M}_{\text{SPH}}^1, \mathcal{F}^1)$ . These measures are precisely the doubly and singly marked grand canonical ensembles of Brownian maps: i.e., they correspond to the measures  $\mu_{\text{SPH}}^2$  and  $\mu_{\text{SPH}}^1$  discussed in Section 1.3. There is a bit of an exercise involved in showing that the map from Brownian snake instances to  $(\mathcal{M}^k, \mathcal{F}^k)$  is measurable w.r.t. the appropriate  $\sigma$ -algebra on the space of Brownian snakes, so that  $\mu_{\text{SPH}}^1$  and  $\mu_{\text{SPH}}^2$  really are well defined as measures on  $(\mathcal{M}_{\text{SPH}}^1, \mathcal{M}^1)$  and  $(\mathcal{M}_{\text{SPH}}^2, \mathcal{M}^2)$ , respectively. In particular, one has to check that the distance-function integrals described in Section 2.4 (the ones used to define the Gromov-weak topology) are in fact measurable functions of the Brownian snake; one can do this by first checking that this is true when the metric is replaced by the function  $d^\circ$  discussed above, and then extending this to the approximations of  $d$  in which the distance between two points is the infimum of the length taken over paths made up of finitely many segments of the geodesic tree described by the process  $X$ . This is a straightforward exercise, and we will not include details here.

Note that switching from  $\Pi$  to  $\Pi_+$  corresponds in some sense to “conditioning” to have the two points coincide; intuitively, the probability that two randomly chosen points coincide should be inversely proportional to the area (i.e., the length of the excursion), so this should correspond to unweighting by the total area measure. (This can be made precise using  $\epsilon$  approximations as briefly discussed above.) Similarly, if one considers the measure  $\Pi_+$  and weights the measure by total area — and samples an extra marked point uniformly from that area — one obtains the measure  $\Pi$ .

Given a snake excursion  $s$  chosen from  $\Pi$ , we define the snake excursion  $\hat{s}$  so that its associated surface is the surface associated to  $s$  *rescaled* to have total area 1. In other words,  $\hat{s}$  is the snake whose corresponding head process is

$$(\hat{X}_t, \hat{Y}_t) = (\zeta^{-1/4} X_{\zeta t}, \zeta^{-1/2} Y_{\zeta t}).$$

Here we have scaled  $t$  by a factor of  $\zeta$ , we have scaled  $Y_t$  by a factor of  $\zeta^{-1/2}$ , and we have scaled  $X_t$  by a factor of  $\zeta^{-1/4}$ . An excursion  $s$  can be represented as the pair  $(\hat{s}, \zeta(s))$  where  $\zeta(s)$  represents the length of the excursion — or equivalently, the area of the corresponding surface. Since a sample from the Brownian excursion measure  $\mathbf{n}$  is an excursion whose length has law  $\zeta^{-3/2} d\zeta$  [RY99, Chapter XII], where  $d\zeta$  is Lebesgue measure on  $\mathbf{R}_+$ , we have the following:

**Proposition 4.1.** *If we interpret  $\Pi$  as a measure on pairs  $(\hat{s}, \zeta)$ , then  $\Pi$  can be written as  $\hat{\Pi} \otimes t^{-3/2} dt$ , where  $dt$  represents Lebesgue measure on  $\mathbf{R}_+$ , and  $\hat{\Pi}$  is a probability measure on the space of excursions of unit length. Similarly,  $\Pi_+$  has the form  $\hat{\Pi}_+ \otimes \zeta^{-5/2} d\zeta$  where  $d\zeta$  denotes Lebesgue measure on  $\mathbf{R}_+$ . The marginal law of the labeled CRT re-rooted at the root of the geodesic tree is the same under  $\Pi_+$  and  $\hat{\Pi}_+$ .*

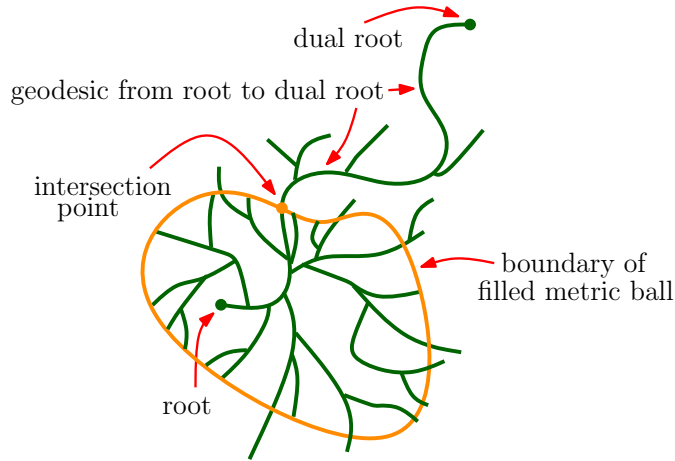


Figure 4.3: The snake trajectory corresponds to a path that traces the boundary of a (space-filling) tree of geodesics in the doubly marked Brownian map. The figure illustrates several branches of the geodesic tree (the tree itself is space-filling) and along with the outer boundary (as viewed from the dual root) of a radius- $r$  metric ball centered at the root. From a generic point on the doubly marked Brownian map, there is a unique path in the dual tree back to the dual root. The distances from the root vary as one moves along that path; this variation encodes the shape of the body of the snake, and the total quadratic variation along this path encodes the height of the snake’s head. During the snake trajectory (as the snake itself changes) the *first* and *last* times that the horizontal coordinate of the snake’s head reaches  $a = \inf\{X_t\} + r$  correspond to the intersection point (shown in orange) on the dual-root-to-root geodesic whose distance from the root is  $r$ . Intuitively, as one traces the boundary of the space-filling geodesic tree (beginning and ending at the dual root), the orange dot is the first and last point that the path visits within the closed orange disk.

## 4.2 Brownian maps and Lévy nets

The purpose of this subsection is to prove that the metric net of the doubly marked Brownian map has the law of a  $3/2$ -stable Lévy net. We will refer to the (countably many) components of the complement of this net as “bubbles” and will describe a one-to-one correspondence between these bubbles and the “holes” in the corresponding Lévy net. The two jump processes in Figure 3.7 correspond to different orders in which one might explore these holes. The first explores holes in a “depth-first” order — i.e., the order in which they are encountered by a path that traces the boundary of the geodesic tree; the second explores holes in a “breadth-first” order — i.e., in order of their distance from a root vertex. We will see what these two orderings look like within the context of the Brownian map, as constructed from a Brownian snake excursion.

In order to begin understanding the metric net of the Brownian map, we need a way to make sense of the boundary length measure on a metric ball within the Brownian

map. Observe that for any real number  $a < 0$ , the snake diffusion process has the property that if the snake lies in  $\mathcal{S}_{\leq a}$  at time  $t$ , then its distance (in the snake space metric as defined in (4.1)) from the boundary of  $\mathcal{S}_{>a}$  is given by  $Y_t - Y_s$ , where  $s$  is supremum of the set of times before  $t$  at which the snake was in  $\mathcal{S}_{>a}$ ; see Figure 4.1. This distance clearly evolves as a Brownian motion until the next time it reaches zero. Let us define  $i_a(t)$  to be the total time before  $t$  that the snake process spends inside  $\mathcal{S}_{>a}$ , and  $o_a(t) = t - i_a(t)$  the total amount of time before  $t$  that the snake process spends in  $\mathcal{S}_{\leq a}$ . Then we find that when we parameterize time by  $o_a(t)$ , this process is a positive, reflected Brownian motion, and hence has a well-defined notion of local time  $\ell_a(t)$  for any given value of  $a$  (see [RY99, Chapter VI] for more on the construction of Brownian local time).

In fact, it is not hard to see that a sample from  $\Pi$  may be obtained in two steps:

1. First sample the behavior of the snake restricted to  $\mathcal{S}_{>a}$ , parameterized by  $i_a(t)$ . We claim that this determines the local time  $\ell_a(t)$  as parameterized by  $i_a(t)$ . To see this, let  $Y_t^1$  be the difference between  $Y_t$  and the height of the ancestor snake head at time  $t$  (as in Figure 4.1), and define  $Y_t^2 = Y_t - Y_t^1$  so that  $Y_t = Y_t^1 + Y_t^2$ . As explained just above, we know that  $Y_t^1$  evolves as a reflected Brownian motion when we parameterize by  $o_a(t)$  time. Thus it follows that  $Y_t^1 - \ell_a(t)$  is a continuous martingale (see, e.g., the Itô-Tanaka formula). Consequently,  $Y_t^2 + \ell_a(t)$  is a martingale, and hence one can use the Doob-Meyer decomposition to recover this local time from the process  $Y_t^2$  as parameterized by  $i_a(t)$  time.
2. Then, conditioned on the boundary length, sample the set of excursions into  $\mathcal{S}_{\leq a}$  using a Poisson point process on the product of Lebesgue measure on  $[0, \ell_a(T)]$  (an interval which is now known, even though  $T$  is not itself yet determined) and  $\Pi$ . Note that each excursion is translated so that it is “rooted” at some point along the vertical line through  $(a, 0)$ , instead of at  $(0, 0)$ .

From this discussion, the following is easy to derive:

**Proposition 4.2.** *As  $a$  decreases, the quantity  $\ell_a(T)$  evolves as a  $3/2$ -stable CSBP.*

*Proof.* The proof is nearly the same as the proof of Proposition 3.12. One has only to verify that the process satisfies the hypotheses Proposition 3.10. Again, the scaling factor is obvious (one may rescale time by a factor of  $C^2$ , the  $Y_t$  process values by a factor of  $C$  and the  $X_t$  process values by a factor of  $C^{1/2}$ ); and the value of the  $\ell_a(T)$  process then scales by  $C$  and its time to completion scales by  $C^{1/2}$ , suggesting that the scaling hypothesis of Proposition 3.12 is satisfied with  $\alpha - 1 = 1/2$ , so that  $\alpha = 3/2$ . The CSBP property (3.1) is also immediate from construction.  $\square$

**Proposition 4.3.** *The jumps in  $\ell_a(T)$  are in one-to-one correspondence with the bubbles of the metric net from the root to the dual root of the Brownian map. If one keeps*

track of the location along the boundary at which each bubble root occurs, one obtains an object with the law of the marked process  $Z_s$  shown in Figure 3.7. In particular, conditioned on the process  $\ell_a(T)$ , the heights of the marks shown in Figure 3.7 are independent random variables, each chosen uniformly between 0 and the lower endpoint of the corresponding jump in  $\ell_a(T)$ .

*Proof.* If one conditions on the Brownian snake growth within the set  $\mathcal{S}_{>a}$ , one can resample the locations of the excursions into  $\mathcal{S}_{\leq a}$ . In particular (taking limits as  $a$  approaches a bubble root time, along the dyadic rationals say) we find that the location at which each bubble occurs with respect to the a.s. unique point on the boundary which is visited by the geodesic connecting the root and dual root is uniform, independently of everything else.  $\square$

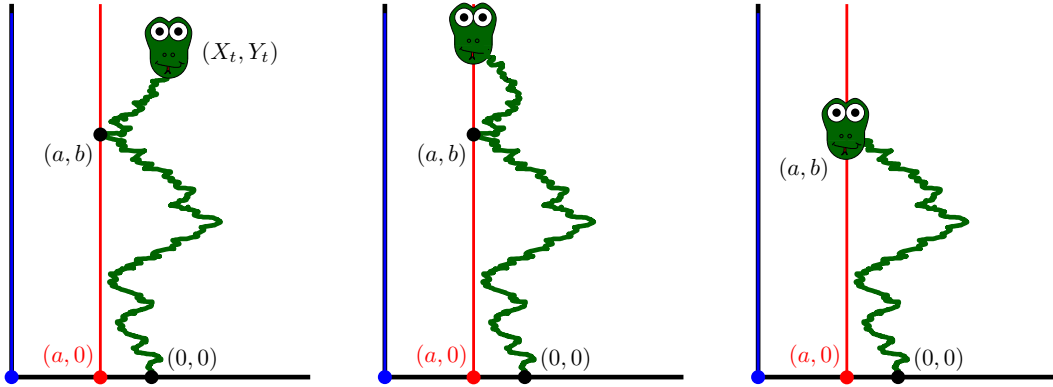


Figure 4.4: **Left:** the snake shown in Figure 4.1 with  $a$  shifted to the smallest value for which the red line intersects the snake, and the point of this first intersection marked as  $(a, b)$ . For almost all times  $t$ , the snake will have a unique minimum point of this kind; a.s., only countably many pairs  $(a, b)$  arise as minima for any snake in the trajectory. We let  $\mathcal{B}_{(a,b)}$  denote the collection of all snakes in the trajectory with leftmost point at  $(a, b)$ , and the head *not* at  $(a, b)$  itself; e.g., the left snake shown belongs to  $\mathcal{B}_{(a,b)}$ . The set  $\mathcal{B}_{(a,b)}$  represents a “bubble” of the corresponding doubly marked Brownian map i.e., an open component of the complement of the metric net between the root and the dual root. **Middle:** A snake on the bubble boundary  $\partial\mathcal{B}_{(a,b)}$ . **Right:** The “bubble root” of  $\mathcal{B}_{(a,b)}$ . (Note: not every snake whose head lies left of its body is a bubble root; there are a.s. only countably many such points in the trajectory, one per bubble.)

**Proposition 4.4.** *The metric net of a sample from  $\mu_{\text{SPH}}^2$  has the law of a 3/2-stable Lévy net. In this correspondence, the 3/2-stable CSBP excursion  $\ell_a(T)$  described above for a sample from  $\mu_{\text{SPH}}^2$  agrees with the 3/2-stable CSBP excursion  $Z_s$  described in Figure 3.7, up to an affine transformation relating  $a$  and  $s$ . Indeed, a sample  $(S, d, \nu, x, y)$  from  $\mu_{\text{SPH}}^2$  can be generated as follows: first sample an instance of the 3/2-stable Lévy net to be the metric net between  $x$  and  $y$ . Then glue a conditionally independent disk*

from a probability measure  $\mu_{\text{DISK}}^L$  for each hole in the Lévy net (which occurs in the canonical embedding of the Lévy net into  $\mathbf{S}^2$ ) where  $L$  is the boundary length of that hole and the gluing is done in a length-preserving way (and one defines the metric quotient in the usual way: as the largest metric compatible with the identification, see the end of Section 2.2).

*Proof.* The correspondence between the metric net and the  $3/2$ -stable Lévy net follows from Proposition 4.2 and Proposition 4.3. The problem is to condition on the metric net and consider the conditional law, given the metric net, of what happens inside each of the disks in the complement of the metric net. Each such disk can be understood as a set of the form  $\mathcal{B}_{(a,b)}$ , as in Figure 4.4. Let  $[t_1, t_2]$  be the time interval between the first and last times the snake on the right hand side of Figure 4.4 is hit. The snake process makes a number of excursions into  $\mathcal{S}_{\leq a}$  (as described in Figure 4.1) during this interval and there is a well defined local time corresponding to the time spent on the boundary of  $\mathcal{S}_{>a}$  during this interval, which corresponds to the length of the bubble boundary. One can produce a truncated snake process by “excising” from  $[t_1, t_2]$  all the time intervals in which the snake lies in  $\mathcal{S}_{\leq a}$ . The truncated process corresponds to an excursion into  $\mathcal{S}_{>a}$  that begins at  $(a, b)$  and reflects off the boundary of  $\mathcal{S}_{>a}$  (when the head is at position  $a$ ) for some amount of local time. It is not hard to see that conditioned on this amount of local time, one may resample (independently of the set of excursions into  $\mathcal{S}_{\leq a}$ , where the latter are interpreted as excursions modulo vertical translation) this truncated process. The metric disk produced by the truncated process is what we call  $\mu_{\text{DISK}}^L$ . From the definition, it is clear that its law depends only on the boundary length  $L$  and possibly one additional marked point on the boundary. This marked point corresponds to when the path which traces the geodesic tree first enters the corresponding disk in the Brownian map. (This is the point which corresponds to the snake on the right side of Figure 4.4.) However, the argument in Lemma 4.13 given below implies that the law  $\mu_{\text{DISK}}^L$  is given by unweighting the law of the complement of the metric ball which contains the dual root by the square of its boundary length. Since this latter law obviously does not have a marked boundary point, neither does  $\mu_{\text{DISK}}^L$ .  $\square$

*Remark 4.5.* In the case that  $\alpha = 3/2$ , we now have that up to time parameterization, both the process  $\ell$  defined for Brownian maps and the process  $Z$  defined for the Lévy net can be understood as descriptions of the natural boundary length measure  $L_t$  discussed in Section 1.

### 4.3 Axioms that characterize the Brownian map

Most of this subsection will be devoted to a proof of the following Lévy net based characterization of the Brownian map. At the end of the section, we will explain how to use this result to derive Theorem 1.1.

**Theorem 4.6.** *The doubly marked Brownian map measure  $\mu_{\text{SPH}}^2$  is the unique (infinite) measure on  $(\mathcal{M}_{\text{SPH}}^2, \mathcal{F}^2)$  which satisfies the following properties, where an instance is denoted by  $(S, d, \nu, x, y)$ .*

1. *Given  $(S, d, \nu)$ , the conditional law of  $x$  and  $y$  is that of two i.i.d. samples from  $\nu$ . In other words, the law of the doubly marked surface is invariant under the Markov step in which one “forgets”  $x$  (or  $y$ ) and then resamples it from the given measure.*
2. *The law of the metric net from  $x$  to  $y$  (an infinite measure) agrees with the law of an  $\alpha$ -Lévy net for some  $\alpha \in (1, 2)$ . More precisely: the metric net of  $(S, d, x, y)$  can be coupled with the  $\alpha$ -Lévy net in such a way that there is a.s. a unique homeomorphism between the two doubly marked topological spaces such that under this homeomorphism all of the distinguished left and right geodesics in the Lévy net map to actual geodesics (of the same length) in  $(S, d)$ .*
3. *Fix  $r > 0$  and consider the circle that forms the boundary  $\partial B^\bullet(x, r)$  (an object that is well-defined a.s. on the finite-measure event that the distance from  $x$  to  $y$  is at least  $r$ ). Then the inside and outside of  $B^\bullet(x, r)$  (each viewed as an element of  $\mathcal{M}^1$ ) are conditionally independent, given the boundary length of  $\partial B^\bullet(x, r)$  (as defined from the Lévy net structure).*

Let us emphasize a few points before we give the proof of Theorem 4.6.

- Recalling Proposition 4.4, in the case of  $\mu_{\text{SPH}}^2$  one has  $\alpha = 3/2$ . Moreover, Proposition 4.4 implies that  $\mu_{\text{SPH}}^2$  satisfies the second hypothesis of Theorem 4.6 and the discussion before Proposition 4.2 implies that  $\mu_{\text{SPH}}^2$  satisfies the third assumption.
- The second assumption together with Proposition 3.27 implies that the boundary length referenced in the third assumption is a.s. well-defined and has the law of a CSBP excursion (just like the CSBP used to encode the Lévy net). In particular, this implies that for any  $r > 0$ , the measure of the event  $d(x, y) > r$  is positive and finite.
- In the coupling between the metric net and the Lévy net described above, we have made no assumptions about whether *every* geodesic in the metric net, from some point  $z$  to the root  $x$ , corresponds to one of the distinguished left or right geodesics in the Lévy net. That is, we allow *a priori* for the possibility that the metric net contains many additional geodesics besides these distinguished ones. Each of these additional geodesics would necessarily pass through the filled ball boundaries  $\partial B^\bullet(x, r)$  in decreasing order of  $r$ , but in principle they could continuously zigzag back and forth in different ways. We also do not assume *a priori* that the distinguished geodesics in the metric net of  $(S, d, x, y)$  (i.e., the ones that correspond to the left and right distinguished Lévy net geodesics) are

actually leftmost or rightmost when viewed as geodesics in  $(S, d)$ . We similarly make no assumption about the lengths of the shortest paths in the metric net that connect points in the metric net that are both distinct from  $x$ . That is, we allow *a priori* for the possibility that there might be a path in the metric net between two endpoints that is strictly shorter than the shortest path obtained by concatenating finitely many segments of distinguished geodesics.

- The measurability results of Section 2.4 imply that the objects referred to in the statement of Theorem 4.6 are random variables. In particular, Proposition 2.17 implies that the inside and the outside of  $B^\bullet(x, r)$  (viewed as elements of  $\mathcal{M}^1$ ) are measurable functions of an element of  $\mathcal{M}_{\text{SPH}}^2$  and Proposition 2.18 implies that the metric net (viewed as an element of  $\mathcal{X}^2$ ) is a measurable function of an element of  $\mathcal{M}_{\text{SPH}}^2$ .

Now we proceed to prove Theorem 4.6. This proof requires several lemmas, beginning with the following.

**Lemma 4.7.** *If  $\tilde{\mu}_{\text{SPH}}^2$  satisfies the hypotheses of Theorem 4.6, and  $(S, d, \nu, x, y)$  denotes a sample from  $\tilde{\mu}_{\text{SPH}}^2$ , then it is a.s. the case that the metric net from  $x$  to  $y$  has  $\nu$  measure zero. That is, the set of  $(S, d, \nu, x, y)$  for which this is not the case has  $\tilde{\mu}_{\text{SPH}}^2$  measure zero.*

*Proof.* Suppose that the metric net does not have  $\nu$  measure 0 with positive  $\tilde{\mu}_{\text{SPH}}^2$  measure. Then if we fix  $x$  and resample  $y$  from  $\nu$  to obtain  $\tilde{y}$ , there is some positive probability that  $\tilde{y}$  is in the metric net from  $x$  to  $y$ . Let  $L_r$  be the process that encodes the boundary length of the complementary component of  $B(x, r)$  which contains  $\tilde{y}$ . Then we have that  $L_r$  does not a.s. tend to 0 as  $\tilde{y}$  is hit. This is a contradiction as, in the Lévy net definition, we do have that  $L_r$  almost surely tends to 0 as the target point is reached.  $\square$

If  $\tilde{\mu}_{\text{SPH}}^2$  satisfies the hypotheses of Theorem 4.6, then we let  $\tilde{\mu}_{\text{DISK}}^{1,L}$  denote the conditional law of  $S \setminus B^\bullet(x, r)$ , together with its internal metric and measure, given that the boundary length of  $\partial B^\bullet(x, r)$  is equal to  $L$ . Once we have shown that  $\tilde{\mu}_{\text{SPH}}^2$  agrees with  $\mu_{\text{SPH}}^2$ , we will know that  $\tilde{\mu}_{\text{DISK}}^{1,L}$  agrees with  $\mu_{\text{DISK}}^{1,L}$ , which will imply in particular that  $\tilde{\mu}_{\text{DISK}}^{1,L}$  depends on  $L$  in a scale invariant way. That is, we will know that sampling from  $\tilde{\mu}_{\text{DISK}}^{1,L}$  is equivalent to sampling from  $\tilde{\mu}_{\text{DISK}}^{1,1}$  and then rescaling distances and measures by the appropriate powers of  $L$ . However, this is not something we can deduce directly from the hypotheses of Theorem 4.6 as stated. We can however deduce a weaker statement directly: namely, that at least the probability measures  $\tilde{\mu}_{\text{DISK}}^{1,L}$  in some sense depend on  $L$  in a continuous way. Note that given our definition in terms of a regular conditional probability, the family of measures  $\tilde{\mu}_{\text{DISK}}^{1,L}$  is *a priori* defined only up to redefinition on a Lebesgue measure zero set of  $L$  values, so the right statement will be that there is a certain type of a continuous modification.

**Lemma 4.8.** *Suppose that  $\tilde{\mu}_{\text{SPH}}^2$  satisfies the hypotheses of Theorem 4.6. Let  $\tilde{\mu}_{\text{DISK}}^{1,L}$  denote the conditional law of  $S \setminus B^\bullet(x, r)$ , together with its internal metric and measure, given that the boundary length of  $\partial B^\bullet(x, r)$  is  $L$ . For  $L_1, L_2 > 0$ , define  $\rho(\tilde{\mu}_{\text{DISK}}^{1,L_1}, \tilde{\mu}_{\text{DISK}}^{1,L_2})$  to be the smallest  $\epsilon > 0$  such that one can couple a sample from  $\tilde{\mu}_{\text{DISK}}^{1,L_1}$  with a sample from  $\tilde{\mu}_{\text{DISK}}^{1,L_2}$  in such way that with probability at least  $1 - \epsilon$  the two metric/measure-endowed disks agree when restricted to the  $y$ -containing component of the complement of the set of all points of distance  $\epsilon$  from the disk boundary (and both such components are nonempty). Then the  $\tilde{\mu}_{\text{DISK}}^{1,L}$  (after redefinition on a zero Lebesgue measure set of  $L$  values) have the property that as  $L_1$  tends to  $L_2$  the  $\rho$  distance between the  $\tilde{\mu}_{\text{DISK}}^{1,L_i}$  tends to zero. In other words, the map from  $L$  to  $\tilde{\mu}_{\text{DISK}}^{1,L}$  has a modification that is continuous w.r.t. the metric described by  $\rho$ .*

*Proof.* It is clear that a sample from  $\tilde{\mu}_{\text{DISK}}^{1,L}$  comes equipped with an instance of a time-reversed CSBP starting from  $L$  and stopping when it hits zero (corresponding to a continuation of the  $L_r$  process corresponding to the Lévy net from a point at which it has value  $L$ ). If  $L_1$  and  $L_2$  are close, then we can couple the corresponding time-reversed CSBPs that arise from  $\tilde{\mu}_{\text{DISK}}^{1,L_1}$  and  $\tilde{\mu}_{\text{DISK}}^{1,L_2}$  so that they agree with high probability after some small  $\epsilon$  amount of time. Let us define  $\rho'(L_1, L_2)$  to be the smallest  $\epsilon$  so that the two time-reversed CSBPs, started at different heights  $L_1$  and  $L_2$ , can be coupled to agree and are both non-zero after an  $\epsilon$  interval of time with probability  $1 - \epsilon$ . It is easy to see that  $\rho'(L_1, L_2)$  is continuous in  $L_1$  and  $L_2$  and zero when  $L_1 = L_2$ . Now using the Markov property assumed by the hypotheses of Theorem 4.6, we find  $\rho(\tilde{\mu}_{\text{DISK}}^{1,L_1}, \tilde{\mu}_{\text{DISK}}^{1,L_2}) \leq \rho'(L_1, L_2)$  for almost all  $L_1$  and  $L_2$  pairs. Thus, if a countable dense set  $Q$  of  $L$  values is obtained by i.i.d. sampling from Lebesgue measure, then this bound a.s. holds for all  $L_1$  and  $L_2$  in  $Q$ . Then for almost all other  $L$  values, we have that with probability one,  $\rho(\tilde{\mu}_{\text{DISK}}^{1,L'}, \tilde{\mu}_{\text{DISK}}^{1,L}) \rightarrow 0$  as  $L'$  approaches  $L$  with  $L'$  restricted to the set  $Q$ . We obtain the desired modification by redefining  $\tilde{\mu}_{\text{DISK}}^{1,L}$  on the measure zero set of values for which this is not the case, to be the unique measure for which this limiting statement holds. (It is clear that the limiting statement uniquely determines the law of disk outside of an  $\epsilon$ -neighborhood of the boundary, and since this holds for any  $L$ , it determines the law of the overall disk.)  $\square$

**Lemma 4.9.** *Suppose that  $\tilde{\mu}_{\text{SPH}}^2$  satisfies the hypotheses of Theorem 4.6. Let  $\tilde{\mu}_{\text{DISK}}^{1,L}$  denote the conditional law of  $S \setminus B^\bullet(x, r)$ , together with its internal metric and measure, given that the boundary length of  $\partial B^\bullet(x, r)$  is  $L$ . Then suppose  $\tau$  is any stopping time for the process  $L_r$  such that a.s.  $L_r$  has a jump at time  $\tau$ . (For example  $\tau$  could be the first time at which a jump in a certain size range appears.) Then the conditional law of  $S \setminus B^\bullet(x, \tau)$ , given  $B^\bullet(x, \tau)$  and the process  $L_r$  up to time  $\tau$ , is given by  $\tilde{\mu}_{\text{DISK}}^{1,L}$  with  $L = L_\tau$ .*

*Proof.* This is simply an extension of the theorem hypothesis from a deterministic stopping time to a specific type of random stopping time. The extension to random stopping times is obvious if one considers stopping times that a.s. take one of finitely

many values. In particular this is true for the stopping time  $\tau_\delta$  obtained by rounding  $\tau$  up to the nearest integer multiple of  $\delta$ , where  $\delta > 0$ . It is then straightforward to obtain the result by taking the  $\delta \rightarrow 0$  limit and invoking the continuity described in Lemma 4.8.  $\square$

**Lemma 4.10.** *Let  $\tau$  be as in Lemma 4.9. Then the union of  $\partial B^\bullet(x, r)$  and the boundary of the ball cut off at time  $\tau$  is a.s. a topological figure 8 of the sort shown in Figure 4.5. The boundary length measure along the figure 8 is a.s. well defined. The total boundary length is the value of  $L_\tau$  just before the (downward) jump, while the boundary length of the component surrounding  $y$  is the value of  $L_\tau$  is itself.*

*Proof.* This is immediate from the definition of the Lévy net and Proposition 2.1.  $\square$

If  $\tilde{\mu}_{\text{SPH}}^2$  satisfies the hypotheses of Theorem 4.6, and  $\tau$  is a stopping time as in Lemma 4.9, then we can now define  $\tilde{\mu}_{\text{DISK}}^L$  to be the conditional law of the disk cut out at time  $\tau$  given that the boundary length of that disk (i.e., the size of the jump in the  $L_r$  process that occurs then  $r = \tau$ ) is  $L$ . The following lemma asserts that this conditional law indeed depends only on  $L$  and not on other information about the behavior of the surface outside of this disk.

**Lemma 4.11.** *Assume that  $\tilde{\mu}_{\text{SPH}}^2$  satisfies the hypotheses of Theorem 4.6. Then the conditional probability  $\tilde{\mu}_{\text{DISK}}^L$  described above is well defined and indeed depends only on  $L$ .*

*Proof.* If one explores up until the stopping time  $\tau$ , one can resample the target point  $y$  from the restriction of  $\nu$  to the union of the two disks pinched off at time  $\tau$ . Since  $\nu$  is a.s. a good measure, there will be some positive probability that  $y$  ends up on each of the two sides. The theorem hypotheses imply that the conditional law of each of the two disks bounded by the figure 8, on the event that  $y$  lies in that disk, is given by  $\tilde{\mu}_{\text{DISK}}^{1,L}$ , independently of any other information about the surface outside of that disk. This implies in particular that the two disks are independent of each other once it has been determined which disk contains  $y$ . Now, one can resample the location of  $y$ , resample the disk containing  $y$  from  $\tilde{\mu}_{\text{DISK}}^{1,L}$ , resample the location of  $y$ , resample the disk containing  $y$  again, etc., and it is not hard to see that this process is mixing, so that these assumptions determine the form of  $\tilde{\mu}_{\text{DISK}}^L$ . The explicit relationship between  $\tilde{\mu}_{\text{DISK}}^L$  and  $\tilde{\mu}_{\text{DISK}}^{1,L}$  will be derived in the proof of Lemma 4.13 just below.  $\square$

**Lemma 4.12.** *Given the  $L_r$  process describing the boundary length of  $\partial B^\bullet(x, r)$ , the conditional law of the disks in the complement of the net are given by conditionally independent samples from  $\tilde{\mu}_{\text{DISK}}^{L_i}$  where  $L_i$  are the lengths of the hole boundaries (which in turn correspond to the jumps of  $L_r$ ).*

*Proof.* This is a consequence of Lemma 4.11.  $\square$

**Lemma 4.13.** *Assume that  $\tilde{\mu}_{\text{SPH}}^2$  satisfies the hypotheses of Theorem 4.6, and that  $\tilde{\mu}_{\text{DISK}}^L$  and  $\tilde{\mu}_{\text{DISK}}^{1,L}$  are defined as above. Let  $A$  be the total area measure of a sample from  $\tilde{\mu}_{\text{DISK}}^L$ . Then the  $\tilde{\mu}_{\text{DISK}}^L$  expectation of  $A$  is given by a constant times  $L^{2\alpha-1}$ . Moreover, the Radon-Nikodym derivative of  $\tilde{\mu}_{\text{DISK}}^{1,L}$  w.r.t.  $\tilde{\mu}_{\text{DISK}}^L$  (where one ignores the marked point, so that the two objects are defined on the same space) is given by this same expectation, is hence also given by a constant times  $L^{2\alpha-1}$ .*

*Proof.* Suppose that we evolve  $L_r$  from a positive initial value of  $L$  up to a stopping time at which a jump occurs — for example, the first time at which a jump occurs that would decrease the total boundary length by at least an  $\epsilon$  fraction of its total (where  $0 < \epsilon < 1/2$ ). At such a jump time, the boundary length  $c$  is divided into two components, of lengths  $a$  and  $b$  with  $a + b = c$ . (That is,  $c$  is the value of  $L_r$  just before the downward jump; one of the two  $\{a, b\}$  values is the value of  $L_r$  just after the jump and the other is determined by  $a + b = c$ .)

At this point in the proof, let us relabel slightly and set  $L \in \{a, b\}$  to be the boundary length of the component surrounding  $y$ . By Lemma 4.9, the conditional law of the disk in this component is given by  $\tilde{\mu}_{\text{DISK}}^{1,L}$ . Following Lemma 4.11, we let  $\tilde{\mu}_{\text{DISK}}^L$  denote the probability measure that describes the conditional law of the metric disk inside the loop that *does not* surround  $y$ , when  $L \in \{a, b\}$  is taken to be the length of *that* loop. (Again, we have not yet proved this is equivalent to the  $\tilde{\mu}_{\text{DISK}}^L$  defined from the Brownian map.)

If we condition on the lengths of these two pieces — i.e., on the pair  $(a, b)$  — then what is the conditional probability that  $y$  belongs to the  $a$  loop versus the  $b$  loop? We will address that question in two different ways. First of all, if  $p$  is that probability, then we can write the overall measure for the pair of surfaces as the following weighted average of probability measures

$$p\tilde{\mu}_{\text{DISK}}^{1,a} \otimes \tilde{\mu}_{\text{DISK}}^b + (1-p)\tilde{\mu}_{\text{DISK}}^a \otimes \tilde{\mu}_{\text{DISK}}^{1,b}.$$

Now, observe that if we condition on the pair of areas  $A_1, A_2$ , then the resampling property for  $y$  implies that the conditional probability that  $y$  is in the first area is  $A_1/(A_1 + A_2)$ . This implies the following Radon-Nikodym derivative formula for two (non-probability) measures

$$\frac{d[p\tilde{\mu}_{\text{DISK}}^{1,a} \otimes \tilde{\mu}_{\text{DISK}}^b]}{d[(1-p)\tilde{\mu}_{\text{DISK}}^a \otimes \tilde{\mu}_{\text{DISK}}^{1,b}]} = \frac{A_1}{A_2}. \quad (4.6)$$

From this, we may deduce (by holding one of the two disks fixed and letting the other vary) that the Radon-Nikodym derivative of  $\tilde{\mu}_{\text{DISK}}^{1,L}$  w.r.t.  $\tilde{\mu}_{\text{DISK}}^L$  (ignoring the marked point location) is given by a constant times the area  $A$  of the disk; since both objects are probability measures, this Radon-Nikodym derivative must be the ratio  $A/\mathbf{E}_{\tilde{\mu}_{\text{DISK}}^L}[A]$ .

Plugging this back into (4.6), we find that

$$\frac{p}{1-p} = \frac{\mathbf{E}_{\tilde{\mu}_{\text{DISK}}^a}[A]}{\mathbf{E}_{\tilde{\mu}_{\text{DISK}}^b}[A]}. \quad (4.7)$$

In other words, the probability that  $y$  lies in the disk bounded by the loop of length  $L \in \{a, b\}$  (instead of the other disk) is given by a constant times the  $\tilde{\mu}_{\text{DISK}}^L$ -expected area of a disk bounded by that loop.

Next, we note that there is a second way to determine  $p$ . Namely, we may directly compute the relative likelihood of a jump by  $a$  versus a jump by  $b$  in the time-reversal of an  $\alpha$ -stable Lévy excursion, given that one has a jump of either  $a$  or  $b$ . By Lemma 3.19, the ratio of these two probabilities is  $a^{2\alpha-1}/b^{2\alpha-1}$ . Plugging this into (4.7) gives

$$\frac{a^{2\alpha-1}}{b^{2\alpha-1}} = \frac{\mathbf{E}_{\tilde{\mu}_{\text{DISK}}^a}[A]}{\mathbf{E}_{\tilde{\mu}_{\text{DISK}}^b}[A]}.$$

Since this is true for generic values of  $a$  and  $b$ , we conclude that  $\mathbf{E}_{\tilde{\mu}_{\text{DISK}}^L}[A]$  is given by a constant times  $L^{2\alpha-1}$ .  $\square$

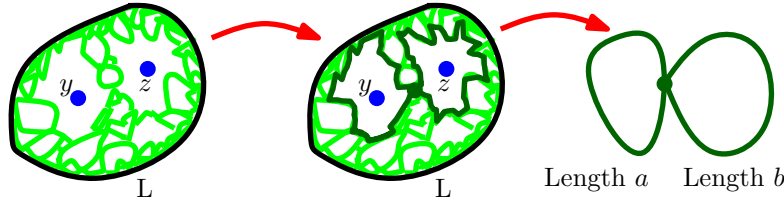


Figure 4.5: The intersection of the metric net from the boundary to  $y$  with the metric net from the boundary to  $z$ . Intuitively, these are the points one finds as one continually “explores” points (in order of distance from the boundary) within the unexplored component containing both  $y$  and  $z$ , stopping at the first time that  $y$  and  $z$  are separated. At the time when  $y$  and  $z$  are separated, the boundaries of the component containing  $y$  and the component containing  $z$  are disjoint topological circles, each of which comes with a length; we denote the two lengths by  $a$  and  $b$ .

As discussed above, at a time when a point  $z$  is disconnected from the target point  $y$ , the boundary has the form of a figure 8 with two loops of distinct lengths  $a$  and  $b$ , as shown in Figure 4.5. At this time the process  $L_r$  jumps from some value  $c = a + b$  down to  $a$  (if the marked point  $y$  is in the component of boundary length  $a$ ) or  $b$  (if  $y$  is in the component of boundary length  $b$ ). We define a *big jump* in the process  $L_r$  associated to  $\tilde{\mu}_{\text{DISK}}^{1,L}$  to be a jump whose lower endpoint is less than half of its upper endpoint. A big jump corresponds to a time when the marked point lies in the disk bounded by the *shorter* of the two figure 8 loops.

In what follows, it will sometimes be useful to consider an alternative form of exploration in which the endpoint  $y$  is not fixed in advance. We already know that if let  $y_1, y_2, \dots$  be independent samples from  $\nu$ , then the metric nets targeted at those points should be in some sense coupled Lévy nets, which agree up until the first time at which those points are separated. Indeed, there will be countably many times at which one of those points is first disconnected from the other, as illustrated in Figure 4.5. This union of all such explorations can be understood as sort of a branching exploration process, where each time the boundary is “pinched” into two (forming a figure 8, as in Figure 4.5) the exploration continues on each of the two sides.

In what follows, it will be useful to consider an alternative form of exploration in which, at each such pinch point, the exploration always continues in the *longer* of these two loops, rather than continuing in the loop that contains some other predetermined point  $y$ . That is, we choose the exploration so that the corresponding boundary length process  $L_r$  has no “big jumps” as we defined them above. It is clear that each  $y_i$  will almost surely fail to lie in the bigger loop of a figure 8 at some point, and hence a.s. all of the points  $y_i$  will lie in disks that are cut off by this exploration process in finite time.

Let  $A_r$  denote the unexplored disk that remains after  $r$  units of exploration of this process. Then  $\overline{A}_r$  is a closed set, which is the closure of the set of points  $y_i$  with the property that Lévy nets explorations targeted at those points have no big jumps before time  $t$ . The intersection of  $\overline{A}_r$ , over all  $r$ , is thus a closed set that we will call the *center* of the disk. We do not need to know this *a priori* but we expect that center contains only a single point. Note that the center can be defined if the surface is sampled from either  $\tilde{\mu}_{\text{DISK}}^L$  or  $\tilde{\mu}_{\text{DISK}}^{1,L}$  (and in the latter case its definition does not depend on the marked point  $y$ ). We refer to the modified version of the Lévy net as the *center net* corresponding to the surface. We are now going to prove an analog of Lemma 4.12 for the center net.

**Lemma 4.14.** *Given the  $M_r$  process describing the center net corresponding to a sample from  $\tilde{\mu}_{\text{DISK}}^L$ , the conditional law of the disks in the complement of the net are given by conditionally independent samples from  $\tilde{\mu}_{\text{DISK}}^{M_i}$  where  $M_i$  are the lengths of the hole boundaries.*

*Proof.* We can condition on the positive probability event that the center net exploration agrees with the exploration with a marked point up to fixed time. Note that this is a positive probability event and, on this event, Lemma 4.12 implies that the conditional law of the disks cut off given  $M$  up to this time is given by i.i.d. samples from  $\tilde{\mu}_{\text{DISK}}^{M_i}$  where  $M_i$  are the lengths of the hole boundaries. The result follows because the disks cut off up to this fixed time are conditionally independent of the unexplored region given their boundary lengths.  $\square$

We now would like to discuss the relationship between the laws of the following processes:

1. The process  $L_r$  obtained by exploring the metric net from a sample from  $\tilde{\mu}_{\text{DISK}}^{1,L}$ , starting with  $L_0$  equal to some fixed value  $L$ .
2. The process  $M_r$  obtained by exploring a sample from  $\tilde{\mu}_{\text{DISK}}^L$  toward the center (again starting with  $M_0 = L$ ).
3. The process  $M_r^1$  obtained by exploring a sample from  $\tilde{\mu}_{\text{DISK}}^{1,L}$  toward the center (again starting with  $M_0^1 = L$ ).

We already know that the Radon-Nikodym derivative of  $\tilde{\mu}_{\text{DISK}}^{1,L}$  w.r.t.  $\tilde{\mu}_{\text{DISK}}^L$  is given by a constant times the area of the disk. This immediately implies the following:

**Lemma 4.15.** *The Radon-Nikodym derivative of the process  $M_r^1$  w.r.t. the process  $M_r$  is given by the expected disk area given the process, which (by Lemma 4.13 and Lemma 4.14) is given by a constant times  $\sum_K K^{2\alpha-1}$  where  $K$  ranges over the jump magnitudes corresponding to the countably many jumps in the process. Moreover, if  $L_r$  and  $M_r^1$  are coupled in the obvious way (i.e., generated from the same instance of  $\tilde{\mu}_{\text{DISK}}^{1,L}$ ) then they agree up until a stopping time: namely, the first time that  $L_r$  experiences a big jump.*

As a side remark, let us note that the stopping time  $\tau$  of the process  $M_r^1$ , as defined in Lemma 4.15, can be constructed in fairly simple way that roughly corresponds to, each time a new figure 8 is created, tossing an appropriately weighted coin to decide whether  $y$  is in the smaller or the larger loop, and then stopping when it first lies in the smaller loop. To formulate this slightly more precisely, suppose that for each  $r \geq 0$  we let  $\chi_r$  be the product of

$$\frac{a^{2\alpha-1}}{a^{2\alpha-1} + b^{2\alpha-1}}$$

over all jumps of  $M^1|_{[0,r]}$  where  $a$  is the size of the jump and  $b$  is equal to the value of  $M^1$  immediately after the jump. Suppose that we choose  $p$  uniformly in  $[0, 1]$ . Then we can write  $\tau = \inf\{r \geq 0 : \chi_r < p\}$ .

We next claim the following:

**Lemma 4.16.** *If one explores the center net of an instance of  $\tilde{\mu}_{\text{DISK}}^L$  up to some stopping time  $\tau$ , then the conditional law the central unexplored disk (i.e., the one in which exploration will continue) is given by an instance of  $\tilde{\mu}_{\text{DISK}}^{L'}$  where  $L' = M_\tau$  is the boundary length at that time. In particular, this implies that the process  $M_r$  is Markovian.*

*Proof.* This follows by combining Lemma 4.9, Lemma 4.13, and Lemma 4.15. □

By Lemma 3.19, the jump density for  $\tilde{\mu}_{\text{DISK}}^{1,L}$  (for a jump of size  $a$  that leaves a loop of size  $b = c - a$  in which  $y$  is contained) is given by a constant times  $a^{-\alpha-1}b^{\alpha-2}$ .

**Lemma 4.17.** *The process  $M_r$  agrees in law with the process  $L_r$  except that the jump law is different. Instead of having the form*

$$\mathbf{1}_{a \in [0, c]} a^{-\alpha-1} (b/c)^{\alpha-2} da, \quad (4.8)$$

*it has the form*

$$\mathbf{1}_{a \in [0, c/2]} a^{-\alpha-1} (b/c)^{-\alpha-1} da, \quad (4.9)$$

*where in both cases  $b$  is simply defined via  $b = c - a$ ,  $c$  is defined to the height of the process just before the jump, and  $da$  denotes Lebesgue measure.*

*Proof.* Now note that  $\tilde{\mu}_{\text{DISK}}^L$  (explored toward the center) and  $\tilde{\mu}_{\text{DISK}}^{1,L}$  (explored toward the marked point) are both Markov processes, whose laws should evolve in an absolutely continuous way (at least up until the first time that  $y$  fails to lie in the larger of the two components). The relative density of the jump measure in the two models can be computed explicitly. Suppose that we explore an instance of  $\tilde{\mu}_{\text{DISK}}^{1,L}$  up until the first time that there is a jump of size at most an  $\epsilon$  fraction of the total boundary length, i.e., we are observing the process  $M_r^1$  up until a time  $\tau'$  at which such a jump in  $M_r^1$  occurs. On the event that  $\tau' \leq \tau$ , the conditional law of the jump size in  $M_r^1$  at the time  $\tau'$  is the same as it would be for  $M_r$  (having observed the same process thus far) except that it would be weighted by the expected area in the corresponding figure 8, namely by a constant times

$$(a/c)^{2\alpha-1} + (b/c)^{2\alpha-1}. \quad (4.10)$$

But we know by Lemma 3.19 that the jump law for  $L_r$  is given by a constant times  $a^{-\alpha-1}(b/c)^{\alpha-2}$ . Since a jump of size  $a$  in  $M_r^1$  can correspond to two kinds of jumps in  $L_r$  (one of size  $a$  and one of size  $b = c - a$ ) we find that the jump law for  $M_r^1$  is given by a constant times

$$\begin{aligned} & (a^{-\alpha-1}(b/c)^{\alpha-2} + (a/c)^{\alpha-2}b^{-\alpha-1}) \mathbf{1}_{a \in [0, c/2]} \\ &= ((a/c)^{2\alpha-1} + (b/c)^{2\alpha-1}) a^{-\alpha-1} (b/c)^{-\alpha-1} \mathbf{1}_{a \in [0, c/2]}, \end{aligned}$$

which is indeed the product of (4.9) and (4.10), which implies that the jump law described by (4.9) must have been the correct one.  $\square$

We remark that from the point of view of the discrete models, the jump law for  $M_r$  described in Lemma 4.17 is precisely what one would expect if the overall *partition function* for a boundary-length  $a$  disk were given by a constant times  $a^{-\alpha-1}$ . Indeed, in this case  $a^{-\alpha-1}b^{\alpha-1}$  would be the weighted sum of all ways to triangulate the loops of a figure 8 with loop lengths  $a$  and  $b$ , which matches the law described in the lemma statement. It is therefore not too surprising that the jump law for  $\tilde{\mu}_{\text{DISK}}^L$  exploration toward the center has to have this form. Furthermore, we may conclude that the  $M_r$  process can be a.s. recovered from the ordered collection of jumps (since this is true for Lévy process, hence true for CSBPs, hence true for time-reversals of these

processes, hence true for this modified time-reversal that corresponds to  $\tilde{\mu}_{\text{DISK}}^L$ ) and the reconstruction procedure is the same as the one that corresponds to the  $L_r$  process.

As explained in Figure 4.6, now that we have constructed the law of the exploration of a sample from  $\tilde{\mu}_{\text{DISK}}^L$  toward the center, we may iterate this construction within each of the unexplored regions and repeat, so that in the limit, we have determined the joint law of the metric net toward all points in some countable dense subset of the metric disk.

*Proof of Theorem 4.6.* By Lemma 4.7 there is a.s. no area in the metric net itself. This implies that if we explore the center net of a sample from  $\tilde{\mu}_{\text{DISK}}^L$  up until a given time, then the center net also a.s. contains zero area. Let  $M_r$  be the boundary length process associated with a sample from  $\tilde{\mu}_{\text{DISK}}^L$ . By Lemma 4.13, Lemma 4.14, and Lemma 4.16 if we perform an exploration towards the center of a sample produced from  $\tilde{\mu}_{\text{DISK}}^L$  up until a given time  $s$  then the conditional

$$A_s := M_s^{2\alpha-1} + \sum |a_i|^{2\alpha-1} \quad (4.11)$$

where the  $a_i$  are an enumeration of the jumps in the process  $M_r$  up to time  $s$ . Thus, (4.11) must evolve as a martingale in  $s$ . Proposition 4.19 (stated and proved in Section 4.5 below) implies that (4.11) evolves as a martingale if and only if  $\alpha = 3/2$ . Thus, the fact that  $\alpha = 3/2$  is a consequence of the properties listed in the theorem statement. For the remainder of the proof, we may therefore assume that  $\alpha = 3/2$ .

Let  $A$  be the overall area measure of a surface sampled from  $\tilde{\mu}_{\text{DISK}}^L$ . Let  $A_k$  denote the conditional expectation of  $A$  given the  $\sigma$ -algebra  $\mathcal{G}_k$  generated by  $k$  exploration iterations, where each iteration corresponds to adding an exploration toward the center of each unexplored component, as described above. Note that since the hypotheses of Theorem 4.6 apply to  $\mu_{\text{SPH}}^2$  with  $\alpha = 3/2$ , all of the lemmas above apply if we use  $\mu_{\text{DISK}}^L$  and  $\mu_{\text{DISK}}^{1,L}$  in place of  $\tilde{\mu}_{\text{DISK}}^L$  in and  $\tilde{\mu}_{\text{DISK}}^{1,L}$ , respectively. We know that the joint law of the processes encoding the iterations  $A_k$ , and the law of the conditional expectation of the area in the unexplored regions, is the same in each case. This implies that  $\mu_{\text{SPH}}^2$  and  $\tilde{\mu}_{\text{SPH}}^2$  can be coupled in such a way that their branching boundary length explorations agree, and that their conditional expected amounts of area in the not-yet-explored regions agree, and their metric net structures are compatible.

But does this imply that the overall areas agree in this coupling? To prove this, it would suffice to show that the  $A_k \rightarrow A$  almost surely. By the martingale convergence theorem, to prove that  $A_k \rightarrow A$  a.s. it suffices to show that  $A$  is a measurable function of the  $\sigma$ -algebra  $\mathcal{G}$  generated by the information encoded by *all* of the countably many exploration iterations. To prove this we will in fact prove a stronger claim: that  $\mathcal{G}$  encodes all of the information about random metric measure space.

Let us first consider this claim in the case of  $\mu_{\text{SPH}}^2$ . That is, we will show that the entire doubly marked Brownian map instance is  $\mathcal{G}$ -measurable. Note that if a point  $z$

is chosen uniformly from the measure on the surface, then it is almost surely the case that, as one explores towards  $z$ , there are only countably many “large jumps” (where the target point lies in the component of the smaller boundary). Thus, as  $k \rightarrow \infty$ , the exploration a.s. gets arbitrarily close to  $z$ . In particular, as  $k \rightarrow \infty$  one obtains the entire Lévy net targeted toward  $z$ . Indeed, this holds for a countable collection of points  $z_i$  chosen i.i.d. from the measure on the surface, and one then recovers the structure of the tree that describes the union of the geodesics from all of the  $z_i$  to the root. Since the  $z_i$  are a.s. a dense set (as the area measure on the Brownian map is a good measure), one obtains from this procedure the entire geodesic tree structure. This, in turn, determines (up to time change) the horizontal component of the snake process that encodes the Brownian map. One then also obtains the vertical component (by observing the quadratic variation along the dual paths of the geodesic) and the time parameter (by observing the quadratic variation of the vertical component).

We now turn to establish the claim in the case of  $\tilde{\mu}_{\text{SPH}}^2$ . We know that an instance of  $\tilde{\mu}_{\text{SPH}}^2$  determines a sample from  $\mu_{\text{SPH}}^2$  in a unique way, and that the expectation of the area measure  $\nu$  corresponding to  $\tilde{\mu}_{\text{SPH}}^2$  given  $\mathcal{G}$  is equivalent to the area measure  $\nu$  corresponding to the sample from  $\mu_{\text{SPH}}^2$ . It could still be the case that the  $\nu$  corresponding to a sample from  $\tilde{\mu}_{\text{SPH}}^2$  differed from its expected value given  $\mathcal{G}$  and, in particular, this corresponding Brownian map structure. For example, this would be the case if the  $\nu$  corresponding to  $\tilde{\mu}_{\text{SPH}}^2$  was chosen as some sort of Poisson point process of atoms, whose expectation was the Brownian map measure; however, since by assumption there are no atoms (as  $\nu$  is required to be a good measure), this type of pathology cannot arise.

To make this precise, we fix  $\epsilon > 0$  and we let  $G_{k,\epsilon}$  be the event that the total amount of area in each of the individual complementary components after performing  $k$  iterations of the exploration is at most  $\epsilon$ . Under  $\tilde{\mu}_{\text{SPH}}^2$ , we know that  $\nu$  is a good measure hence does not have atoms. Recall from the discussion just after the statement of the theorem that, for each fixed  $r > 0$ , the event  $d(x, y) > r$  has positive and finite  $\tilde{\mu}_{\text{SPH}}^2$  mass. Therefore it follows that the  $\tilde{\mu}_{\text{SPH}}^2$  mass of  $G_{k,\epsilon}^c \cap \{d(x, y) > r\}$  tends to 0 as  $k \rightarrow \infty$  (with  $\epsilon$  fixed). For each  $j$ , let  $X_j$  denote the area of the  $j$ th component (according to some ordering) after performing  $k$  iterations of the exploration. Then we have that the total variation distance between the law of  $\sum_j X_j \mathbf{1}_{X_j \leq \epsilon}$  and the law of  $\sum_j X_j$  under  $\tilde{\mu}_{\text{SPH}}^2$  conditioned on  $d(x, y) > r$  tends to 0 as  $k \rightarrow \infty$  (with  $\epsilon$  fixed). As the conditional variance of the former given  $\mathcal{G}_k$  obviously tends to 0 as  $k \rightarrow \infty$  and then  $\epsilon \rightarrow 0$ , it thus follows that the latter concentrates around a  $\mathcal{G}$ -measurable value as  $k \rightarrow \infty$ . This proves the claim.

Finally, now that we have coupled an instance of  $\tilde{\mu}_{\text{SPH}}^2$  with an instance of  $\mu_{\text{SPH}}^2$  in such a way that the measures and iterated center net explorations agree, we would like to argue that the distance functions also agree. We already know that the distances between points  $y_i$  in a countable dense set (sampled i.i.d. from  $\nu$ ) and the root can be made to agree on the two sides. And we know, by definition of distance on the  $\mu_{\text{SPH}}^2$

Brownian map side, the distance between any two such points is the infimum over the lengths of continuous paths between those points made by concatenating finitely many distinguished geodesics to the root (recall (4.3)–(4.5)). This is clearly an *upper* bound on the associated length on the  $\tilde{\mu}_{\text{SPH}}^2$  side.

However, it is easy to see on the Brownian map side, that if one conditions on the total area of the surface, then the expected distance between  $x$  and  $y$  is finite. (This follows from the fact that the  $\mu_{\text{SPH}}^{A=1}$  expectation of the diameter is finite.) If we condition on the total area of the surface, then the expected distance from  $x$  to  $y$  must be the same as the expected distance from  $y_1$  to  $y_2$  when  $y_1$  and  $y_2$  are chosen uniformly from the overall measure. Thus, the one-sided bound described above implies almost sure equality.  $\square$

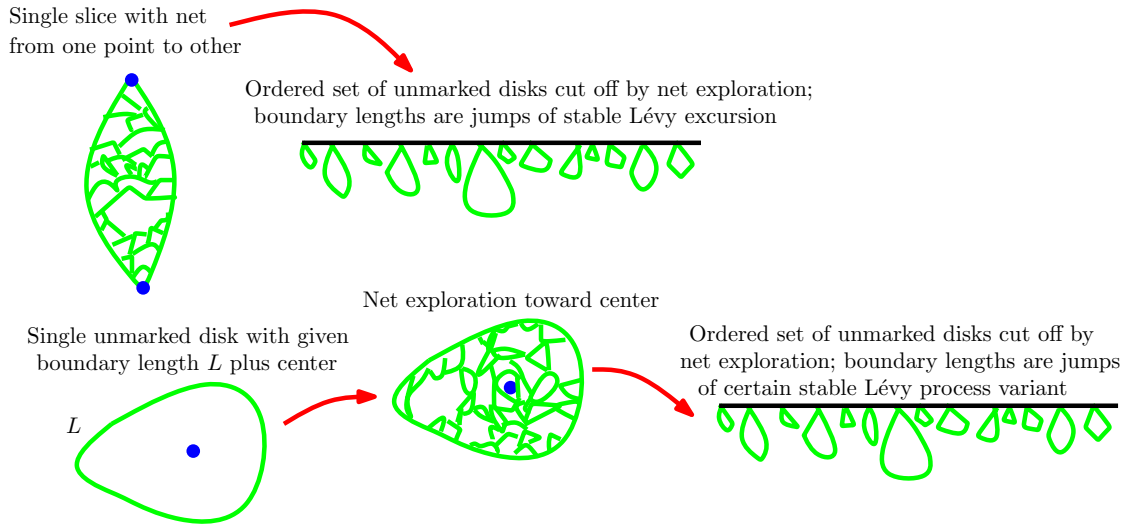


Figure 4.6: A slice (or doubly marked sphere) comes endowed with a Lévy net (as explained in Figure 3.8) and once the Lévy net is given, the disks are conditionally independent unmarked Brownian disks with given boundary lengths. As shown below, even an unmarked disk of given boundary length  $L$  has a special interior point called the *center*. Once one conditions on the exploration net toward that point, the holes are again conditionally independent unmarked Brownian disks with given boundary lengths.

We are now ready to prove Theorem 1.1. The main ideas of the proof already appeared in the proof of Theorem 4.6.

*Proof of Theorem 1.1.* The beginning of the proof of this result appears in Section 2.3 with the statement of Proposition 2.8. In particular, the combination of Proposition 2.8 and Lemma 3.11 implies that for each fixed value of  $r$  the law of the merging times of the leftmost geodesics of  $(S, d, x, y)$  from  $\partial B^\bullet(x, s)$  for  $s = d(x, y) - r$  to  $x$  have the same law in a Lévy a net (when the starting points for the geodesics have the same spacing in

both). Thus in view of the proof of Proposition 3.27, we have that  $L_r$  is almost surely determined by the metric space structure of  $(S, d, x, y)$ . This combined with the second assumption in the statement of Theorem 1.1 implies that  $L_r$  is a non-negative Markov process which satisfies the conditions of Proposition 3.10. That is,  $L_r$  evolves as a CSBP excursion as  $r$  increases, stopped when it hits zero.

This discussion almost implies that the hypotheses of Theorem 4.6 are satisfied for some  $\alpha \in (1, 2)$ . It implies that the intersection of a metric net with  $B^\bullet(x, s)$  looks like a portion of a Lévy net. However, it does not rule out the possibility that the boundary length process  $L_r$  might not tend to zero as  $r$  approaches  $d(x, y)$ . As explained in the proof of Lemma 4.7, this can be ruled out by showing that the metric net from  $x$  to  $y$  almost surely has  $\nu$  measure zero.

If the metric net failed to have measure zero, then the expression (4.12) from Proposition 4.19 would have to fail to be a martingale, which would imply by Proposition 4.19 that we must have  $\alpha \neq 3/2$ .

However, the expression (4.12) *would* have to be a supermartingale, and it would have to become a martingale if an appropriate non-increasing function were added (corresponding to the accumulated amount of mass in the portion of the metric net observed thus far). The Doob-Meyer decomposition implies that the form this function would have to have is uniquely determined. Moreover, it can be determined explicitly from the expression for the drift term associated to (4.12), which is derived in the proof of Proposition 4.19. Indeed, one finds that the accumulated metric net mass would have to be the integral of a power of  $L_r$ , as  $t$  varies from 0 to  $d(x, y)$ . However, it is not hard to see that if this power is anything other than 1, there must be a violation of the independence of slices assumption (since the amount being added would not be a linear function of the slices taken individually). On the other hand, if the power is 1, then the overall scaling exponent would be wrong, since the duration of time scales like  $L^{\alpha-1}$  and the integral would have to scale like  $L^{\alpha-1}L = L^\alpha$ , and not as  $L^{2\alpha-1}$ .  $\square$

## 4.4 Adding a third marked point along the geodesic

In this section, we present Figure 4.7 and use it to informally explain a construction that will be useful in the subsequent works [MS15b, MS15c] by the authors to establish the connection between the  $\sqrt{8/3}$ -Liouville quantum gravity sphere and the Brownian map. This subsection is an “optional” component of the current paper and does not contain any detailed proofs; however, the reader who intends to read [MS15b, MS15c] will find it helpful to have this picture in mind, and it is easier to introduce this picture here.

Roughly speaking, we want to describe the continuum version of the Boltzmann measure on figures such as the one in Figure 1.2, where one has a doubly marked sphere together with two filled metric balls (centered at the two marked points) that touch each other

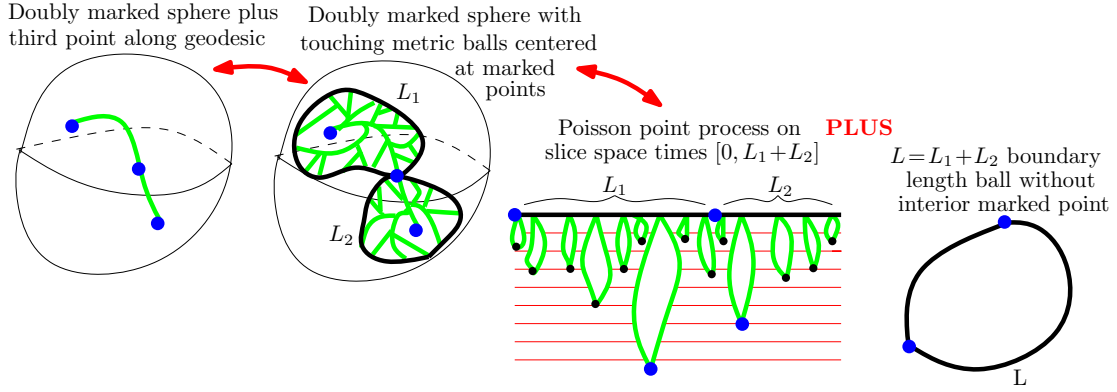


Figure 4.7: To sample from the measure  $\mu_{\text{SPH}}^{2+1}$  on triply marked spheres, one first samples from the measure  $\mu_{\text{SPH}}^2$  *weighted* by the distance  $D = d(x, y)$ ; given a sample from that measure, one then chooses  $r$  uniformly in  $[0, D]$  and marks the point  $r$  units along the (a.s. unique) geodesic. The second figure is a continuum version of Figure 1.2. Given  $L_1$  and  $L_2$ , one may decompose the metric balls as in Figure 1.3 (the first  $L_1$  units of time describing the first ball, the second  $L_2$  units the second ball). The right figure is an independent unmarked Brownian disk, which represents the surface that lies outside of the two metric balls in the second figure. Given the disk, first blue dot is uniform on the boundary; the second is  $L_1$  units clockwise from first. The measure that  $\mu_{\text{SPH}}^{2+1}$  induces on the pair  $(L_1, L_2)$  is (up to multiplicative constant) the measure  $(L_1 + L_2)^{-5/2} dL_1 dL_2$ . This follows from the overall scaling exponent of  $L$  and the fact that given  $L = L_1 + L_2$  the conditional law of  $L_1$  is uniform on  $[0, L]$ .

on the boundary but do not otherwise overlap. Clearly, the Radon-Nikodym derivative of such a measure w.r.t.  $\mu_{\text{TRI}}^2$  should be  $D + 1$  where  $D$  is the distance between the two points, since the radius of the first ball can be anything in the interval  $[0, D]$ . In the discrete version of this story, it is possible for the two metric balls in Figure 1.2 to intersect in more than one point (this can happen if the geodesic between the two marked points is not unique) but in the continuum analog discussed below one would not expect this to be the case (since the geodesic between the marked points is a.s. unique).

To describe the continuum version of the story, we need to define a measure  $\mu_{\text{SPH}}^{2+1}$  on continuum configurations like the one shown in Figure 4.7. To sample from  $\mu_{\text{SPH}}^{2+1}$ , one first chooses a doubly marked sphere from the measure whose Radon-Nikodym derivative w.r.t.  $\mu_{\text{SPH}}^2$  is given by  $D$ . Then, having done so, one chooses a radius  $D_1$  for the first metric ball uniformly in  $[0, D]$ , and then sets the second ball radius to be  $D_2 := D - D_1$ . Now  $\mu_{\text{SPH}}^{2+1}$  is a measure on Brownian map surfaces decorated by two marked points and touching two filled metric balls centered at those points. Let  $L_1$  and  $L_2$  denote the boundary lengths of the two balls and write  $L = L_1 + L_2$ .

1. Based on Figure 1.2 and Figure 4.7, we would expect that one can first choose

the set of slices indexed by time  $L$ , and then randomly choose  $L_1$  uniformly from  $[0, L]$ . Thus, we expect that given  $L$  and  $A$ , the value  $L_1$  is uniform on  $[0, L]$ .

2. It is possible to verify the following scaling properties (which hold up to a constant multiplicative factor):

$$\begin{aligned} \mu_{\text{SPH}}^2[A > a] &\approx a^{-1/2} & \text{and} & & \mu_{\text{SPH}}^{2+1}[A > a] &\approx a^{-1/4}. \\ \mu_{\text{SPH}}^2[L > a] &\approx a^{-1} & \text{and} & & \mu_{\text{SPH}}^{2+1}[L > a] &\approx a^{-1/2}. \\ \mu_{\text{SPH}}^2[D > a] &\approx a^{-2} & \text{and} & & \mu_{\text{SPH}}^{2+1}[D > a] &\approx a^{-1}. \end{aligned}$$

The two properties above suggest that  $\mu_{\text{SPH}}^{2+1}$  induces a measure on  $(L_1, L_2)$  given (up to constant multiplicative factor) by  $(L_1 + L_2)^{-5/2} dL_1 dL_2$ . The measure on  $L$  itself is then  $L^{-3/2} dL$ .

If we condition on the metric ball in Figure 4.7 of boundary length  $L_1$ , we expect that conditional law of the complement to be that of a marked disk of boundary length  $L_1$ , i.e., to be a sample from  $\mu_{\text{DISK}}^{1,L}$  with  $L_1$  playing the role of the boundary length. This suggests the following symmetry (which we informally state but will not actually prove here).

**Proposition 4.18.** *Given  $L_1$ , the following are equivalent:*

1. *Sample a marked disk of boundary length  $L_1$  from the probability measure  $\mu_{\text{DISK}}^{1,L}$  (with  $L_1$  as the boundary length). One can put a “boundary-touching circle” on this disk by drawing the outer boundary of the metric ball whose center is the marked point and whose radius is the metric distance from the marked point to the disk boundary.*
2. *Sample  $L_2$  from the measure  $(L_1 + L_2)^{-5/2} dL_2$  (normalized to be a probability measure) and then create a large disk by identifying a length  $L_2$  arc of the boundary of a sample from  $\mu_{\text{DISK}}^L$ , with the entire boundary of a disk sampled from  $\mu_{\text{MET}}^{L_2}$ . The interface between these two samples is the “boundary-touching circle” on the larger disk.*

Interestingly, we do not know how to prove Proposition 4.18 directly from the Brownian snake constructions of these Brownian map measures, or from the breadth-first variant discussed here. Indeed, from direct considerations, we do not even know how to prove the symmetry of  $\mu_{\text{SPH}}^2$  with respect to swapping the roles of the two marked points  $x$  and  $y$ . However, both this latter fact and Proposition 4.18 can be derived as consequences of the fact that  $\mu_{\text{SPH}}^2$  is a scaling limit of discrete models that have similar symmetries (though again we do not give details here). We will see in [MS15b, MS15c] that these facts can also be derived in the Liouville quantum gravity setting, where certain symmetries are more readily apparent.

We will also present in [MS15b, MS15c] an alternate way to construct Figure 4.7 in the Liouville quantum gravity setting. In this alternate construction, one begins with a measure  $\mu_{\text{LQGSPH}}^2$  on doubly marked LQG spheres. Given such a sphere, one may then decorate it by a whole plane  $\text{SLE}_6$  path from one marked point to the other. Such a path will have certain “cut points” which divide the trace of the path into two connected components. It is possible to define a quantum measure on the set of cut points. One can then define a measure  $\mu_{\text{LQGSPH}}^{2+1}$  on path-decorated doubly marked quantum spheres with a *distinguished* cut point along the path. This is obtained by starting with the law of an  $\text{SLE}_6$ -decorated sample from  $\mu_{\text{LQGSPH}}^2$ , then *weighting* this law by the quantum cut point measure, and then choosing a cut point uniformly from this cut point measure. We will see in [MS15b, MS15c] that a certain QLE “reshuffling” procedure allows us to convert a sample from  $\mu_{\text{LQGSPH}}^{2+1}$  into an object that (once an appropriate metric is defined on it) looks like a sample from  $\mu_{\text{SPH}}^{2+1}$ .

## 4.5 The martingale property holds if and only if $\alpha = 3/2$

**Proposition 4.19.** *Fix  $\alpha \in (1, 2)$  and suppose that  $M_r$  is the process associated with an exploration towards the center of a sample produced from  $\tilde{\mu}_{\text{DISK}}^L$  where  $\tilde{\mu}_{\text{DISK}}^L$  is as in Section 4.3. For each  $r \geq 0$ , we let*

$$A_r = M_r^{2\alpha-1} + \sum_{a \in \mathcal{J}_r} |a|^{2\alpha-1} \quad (4.12)$$

where  $\mathcal{J}_r$  is the set of jumps made by  $M|_{[0,r]}$ . Then  $A_r$  is a martingale if and only if  $\alpha = 3/2$ .

We will need two intermediate lemmas before we give the proof of Proposition 4.19.

**Lemma 4.20.** *Suppose that  $X_t$  is a non-negative, real-valued, continuous-time càdlàg process such that there exists  $p > 1$  with*

$$\sup_{0 \leq t \leq T} \mathbf{E}|X_t|^p < \infty \quad \text{for all } T > 0. \quad (4.13)$$

Let  $\tau = \inf\{t \geq 0 : X_t = 0\}$  and let  $(\mathcal{F}_t)$  be the filtration generated by  $(X_{t \wedge \tau})$ . Suppose that  $q: \mathbf{R}_+ \rightarrow \mathbf{R}_+$  is a non-decreasing function such that  $q(\Delta)/\Delta \rightarrow 0$  as  $\Delta \rightarrow 0$ . Assume that  $Y_t$  is a càdlàg process adapted to  $\mathcal{F}_t$  with  $\mathbf{E}|Y_t| < \infty$  for all  $t$  and that  $a$  is a constant such that

$$\mathbf{E}[Y_t | \mathcal{F}_s] = Y_s + a(t-s)X_{s \wedge \tau} + Z_s \quad \text{where} \quad |Z_s| \leq q(t-s)|X_{s \wedge \tau}| \quad \text{for all } t \geq s.$$

Then  $Y_t$  is a martingale if and only if  $a = 0$ .

*Proof.* Fix  $\Delta > 0$ ,  $s < t$ , and let  $t_0 = s < t_1 < \dots < t_n = t$  be a partition of  $[s, t]$  with  $\Delta/2 < t_j - t_{j-1} \leq \Delta$  for all  $1 \leq j \leq n$ . Then we have that

$$\begin{aligned}\mathbf{E}[Y_t | \mathcal{F}_s] &= Y_s + \sum_{j=1}^n \mathbf{E}[Y_{t_j} - Y_{t_{j-1}} | \mathcal{F}_s] \\ &= Y_s + \sum_{j=1}^n \mathbf{E}[\mathbf{E}[Y_{t_j} - Y_{t_{j-1}} | \mathcal{F}_{t_{j-1}}] | \mathcal{F}_s].\end{aligned}$$

We are going to show that the right hand side above tends to  $Y_s + a \int_s^t \mathbf{E}[X_{u \wedge \tau} | \mathcal{F}_s] du$  in  $L^1$  as  $\Delta \rightarrow 0$ . This turn, implies that there exists a positive sequence  $(\Delta_k)$  with  $\Delta_k \rightarrow 0$  as  $k \rightarrow \infty$  sufficiently quickly so that the convergence is almost sure. This implies the result because if  $s < \tau$  then  $a \int_s^t \mathbf{E}[X_{u \wedge \tau} | \mathcal{F}_s] du = 0$  if and only if  $a = 0$ .

We begin by noting that

$$\begin{aligned}& \sum_{j=1}^n \mathbf{E} \left| \mathbf{E}[(Y_{t_j} - Y_{t_{j-1}}) | \mathcal{F}_{t_{j-1}}] - a(t_j - t_{j-1})X_{t_{j-1} \wedge \tau} \right| \\ & \leq \sum_{j=1}^n q(t_j - t_{j-1}) \mathbf{E}|X_{t_{j-1} \wedge \tau}| \\ & \leq \frac{2q(\Delta)}{\Delta} \sup_{s \leq u \leq t} \mathbf{E}|X_u| \rightarrow 0 \quad \text{as } \Delta \rightarrow 0.\end{aligned}$$

This implies the claim because the càdlàg property implies that

$$\sum_{j=1}^n a(t_j - t_{j-1})X_{t_{j-1} \wedge \tau} \rightarrow a \int_s^t X_{u \wedge \tau} du \quad \text{as } \Delta \rightarrow 0$$

which, combined with the integrability assumption (4.13), implies that

$$\sum_{j=1}^n a(t_j - t_{j-1}) \mathbf{E}[X_{t_{j-1} \wedge \tau} | \mathcal{F}_s] \rightarrow a \int_s^t \mathbf{E}[X_{u \wedge \tau} | \mathcal{F}_s] du \quad \text{as } \Delta \rightarrow 0.$$

□

**Lemma 4.21.** Fix  $\alpha \in (1, 2)$  and suppose that  $M_r$  is the process associated with an exploration towards the center of a sample produced from  $\tilde{\mu}_{\text{DISK}}^L$  where  $\tilde{\mu}_{\text{DISK}}^L$  is as in Section 4.3. There exists constants  $c_0, c_1 > 0$  such that

$$\mathbf{P}[M_r \geq u] \leq c_0 e^{-c_1 r^{-1/\alpha} u} \quad \text{for all } u, r > 0. \quad (4.14)$$

In particular,

$$\mathbf{E}|M_r|^p < \infty \quad \text{for all } r, p > 0. \quad (4.15)$$

*Proof.* We first note that (4.14) in the case of an  $\alpha$ -stable process with only downward jumps follows from [Ber96, Chapter VII, Corollary 2]. The result in the case of  $M_r$  follows by comparing the jump law for  $M_r$  as computed in Lemma 4.17 with the jump law for an  $\alpha$ -stable process (which we recall has density  $x^{-\alpha-1}$  with respect to Lebesgue measure on  $\mathbf{R}_+$ ).  $\square$

*Proof of Proposition 4.19.* Let  $\mathcal{J}_r$  be the set of jumps made by  $M|_{[0,r]}$  and, for each  $\epsilon, \delta > 0$ , let  $\mathcal{J}_r^\epsilon$  (resp.  $\mathcal{J}_r^{\epsilon, \delta}$ ) consist of those jumps in  $\mathcal{J}_r$  with size at least  $\epsilon$  (resp. size in  $[\epsilon, \delta]$ ). Let  $J_r^\epsilon$  (resp.  $J_r^{\epsilon, \delta}$ ) be the sum of the elements in  $\mathcal{J}_r^\epsilon$  (resp.  $\mathcal{J}_r^{\epsilon, \delta}$ ) and let

$$C^\epsilon = \int_\epsilon^\infty x \cdot x^{-\alpha-1} dx = \int_\epsilon^\infty x^{-\alpha} dx = \frac{1}{\alpha-1} \epsilon^{1-\alpha} \quad \text{and} \quad C^{\epsilon, \delta} = \int_\epsilon^\delta x^{-\alpha} dx.$$

Then we have that

$$M_r = \lim_{\epsilon \rightarrow 0} M_r^\epsilon \quad \text{where} \quad M_r^\epsilon = (J_r^\epsilon + rC^\epsilon)_+.$$

We also let  $A_r^\epsilon$  be given by

$$A_r^\epsilon = (M_r^\epsilon)^{2\alpha-1} + \sum_{a \in \mathcal{J}_r^\epsilon} |a|^{2\alpha-1}.$$

We note that

$$A_r - A_r^\epsilon = M_r^{2\alpha-1} - (M_r^\epsilon)^{2\alpha-1} - \sum_{a \in \mathcal{J}_r \setminus \mathcal{J}_r^\epsilon} |a|^{2\alpha-1} \quad (4.16)$$

and that the expectation of (4.16) tends to 0 as  $\epsilon \rightarrow 0$ .

We assume without loss of generality that  $L = 1$ . Using that  $A_0^\epsilon = M_0 = 1$ , we have that

$$A_r^\epsilon - A_0^\epsilon = (M_r^\epsilon)^{2\alpha-1} + \sum_{a \in \mathcal{J}_r^\epsilon} |a|^{2\alpha-1} - 1 = (1 + J_r^\epsilon + rC^\epsilon)^{2\alpha-1} + \sum_{a \in \mathcal{J}_r^\epsilon} |a|^{2\alpha-1} - 1.$$

With  $\Pi$  denoting the jump law of  $M_r$ , we let

$$I_\alpha^\delta = \int_\delta^{1/2} (x^{2\alpha-1} + (1-x)^{2\alpha-1} - 1) d\Pi(x) + (2\alpha-1)C^\delta \quad \text{and} \quad (4.17)$$

$$I_\alpha = \lim_{\delta \rightarrow 0} I_\alpha^\delta. \quad (4.18)$$

We will show later in the proof that the limit in (4.18) converges, compute its value, and show that  $I_\alpha = 0$  precisely for  $\alpha = 3/2$ .

Assuming for now that this is the case, we are going to prove the result by showing that

$$\mathbf{E}[A_r - A_0] = \lim_{\epsilon \rightarrow 0} \mathbf{E}[A_r^\epsilon - A_0^\epsilon] = rI_\alpha + o(r) \quad \text{as } r \rightarrow 0 \quad (4.19)$$

where  $I_\alpha$  is as in (4.18). This suffices because then we can invoke Lemma 4.20.

Let  $E_r^{0,\delta}$  (resp.  $E_r^{1,\delta}$ ) be the event that  $M|_{[0,r]}$  does not make a (resp. makes exactly 1) jump of size at least  $\delta$  and let  $E_r^{2,\delta}$  be the event that  $M|_{[0,r]}$  makes at least two jumps of size at least  $\delta$ .

Assume  $\epsilon \in (0, \delta)$ . We will now establish (4.19) by estimating  $\mathbf{E}[(A_r^\epsilon - A_0^\epsilon)\mathbf{1}_{E_r^{j,\delta}}]$  for  $j = 0, 1, 2$ .

We start with the case  $j = 0$ . Let

$$X = J_r^{\epsilon,\delta} + rC^\epsilon = J_r^{\epsilon,\delta} + r(C^{\epsilon,\delta} + C^\delta). \quad (4.20)$$

On  $E_r^{0,\delta}$ , we have that

$$A_r^\epsilon - A_0^\epsilon = (1 + X)_+^{2\alpha-1} + \sum_{a \in \mathcal{J}_r^\epsilon} |a|^{2\alpha-1} - 1. \quad (4.21)$$

By performing a Taylor expansion of  $u \mapsto (1 + u)_+^{2\alpha-1}$  around  $u = 0$ , we see that (4.21) is equal to

$$(2\alpha - 1)X + O(X^2) + O(|X|^3) + \sum_{a \in \mathcal{J}_r^\epsilon} |a|^{2\alpha-1} \quad (4.22)$$

where the implicit constants in the  $O(X^2)$  and  $O(|X|^3)$  terms are non-random. (The presence of the  $O(|X|^3)$  term is so that we have a uniform bound which holds for all  $X$  values, not just small  $X$  values; we are using that  $\alpha \in (1, 2)$  so that  $2\alpha - 1 < 3$ .)

The form of the jump law implies that

$$\mathbf{E} \sum_{a \in \mathcal{J}_r^\epsilon} |a|^{2\alpha-1} = O(r\delta^{\alpha-1}) \quad (4.23)$$

$$\mathbf{P}[(E_r^{0,\delta})^c] = O(r\delta^{-\alpha}), \quad \mathbf{P}[E_r^{1,\delta}] = O(r\delta^{-\alpha}), \quad \mathbf{P}[E_r^{2,\delta}] = O_\delta(r^2) \quad (4.24)$$

$$\mathbf{E}[|J_r^{\epsilon,\delta} + rC^{\epsilon,\delta}|] = O(r\delta^{1-\alpha/2}), \quad (4.25)$$

$$\mathbf{E}[(J_r^{\epsilon,\delta} + rC^{\epsilon,\delta})^2] = O_\delta(r^2), \quad \text{and} \quad (4.26)$$

$$\mathbf{E}[|J_r^{\epsilon,\delta} + rC^{\epsilon,\delta}|^3] = O_\delta(r^3). \quad (4.27)$$

In (4.24), (4.26), and (4.27) the subscript  $\delta$  in  $O_\delta$  means that the implicit constant depends on  $\delta$ . Thus by the Cauchy-Schwarz inequality and (4.24), (4.25), (4.26) we have that

$$\mathbf{E}[(J_r^{\epsilon,\delta} + rC^{\epsilon,\delta})\mathbf{1}_{E_r^{0,\delta}}] = O(r\delta^{1-\alpha/2}) - \mathbf{E}[(J_r^{\epsilon,\delta} + rC^{\epsilon,\delta})\mathbf{1}_{(E_r^{0,\delta})^c}]$$

$$= O(r\delta^{1-\alpha/2}) + O_\delta(r^{3/2}). \quad (4.28)$$

Moreover, using (4.26) we have that

$$\mathbf{E}[X^2] \leq 4 \left( \mathbf{E}[(J_r^\epsilon + rC^{\epsilon,\delta})^2] + (rC^\delta)^2 \right) = O_\delta(r^2). \quad (4.29)$$

and from (4.27) we have

$$\mathbf{E}[|X|^3] \leq 8 \left( \mathbf{E}[|J_r^\epsilon + rC^{\epsilon,\delta}|^3] + (rC^\delta)^3 \right) = O_\delta(r^3). \quad (4.30)$$

Therefore taking expectations of (4.22) and using (4.23), (4.28), (4.29), and (4.30), we see that

$$\mathbf{E}[(A_r^\epsilon - A_0^\epsilon)\mathbf{1}_{E_r^{0,\delta}}] = r(2\alpha - 1)C^\delta + O(r\delta^{1-\alpha/2}) + O(r\delta^{\alpha-1}) + O_\delta(r^{3/2}). \quad (4.31)$$

We turn to the case  $j = 1$ . On  $E_r^{1,\delta}$ , with  $J$  the size of the single jump larger than  $\delta$ , we have that

$$A_r^\epsilon - A_0^\epsilon = (1 + J + X)_+^{2\alpha-1} + |J|^{2\alpha-1} + \sum_{a \in \mathcal{J}_r^\epsilon \setminus \mathcal{J}_r^\delta} |a|^{2\alpha-1} - 1. \quad (4.32)$$

By performing a Taylor expansion of  $u \mapsto (1 + J + u)_+^{2\alpha-1}$  about  $u = 0$ , we see that (4.32) is equal to

$$(1 + J)_+^{2\alpha-1} + |J|^{2\alpha-1} + \sum_{a \in \mathcal{J}_r^\epsilon \setminus \mathcal{J}_r^\delta} |a|^{2\alpha-1} + O(X) + O(|X|^3) - 1$$

where  $X$  is as in (4.20) and the implicit constant in the  $O(X)$  and  $O(|X|^3)$  terms are non-random. By (4.24) and the Cauchy-Schwarz inequality we have  $\mathbf{E}[X\mathbf{1}_{E_r^{1,\delta}}] = O_\delta(r^{3/2})$ . Combining, we have that

$$\mathbf{E}[(A_r^\epsilon - A_0^\epsilon)\mathbf{1}_{E_r^{1,\delta}}] = r(I_\alpha^\delta - (2\alpha - 1)C^\delta) + O(r\delta^{\alpha-1}) + O(r\delta^{1-\alpha/2}) + O_\delta(r^{3/2}). \quad (4.33)$$

We finish with the case  $j = 2$ . Using Lemma 4.21, it is easy to see that  $A_r^\epsilon$  has finite moments of all order uniformly in  $\epsilon$ . Thus using (4.24) and Hölder's inequality, we have for any  $p > 1$  that

$$\mathbf{E}[(A_r^\epsilon - A_0^\epsilon)\mathbf{1}_{E_r^{2,\delta}}] = O_{\delta,p}(r^{2/p}) \quad (4.34)$$

where the implicit constant in  $O_{\delta,p}(r^{2/p})$  depends on both  $\delta$  and  $p$ .

Combining (4.31), (4.33), and (4.34) (with  $p \in (1, 2)$  so that  $2/p > 1$ ), and taking a limit as  $\epsilon \rightarrow 0$  we see that

$$\mathbf{E}[A_r - A_0] = rI_\alpha + o(r) \quad \text{as } r \rightarrow 0.$$

Indeed, this follows because each of the error terms which have a factor of  $r$  also have a positive power of  $\delta$  as a factor, except for the term with  $I_\alpha$ . Thus we can make these terms arbitrarily small compared to  $r$  by taking  $\delta$  small. The remaining error terms have a factor with a power of  $r$  which is strictly larger than 1, so we can make these terms arbitrarily small compared to  $r$  by taking  $r$  small.

Therefore to finish the proof we need to show that  $I_\alpha = 0$  precisely for  $\alpha = 3/2$ . The indefinite integral

$$\int (x^{2\alpha-1} + (1-x)^{2\alpha-1} - 1) \Pi(dx) - (2\alpha - 1) \int x^{-\alpha} dx \quad (4.35)$$

can be directly computed (most easily using a computer algebra package such as Mathematica) to give

$$x^{-\alpha} \left( \frac{{}_2F_1(1-\alpha, \alpha+1; 2-\alpha; x)x}{\alpha-1} + \frac{{}_2F_1(-\alpha, \alpha; 1-\alpha; x)}{\alpha} + \frac{(\alpha-x)x^{2\alpha-1}(1-x)^{-\alpha}}{(\alpha-1)\alpha} - \frac{(\alpha+x-1)(1-x)^{\alpha-1}}{(\alpha-1)\alpha} + \frac{x-2\alpha x}{\alpha-1} \right)$$

where  ${}_2F_1$  is the hypergeometric function. In particular, the limit in (4.17) is equal to

$$-\frac{4^\alpha}{\alpha} - 2B_{\frac{1}{2}}(-\alpha, 1-\alpha) + \frac{2^{\alpha-1}(1-2\alpha)}{\alpha-1} + (2\alpha-1) \int_{1/2}^{\infty} x^{-\alpha} dx, \quad (4.36)$$

where  $B_x(a, b) = \int_0^x u^{a-1}(1-u)^{b-1} du$  is the incomplete beta function.

By evaluating the integral in (4.36), we see that (4.36) is equal to

$$-\frac{4^\alpha}{\alpha} - 2B_{\frac{1}{2}}(-\alpha, 1-\alpha).$$

Direct computation shows that this achieves the value 0 when  $\alpha = 3/2$  and (since this is an increasing function of  $\alpha$ ) is non-zero for other values of  $\alpha \in (1, 2)$ . Thus, (4.17) is equal to zero if and only if  $\alpha = 3/2$ , and as noted above, the lemma statement follows from this.  $\square$

## References

- [Ald91a] D. Aldous. The continuum random tree. I. *Ann. Probab.*, 19(1):1–28, 1991. MR1085326 (91i:60024)
- [Ald91b] D. Aldous. The continuum random tree. II. An overview. In *Stochastic analysis (Durham, 1990)*, volume 167 of *London Math. Soc. Lecture Note Ser.*, pages 23–70. Cambridge Univ. Press, Cambridge, 1991. MR1166406 (93f:60010)

- [Ald93] D. Aldous. The continuum random tree. III. *Ann. Probab.*, 21(1):248–289, 1993. MR1207226 (94c:60015)
- [ALG15] C. Abraham and J.-F. Le Gall. 2015. In preparation.
- [Ang03] O. Angel. Growth and percolation on the uniform infinite planar triangulation. *Geom. Funct. Anal.*, 13(5):935–974, 2003. MR2024412 (2005b:60015)
- [AS03] O. Angel and O. Schramm. Uniform infinite planar triangulations. *Comm. Math. Phys.*, 241(2-3):191–213, 2003. MR2013797 (2005b:60021)
- [BBI01] D. Burago, Y. Burago, and S. Ivanov. *A course in metric geometry*, volume 33 of *Graduate Studies in Mathematics*. American Mathematical Society, Providence, RI, 2001.
- [BCK15] J. Bertoin, N. Curien, and I. Kortchemski. 2015. In preparation.
- [Beg44] E. G. Begle. Regular convergence. *Duke Math. J.*, 11:441–450, 1944. MR0010964 (6,95e)
- [Ber96] J. Bertoin. *Lévy processes*, volume 121 of *Cambridge Tracts in Mathematics*. Cambridge University Press, Cambridge, 1996. MR1406564 (98e:60117)
- [Ber07] O. Bernardi. Bijective counting of tree-rooted maps and shuffles of parenthesis systems. *Electron. J. Combin.*, 14(1):Research Paper 9, 36 pp. (electronic), 2007. math/0601684. MR2285813 (2007m:05125)
- [BM15] J. Bettinelli and G. Miermont. Compact Brownian surfaces i. Brownian disks. 2015. In preparation.
- [BMS00] M. Bousquet-Mélou and G. Schaeffer. Enumeration of planar constellations. *Adv. in Appl. Math.*, 24(4):337–368, 2000. MR1761777 (2001g:05006)
- [CK13] N. Curien and I. Kortchemski. Random stable looptrees. *ArXiv e-prints*, April 2013, 1304.1044.
- [CL14a] N. Curien and J.-F. Le Gall. Scaling limits for the peeling process on random maps. *ArXiv e-prints*, December 2014, 1412.5509.
- [CL14b] N. Curien and J.-F. Le Gall. The hull process of the Brownian plane. *ArXiv e-prints*, September 2014, 1409.4026.
- [CLGM13] N. Curien, J.-F. Le Gall, and G. Miermont. The Brownian cactus I. Scaling limits of discrete cactuses. *Ann. Inst. Henri Poincaré Probab. Stat.*, 49(2):340–373, 2013. MR3088373

- [CLUB09] M. E. Caballero, A. Lambert, and G. Uribe Bravo. Proof(s) of the Lamperti representation of continuous-state branching processes. *Probab. Surv.*, 6:62–89, 2009. MR2592395 (2011a:60305)
- [CS02] P. Chassaing and G. Schaeffer. Random planar lattices and integrated super-Brownian excursion. In *Mathematics and computer science, II (Versailles, 2002)*, Trends Math., pages 127–145. Birkhäuser, Basel, 2002. MR1940133
- [Cur13] N. Curien. A glimpse of the conformal structure of random planar maps. *ArXiv e-prints*, August 2013, 1308.1807.
- [CV81] R. Cori and B. Vauquelin. Planar maps are well labeled trees. *Canad. J. Math.*, 33(5):1023–1042, 1981. MR638363 (83c:05070)
- [DK88] B. Duplantier and K.-H. Kwon. Conformal invariance and intersections of random walks. *Phys. Rev. Lett.*, 61:2514–2517, 1988.
- [DLG02] T. Duquesne and J.-F. Le Gall. Random trees, Lévy processes and spatial branching processes. *Astérisque*, (281):vi+147, 2002. MR1954248 (2003m:60239)
- [DLG05] T. Duquesne and J.-F. Le Gall. Probabilistic and fractal aspects of Lévy trees. *Probab. Theory Related Fields*, 131(4):553–603, 2005. MR2147221 (2006d:60123)
- [DLG06] T. Duquesne and J.-F. Le Gall. The Hausdorff measure of stable trees. *ALEA Lat. Am. J. Probab. Math. Stat.*, 1:393–415, 2006. MR2291942 (2008c:60081)
- [DLG09] T. Duquesne and J.-F. Le Gall. On the re-rooting invariance property of Lévy trees. *Electron. Commun. Probab.*, 14:317–326, 2009. MR2535079 (2010k:60291)
- [DMS14] B. Duplantier, J. Miller, and S. Sheffield. Liouville quantum gravity as a mating of trees. *ArXiv e-prints*, September 2014, 1409.7055.
- [DS89] B. Duplantier and H. Saleur. Exact fractal dimension of 2D Ising clusters. *Phys. Rev. Lett.*, 63:2536, 1989.
- [Dup98] B. Duplantier. Random walks and quantum gravity in two dimensions. *Phys. Rev. Lett.*, 81(25):5489–5492, 1998. MR1666816 (99j:83034)
- [Dur10] R. Durrett. *Probability: theory and examples*. Cambridge Series in Statistical and Probabilistic Mathematics. Cambridge University Press, Cambridge, fourth edition, 2010. MR2722836 (2011e:60001)

- [FT83] B. Fristedt and S. J. Taylor. Constructions of local time for a Markov process. *Z. Wahrsch. Verw. Gebiete*, 62(1):73–112, 1983. MR684210 (85c:60121)
- [GPW09] A. Greven, P. Pfaffelhuber, and A. Winter. Convergence in distribution of random metric measure spaces ( $\Lambda$ -coalescent measure trees). *Probab. Theory Related Fields*, 145(1-2):285–322, 2009. MR2520129 (2011c:60008)
- [Jir58] M. Jiřina. Stochastic branching processes with continuous state space. *Czechoslovak Math. J.*, 8 (83):292–313, 1958. MR0101554 (21 #364)
- [JS98] B. Jacquard and G. Schaeffer. A bijective census of nonseparable planar maps. *J. Combin. Theory Ser. A*, 83(1):1–20, 1998. MR1629428 (99f:05054)
- [Kri05] M. Krikun. Uniform infinite planar triangulation and related time-reversed critical branching process. *Journal of Mathematical Sciences*, 131(2):5520–5537, 2005.
- [Kyp06] A. E. Kyprianou. *Introductory lectures on fluctuations of Lévy processes with applications*. Universitext. Springer-Verlag, Berlin, 2006. MR2250061 (2008a:60003)
- [Lam67a] J. Lamperti. Continuous state branching processes. *Bull. Amer. Math. Soc.*, 73:382–386, 1967. MR0208685 (34 #8494)
- [Lam67b] J. Lamperti. The limit of a sequence of branching processes. *Z. Wahrscheinlichkeitstheorie und Verw. Gebiete*, 7:271–288, 1967. MR0217893 (36 #982)
- [Law05] G. F. Lawler. *Conformally invariant processes in the plane*, volume 114 of *Mathematical Surveys and Monographs*. American Mathematical Society, Providence, RI, 2005. MR2129588 (2006i:60003)
- [Le 14] J.-F. Le Gall. Random geometry on the sphere. *ArXiv e-prints*, March 2014, 1403.7943.
- [LG99] J.-F. Le Gall. *Spatial branching processes, random snakes and partial differential equations*. Lectures in Mathematics ETH Zürich. Birkhäuser Verlag, Basel, 1999. MR1714707 (2001g:60211)
- [LG10] J.-F. Le Gall. Geodesics in large planar maps and in the Brownian map. *Acta Math.*, 205(2):287–360, 2010. 0804.3012. MR2746349 (2012b:60272)
- [LG13] J.-F. Le Gall. Uniqueness and universality of the Brownian map. *Ann. Probab.*, 41(4):2880–2960, 2013. 1105.4842. MR3112934
- [LG14] J.-F. Le Gall. The Brownian map: a universal limit for random planar maps. In *XVIIth International Congress on Mathematical Physics*, pages 420–428. World Sci. Publ., Hackensack, NJ, 2014. MR3204495

- [LGLJ98] J.-F. Le Gall and Y. Le Jan. Branching processes in Lévy processes: the exploration process. *Ann. Probab.*, 26(1):213–252, 1998. MR1617047 (99d:60096)
- [LGP08] J.-F. Le Gall and F. Paulin. Scaling limits of bipartite planar maps are homeomorphic to the 2-sphere. *Geom. Funct. Anal.*, 18(3):893–918, 2008. math/0612315. MR2438999 (2010a:60030)
- [Löh13] W. Löh. Equivalence of Gromov-Prohorov- and Gromov’s  $\square_\lambda$ -metric on the space of metric measure spaces. *Electron. Commun. Probab.*, 18:no. 17, 10, 2013. MR3037215
- [Mie08] G. Miermont. On the sphericity of scaling limits of random planar quadrangulations. *Electron. Comm. Probab.*, 13:248–257, 2008. 0712.3687. MRMR2399286 (2009d:60024)
- [Mie13] G. Miermont. The Brownian map is the scaling limit of uniform random plane quadrangulations. *Acta Math.*, 210(2):319–401, 2013. MR3070569
- [Mie14] G. Miermont. Aspects of random planar maps. 2014. <http://perso.ens-lyon.fr/gregory.miermont/coursSaint-Flour.pdf>.
- [Mil04] J. Milnor. Pasting together Julia sets: a worked out example of mating. *Experiment. Math.*, 13(1):55–92, 2004. MR2065568 (2005c:37087)
- [MM06a] J.-F. Marckert and A. Mokkadem. Limit of normalized quadrangulations: the Brownian map. *Ann. Probab.*, 34(6):2144–2202, 2006. MR2294979 (2007m:60092)
- [MM06b] J.-F. Marckert and A. Mokkadem. Limit of normalized quadrangulations: the Brownian map. *Ann. Probab.*, 34(6):2144–2202, 2006. math/0403398. MR2294979 (2007m:60092)
- [Moo25] R. L. Moore. Concerning upper semi-continuous collections of continua. *Trans. Amer. Math. Soc.*, 27(4):416–428, 1925. MR1501320
- [MS12a] J. Miller and S. Sheffield. Imaginary Geometry I: Interacting SLEs. *ArXiv e-prints*, January 2012, 1201.1496.
- [MS12b] J. Miller and S. Sheffield. Imaginary geometry II: reversibility of  $\text{SLE}_\kappa(\rho_1; \rho_2)$  for  $\kappa \in (0, 4)$ . *ArXiv e-prints*, January 2012, 1201.1497.
- [MS12c] J. Miller and S. Sheffield. Imaginary geometry III: reversibility of  $\text{SLE}_\kappa$  for  $\kappa \in (4, 8)$ . *ArXiv e-prints*, January 2012, 1201.1498.
- [MS13a] J. Miller and S. Sheffield. Imaginary geometry IV: interior rays, whole-plane reversibility, and space-filling trees. *ArXiv e-prints*, February 2013, 1302.4738.

- [MS13b] J. Miller and S. Sheffield. Quantum Loewner Evolution. *ArXiv e-prints*, December 2013, 1312.5745.
- [MS15a] J. Miller and S. Sheffield. Finite volume Liouville quantum gravity spheres as matings of finite trees. 2015.
- [MS15b] J. Miller and S. Sheffield. Liouville quantum gravity and the Brownian map I: the QLE(8/3, 0) metric. 2015. In preparation.
- [MS15c] J. Miller and S. Sheffield. Liouville quantum gravity and the Brownian map II: geodesics and continuity of the embedding. 2015. In preparation.
- [MS15d] J. Miller and S. Sheffield. Liouville quantum gravity and the Brownian map III: the embedding is determined. 2015. In preparation.
- [Mul67] R. C. Mullin. On the enumeration of tree-rooted maps. *Canad. J. Math.*, 19:174–183, 1967. MR0205882 (34 #5708)
- [RRT14] R. B. Richter, B. Rooney, and C. Thomassen. Commentary for “On planarity of compact, locally connected, metric spaces” [mr2835298]. *Combinatorica*, 34(2):253–254, 2014. MR3213849
- [RT02] R. B. Richter and C. Thomassen. 3-connected planar spaces uniquely embed in the sphere. *Trans. Amer. Math. Soc.*, 354(11):4585–4595 (electronic), 2002. MR1926890 (2003h:57004)
- [RY99] D. Revuz and M. Yor. *Continuous martingales and Brownian motion*, volume 293 of *Grundlehren der Mathematischen Wissenschaften [Fundamental Principles of Mathematical Sciences]*. Springer-Verlag, Berlin, third edition, 1999. MR2000h:60050
- [Sat99] K.-i. Sato. *Lévy processes and infinitely divisible distributions*, volume 68 of *Cambridge Studies in Advanced Mathematics*. Cambridge University Press, Cambridge, 1999. Translated from the 1990 Japanese original, Revised by the author. MR1739520 (2003b:60064)
- [Sch97] G. Schaeffer. Bijective census and random generation of Eulerian planar maps with prescribed vertex degrees. *Electron. J. Combin.*, 4(1):Research Paper 20, 14 pp. (electronic), 1997. MR1465581 (98g:05074)
- [Sch99] G. Schaeffer. Random sampling of large planar maps and convex polyhedra. In *Annual ACM Symposium on Theory of Computing (Atlanta, GA, 1999)*, pages 760–769 (electronic). ACM, New York, 1999. MR1798101 (2001i:05142)

- [Sch00] O. Schramm. Scaling limits of loop-erased random walks and uniform spanning trees. *Israel J. Math.*, 118:221–288, 2000. math/9904022. MR1776084 (2001m:60227)
- [She10] S. Sheffield. Conformal weldings of random surfaces: SLE and the quantum gravity zipper. *ArXiv e-prints*, December 2010, 1012.4797.
- [She11] S. Sheffield. Quantum gravity and inventory accumulation. *ArXiv e-prints*, August 2011, 1108.2241.
- [SW12] S. Sheffield and W. Werner. Conformal loop ensembles: the Markovian characterization and the loop-soup construction. *Ann. of Math. (2)*, 176(3):1827–1917, 2012. 1006.2374. MR2979861
- [Tut62] W. T. Tutte. A census of planar triangulations. *Canad. J. Math.*, 14:21–38, 1962. MR0130841 (24 #A695)
- [Tut68] W. T. Tutte. On the enumeration of planar maps. *Bull. Amer. Math. Soc.*, 74:64–74, 1968. MR0218276 (36 #1363)
- [Vil09] C. Villani. *Optimal transport*, volume 338 of *Grundlehren der Mathematischen Wissenschaften [Fundamental Principles of Mathematical Sciences]*. Springer-Verlag, Berlin, 2009. Old and new. MR2459454 (2010f:49001)
- [Wat95] Y. Watabiki. Construction of non-critical string field theory by transfer matrix formalism in dynamical triangulation. *Nuclear Phys. B*, 441(1-2):119–163, 1995. MR1329946 (96k:81224)

Department of Mathematics  
 Massachusetts Institute of Technology  
 Cambridge, MA, USA